EFFECT OF SOLVENTS AND pH ON ABSORPTION AND FLUORE SCENCE SPECTRA OF SOME SELECTED ORGANIC COMPOUNDS

A Thesis Submitted
In Partial Fulfilment of the Requirements
for the Degree of

DOCTOR OF PHILOSOPHY

By
ASHOK KUMAR MISHRA

to the
DEPARTMENT OF CHEMISTRY
INDIAN INSTITUTE OF TECHNOLOGY, KANPUR
MARCH, 1984

TO

MY PARENTS

STATEMENT

I hereby declare that the work embodied in this thesis entitled, "EFFECT OF SOLVENTS AND pH ON ABSORPTION AND FLUORES-CENCE SPECTRA OF SOME SELECTED ORGANIC COMPOUNDS" has been carried out by me under the supervision of Dr. S.K. Dogra.

In keeping with scientific tradition, wherever work done by others has been utilized, due acknowledgement has been made.
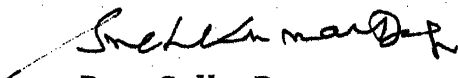
A.K. Mishra

CERTIFICATE-I

Certified that the work presented in this thesis entitled, "EFFECT OF SOLVENTS AND pH ON ABSORPTION AND FLUORESCENCE SPECTRA OF SOME SELECTED ORGANIC COMPOUNDS" by Mr. Ashok Kumar Mishra, has been carried out under my supervision and not submitted elsewhere for a degree.

Dr. S.K. Dogra
Department of Chemistry
I.I.T., Kanpur-208016

March, 1984

DEPARTMENT OF CHEMISTRY
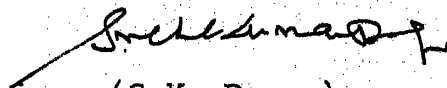INDIAN INSTITUTE OF TECHNOLOGY, KANPUR

CERTIFICATE-II

This is to certify that Mr. Ashok Kumar Mishra has satis-factorily completed all the courses required for the Ph.D. degree programme. These courses include:

Chm 500 Mathematics for Chemists
Chm 521 Chemical Binding
Chm 523 Chemical Thermodynamics
Chm 524 Modern Physical Methods in Chemistry
Chm 534 Electronics for Chemists
Chm 800 General Seminar
Chm 801 Graduate Seminar
Chm 900 Post-Graduate Research

Mr. Ashok Kumar Mishra was admitted to the candidacy of the Ph.D. degree programme in February, 1981 after he success-fully completed the written and oral qualifying examinations.

(P.S. Goel)   (S.K. Dogra)
Professor and Head   Convenor
Department of Chemistry   Departmental Post-Graduate Committee,
I.I.T., Kanpur   I.I.T., Kanpur

CONTENTS

*****

ACKNOWLEDGEMENTS

SYNOPSIS

An organic molecule in its excited state can have a different charge distribution at different atoms as compared to that in its ground state and thus can be considered a new chemical species, thereby opening a new range of reaction pathways which can be different from the ground state reactions. Proton transfer reactions in the excited state have a special significance in heterocyclic chemistry but not much is known about the acid-base behaviour of complex heterocyclic molecules containing polyfunctional groups in their excited states.

In this thesis I have attempted to study (i) the effect of solvents of varying polarity and hydrogen bonding ability and (ii) the acid-base properties of nine organic molecules in their ground (S_o) and the first excited singlet state (S_1). These include two amino-hydrocarbons (aminochrysene and aminofluoranthene), 6-aminoindazole and six benzimidazoles (2-hydroxybenzimidazole, 2-aminobenzimidazole, 2-phenylbenzimidazole, 2-(o-aminophenyl) benzimidazole, 2-(m-aminophenyl)benzimidazole and 2-(p-aminophenyl)benzimidazole.

The thesis contains four chapters. Chapter 1 reviews the literature on the excited state acid-base properties as well as solvent effect on absorption and fluorescence spectra of organic molecules having acidic or basic functional groups. A brief account of the scope of the present investigation and justification of the selection of compounds is also given.

Chapter 2 describes the instrumentation and the materials used. A description of the spectrofluorimeter used which has been fabricated in our laboratory is followed by methods of preparation of certain compounds and the degree of purity of the solvents used for spectral studies.

Chapter 3 has a brief description of the theory of solvent effect on absorption and fluorescence and the effect of solvents on absorption and fluorescence behaviour of the compounds under investigation is discussed. It was found that in most of the compounds the absorption spectrum is not much affected by the polarity or hydrogen bonding ability of solvents. From the nature of the shifts of absorption and fluorescence spectra it was suggested that in many amino compounds like amino-hydrocarbons, 2-amino-benzimidazole, 6-aminoindazole, 2-(m-aminophenyl)benzimidazole and 2-(p-aminophenyl)benzimidazole, the amino group acts as hydrogen bond acceptor in the S_o state and hydrogen bond donor in the S_1 state.

2-(o-Aminophenyl)benzimidazole showed evidence of the presence of two different hydrogen bonded forms: the hydrogen atom of amino group in the phenyl ring forming a hydrogen bond with pyridinic nitrogen in the adjacent ring in one form and the lone pair of amino group with the pyrrolic hydrogen atom in the other form. Both these forms are stable enough in less polar media to give their own absorption and fluorescence spectra. The excitation

spectra of both the forms could be taken thus confirming their presence. The latter form was found to be more stable in protic solvents.

2-Hydroxybenzimidazole showed a blue shift with solvent polarity both in absorption and fluorescence, which is contrary to the behaviour of the rest of the molecules. From the nature of the spectra, solvent effect and prototropic behaviour, it was suggested that it exists in its isomeric 2-(3H)benzimidazolone form. N-Methylbenzimidazolone was prepared and its spectral nature studied to confirm the idea.

Chapter 4 gives the acid-base properties of the molecules in the ground and excited state, following a review of the theories of acidity and basicity change and methods of determination of excited state dissociation constants. In the amino-hydrocarbons and some other amino compounds proton induced fluorescence quenching was found to compete with the protonation equilibria. An attempt is made to calculate the quenching rate constants by Stern-Volmer plot taking approximate lifetimes calculated using Strickler and Berg equation.

In all benzimidazoles except 2-phenylbenzimidazole, a dication, a cation, a neutral form and an anion form were identified in both ground and excited states. The rotation of the phenyl ring on protonation was clearly evident from the blue shift of its cation absorption.

The acid-base properties of 2-hydroxybenzimidazole could be nicely explained by its tautomeric 2-(3H)benzimidazolone form and its conversion to benzamidazole form in dication. 2-Amino-benzimidazole also showed a cyclic amidine structure in its mono-cation form.

The acid-base properties of 2-(o-aminophenyl) benzimidazole very clearly showed the presence of the two hydrogen bonded isomers. The amino group in 2-(m-aminophenyl) benzimidazole behaved almost independent of the rest of the molecule in the ground state, indicating very less conjugation in ground state and an improved conjugation in the excited state. 2-(p-aminophenyl) benzimidazole showed an extensive reorganization of charges in ground and excited states.

6-Aminoindazole showed five prototropic species in the excited state. Apart from the usual dication, neutral and anion species, two monocation forms: one pyridine protonated and the other amino protonated, were identified in the excited state from the fluorescence spectral behaviour where as only the amino protonated monocation existed in the ground state.

Ground and excited state pKa values were determined for all the prototropic equilibria. The excited state pKa values were determined both by 'Förster Cycle' and 'Fluorimetric Titration' methods. The shifts of pKa* values with respect to pKa or the

absence shift in pKa* were rationalized by existing theories of charge density distribution in ground and excited states in various basic centers.

A summary of work done and work could be extended is given at the end of the thesis.

LIST OF FIGURES

LIST OF TABLES

CHAPTER-1

GENERAL INTRODUCTION

A molecule in its electronically excited state has a different electronic charge distribution on different atoms, as compared to that in its ground state. As the physical and chemical properties of a molecule are mostly dependent on its electronic charge distribution, the excited molecule tends to show different physical and chemical properties than the molecule in the ground state. The study of photophysical and photochemical processes of organic molecules, specially heterocyclic molecules, has always been of special interest to chemists.

The energy and sometimes the nature of electronic transitions in a molecule (like absorption, fluorescence or phosphorescence) are largely dependent upon the nature of solute-solvent interaction and hence a study of such transitions in presence of different solvents can provide vital information regarding the charge distribution in the solute molecule, geometry of the molecule, the nature of transition etc., in the ground and excited states. The information on the acid-base properties of molecules in the excited

states and their relation to structure is of prime importance in the mechanistic elucidation of photochemical reactions. For reactions proceeding through excited singlet state or triplet state and dependent on acidity of the system, the information on the excited state pK_a value is necessary to optimize the reaction conditions. In this chapter a brief history of the study of solvent dependence of absorption and fluorescence and excited state proton transfer equilibria, relevant to this study, has been given followed by a description of the scope of the present work.

1.1   Solvent dependence of absorption and fluorescence spectra

The first systematic study of solvent effects on absorption spectra was done in the fifties. A similar study of fluorescence spectra also started during the same time. Kasha[1] and McConnel[2] generalised in 1950 that the nature of the shift of electronic absorption band can be a criterion for distinguishing n π^* from $\pi \pi^*$ transitions. Thus a blue shift for n π^* and a red shift for $\pi \pi^*$ transition is expected with increasing solvent polarity. In 1954 Bayliss and McRae[3] observed that the interactions of solvent and solute molecules are predominantly electrostatic and may be of the induced dipole-induced dipole, dipole-induced dipole, dipole-dipole or hydrogen bonding types. Thus the shift could be nicely related to the dipole moment of the solute molecules and the calculation of dipole moments from shifts was attempted by some workers like Lippert,[4] McRae,[5] Suppan and Tsiamis[6] and Mataga and

coworkers.[7] A very consolidated and comprehensive account of electronic absorption spectroscopy is given in the books written by Jaffe and Orchin,[8] Suzuki[9a] and Mataga and Kubota.[9b] Pring-sheim[10] in 1949 and Förster[11] in 1951 made the first systematic study of the environmental effects on the fluorescence spectra of aromatic compounds. In 1963 Van Duuren[12] reviewed the subject giving a detailed account of the solvent effects for various types of aromatic compounds and their derivatives. He discussed the λ_{max} shifts and the quenching of fluorescence in addition to the viscosity effect caused by the solvents. The λ_{max} shifts were explained using the Frank-Condon principle.

Mataga and co-workers[13-15] studied the effect of hydrogen bonding extensively. The site and nature of hydrogen bonding in terms of hydrogen bond acceptor and hydrogen bond donor type interactions could cause either a blue or a red shift in fluorescence in naphthylamines.

In 1970, Berlman[16] tried to correlate empirically the absorption and fluorescence characteristics of aromatic ring and ring-chain systems with the nuclear conformation of the molecules in ground and excited states. Thus he classified these compounds into five different classes, depending upon spectral shifts, shape of absorption and emission bands, medium effects etc.

Recently a study of dipole moments and geometries of aromatic esters has been attempted by Costa and coworkers[17] from the

absorption and emission data in different solvents. As recent as in 1983, a method of determining excited state dipole moments from absorption/fluorescence solvatochromic ratios is discussed by Suppan.[18]

Few papers have tried to rationalize intramolecular photo-tautomerism,[19,20] nature of hydrogen bonding,[21] chemical structure[2] and geometry[17] in the ground and excited states on the basis of solvent effects on absorption and fluorescence.

1.2 Excited state pK_a studies

In 1931, an 'abnormal' fluorescence due to protolytic dissociation of 1-naphthylamine-4-sulphonate was reported by Weber,[23] which occurred in a pH range where there was no change in absorption spectrum. After some more such observations[24-26] in hydroxy and amino-pyrene sulphonates, hydroxy and other naphthalene derivatives, Förster[24,25] in 1950 suggested a method to determine the excited state pK_a (pK_a^*) values from the electronic transition energy. This method was based on the thermodynamic equivalence of all routes from the ground state of the acid to the excited state of the conjugate base and is commonly known as 'Förster Cycle'.

In 1952 Weller[27] developed a method of plotting fluorescence intensity of a species as a function of hydrogen ion concentration. The point of inflection of the resultant sigmoid curve is a measure of the dissociation constant in the excited

state provided the excited state equilibrium is attained. This method is known as 'Fluorimetric Titration'.

These two constitute the most important methods to obtain excited state pKa values, besides the dynamic methods involving time dependent fluorescence spectroscopy.[112] Although use of photo-potentiometry has been tried for the same,[28] it has not received wide attention, may be because of an insufficient generation of photopotential in many organic molecules.

The 'Förster Cycle' and the 'Fluorimetric titration' methods have been subjected to many critical discussions regarding their scope and applicability by many authors after they were formulated. From an estimation of pKa^* values of some p-substituted phenols, Bartok et al.[29] suggested that pKa^* calculated by using the average of absorption and fluorescence maxima could be more accurate than the pKa^* values obtained by either absorption or emission data. Haylock et al.,[30] suggested that the discrepancy observed between the pKa^* obtained from spectroscopic data and that obtained from fluorimetric titration for some substituted quinolines is due to an unequal entropy change in the ground and excited state. Mason[31], Jaffe and Jones,[32] Jaffe et al,[33] Wehry and Rogers[34] and many others, while studying various classes of compounds like quinolines, azobenzenes, azoxybenzenes and substituted phenols have further highlighted the differences between estimated and experimental pKa^* values and discussed the possible reasons.

Van der Donckt[35] reviewed the acid base properties of the excited states, wherein he discussed the effect of excited state geometrical relaxation on the 'Förster cycle' calculations. Subsequently more pKa^* data have accumulated and the subject has been reviewed by several authors.[36-38] The review by Ireland and Wyatt[37] contains extensive references of experimental results available in the litrature till 1974. Schulman et al.[19,21,39-45] have done extensive work on pKa^* of many classes of organic compounds including compounds of biological importance. ~~He has~~ They have tried to explain the shapes of fluorimetric titration curves on the basis of the kinetics of the S_1 state proton transfer. Schulman and Capomacchia[40] have proposed a modified Förster cycle which includes vibrational, solvent and geometrical relaxation in both the states and have derived equations similar to those of the Förster cycle. In his recent review[44] and book[45] Schulman has given a nice and detailed picture of the acid-base chemistry of S_1 state.

1.3 Scope of present work

One of the major objectives of this study has been to determine the acid-base properties of some compounds in the ground and the first excited singlet states. Nitrogen, oxygen or sulphur heterocyclic molecules or molecules containing functional groups with a basic center are the main classes of compounds for which such a study could be of fundamental importance. In this thesis,

attention has been focussed on nitrogen containing aromatic molecules like some aromatic amines and some diaza-heterocyclic compounds with various substituents.

In the condensed aromatic amines series, α-and β-naphthylamines[46] and phenanthrylamines[47,48] have earlier been studied in detail. The following facts have been observed:

(i)   At moderate hydrogen ion concentration, proton induced fluorescence quenching competes with protonation equilibria of the amino compounds.

(ii)   The ammonium ion becomes more acidic in the excited state, thus shifting the excited state protonation equilibrium constant to a very low H_o value. Similarly pyrrolic and amino group hydrogen atoms become more acidic, thus the deprotonation constant comes down to ~ 12 in S_1 from a much higher (> 14) value in S_o. A higher member in the series viz. 6-aminochrysene has been considered to test the above results.

It has been established that due to an uneven charge distribution even in the ground state, nonalternant hydrocarbons behave differently than the alternant hydrocarbons.[146] Hence a nonalternant amino hydrocarbon is likely to show some difference in its ground and excited state property, especially with respect to prototropic equilibria. 3-Aminofluoranthene, which is a nonalternant hydrocarbon, has been taken for its photophysical and photochemical studies.

There has hardly been any detailed photophysical study of more complex heterocyclic systems. The compounds which have been selected for this study, mostly have three basic centers, all of different types: one pyridinic nitrogen center, one pyrrolic nitrogen center and an exocyclic amino group which itself can behave in two ways. A redistribution of charge on excitation can result in a change in the basicity of the basic centers in varying degrees and it would be interesting to study their behaviour.

An unusual biprotonic phototautomerism has been observed for 5-aminoindazole.[49] It has been observed that the exocyclic amino group gets protonated in the ground state, but on excitation, the basicity of the pyridinic nitrogen center increases and that of the exocyclic amino group decreases; thus the pyridinic protonated form is observed in the excited state. 6-aminoindazole has been studied to have a further insight into the phenomenon, because, as such 5- and 6- positions in indazole are non-equivalent but both are in the carbocyclic ring, thereby affecting the longer wave-length $^{1}L_{b}$ band most.

The absorption and emission characteristics of benzimidazole as a function of pH have been studied extensively.[50-55] It has been shown by Tway and Love[61] that the transitions in benzimidazole molecule are of $\pi\pi^*$ character and the absorption and fluorescence spectra are weakly affected by the polarity or hydrogen bonding ability of the solvents. The absorption maximum of benzimidazole

cation is blue shifted whereas the fluorescence maximum is largely red shifted as compared to the absorption and fluorescence spectra of the neutral molecule respectively. Borrensen[53] explained this large red shift in emission because of the formation of a stoichiometric complex with the solvent in the excited state whereas Kondo and Kuwano[54] have demonstrated that this is due to the reversal of the two electronic states i.e. in neutral molecule the fluorescence takes place from the less polar ^1L_b state and in the cation the more polar electronic state ^1L_a is S_1. A similar phenomenon has been observed in the cations of other substituted benzimidazoles,[54] for example 2-methylbenzimidazole shows two fluorescence bands, depending upon the energy difference between the L_a and L_b electronic states of the specific cation. Not much work is reported on the substituted benzimidazoles except the recent work of Tway and Love.[61]

Spectroscopic and pKa studies have shown that 2- and 4-hydroxy quinolines[56] exist in 2- and 4-quinolone forms in both S_o and S_1 states, whereas the monocation and monoanion of these compounds behave like the other normal hydroxy derivatives of quinoline. A similar study for isomeric aminoquinolines[57-60] reveals that the structures of 2- and 4-aminoquinolines derived by protonating the pyridinic nitrogen atom possesses the cyclic amidine structure. Thus a nice correlation between 2- and 4-hydroxy and amino quinolines have been made as follows: the anions derived from 2- and

4- quinolinols correspond electronically to neutral 2- and 4-
aminoquinolines, the neutral 2- and 4- quinolones correspond to
the singly charged cations derived from 2- and 4- aminoquinolines
and the cations derived from 2- and 4- quinolinols correspond to
the doubly charged cations derived from 2- and 4- aminoquinolines.
2-Amino and 2-hydroxybenzimidazoles resemble to 2-amino and
2-hydroxyquinolines. Thus to ascertain whether similar behaviour
is expected in the respective benzimidazole molecules, this study
was carried out. In fact 2-hydroxybenzimidazole is known to exist
mainly in its tautomeric 2(3H)-benzimidazolone form, whereas
2-aminobenzimidazole exists in natural arylamine form. 1-Methyl-2-
benzimidazolinone was prepared and studied to confirm some of the
behaviours of 2(3H)-benzimidazolone.

All the three possible isomers in the series of 2-substituted
(aminopheny)benzimidazoles have been studied. All the three of
them are expected to be entirely different from each other in the
following fashion. 2-(o-aminophenyl)benzimidazole has an amino
group which can very nicely form hydrogen bond with pyridinic
nitrogen or pyrrolic hydrogen in the adjacent ring thereby forming
six-membered stable ring structure. The nature and site of this
hydrogen bonding could be different in different medium and hydrogen
ion concentration. The amino group in 2-(m-aminophenyl)benzimida-
zole should almost behave independently without interacting much
with the basic center in the imidazole ring due to lack of direct
conjugation. But the amino group in 2-(p-aminophenyl)benzimidazole

can very nicely interact with the whole molecule and an extensive reorganisation of charges in ground and excited state is expected.

The study of the parent 2-phenylbenzimidazole becomes inevitable to see any steric interaction due to the phenyl ring rotation. This also forms a nice basis for comparison of the properties of the (aminophenyl)benzimidazole compounds. More expecially, after the amino group has been protonated, these molecules should very closely resemble each other and with 2-phenyl-benzimidazole.

A study of absorption and fluorescence of the salts of the amino compounds in different solvents can give further confirmation regarding the nature of the monoprotonated species. This has been done whereever necessary.

The study of fluorescence in a rigid matrix at low temperature (77K) can give valuable informations. Freezing 'locks' the fluorescing molecule in to the ground state equilibrium solvent cage and molecular conformation and thereby prevents solvent cage relaxation and functional group rehybridization subsequent to excitation. Thus, the comparison of absorption and fluorescence spectra taken in frozen solutions with those taken in fluid media permits distinction between solvent and conformational effects arising from the ground state circumstances of the molecule and those arising from the extra-electronic circumstances of the thermally equilibrated excited molecule. Low temperature

fluorescence spectra, whereever necessary to supplement our ideas, have been recorded.

INSTRUMENTATION AND MATERIALS

2.1 Spectrofluorimeter

Fluorescence spectra were recorded on a scanning spectro-
fluorimeter, fabricated in our laboratory. The block diagrams of
the spectrofluorimeter and the arrangement to take spectra at low
temperatures are given in Figs. 2.1 and 2.2 respectively. A brief
description of each part is given below.

A stabilized power supply (PS) for the lamp (LPS 251 HR) and
the lamp housing (LH 150) were procured from Schoeffel Instruments.
They can accomodate 150W Xe lamp, 200W Xe-Hg lamp and 200W Hg lamp.
The total energy output from the lamp could be monitored and kept
constant by the power supply.

Two Jarrell-Ash 0.25 m and f/3.5 Ebert grating monochromators
(82-410 and 82-415) were used. The monochromator (M_1) with one
grating, blazed at 300 nm (1180 grooves/mm with a reciprocal
linear dispersion of 3.3 nm/mm) was used for selecting the excita-
tion wavelength. The monochromator (M_2) with two gratings, one
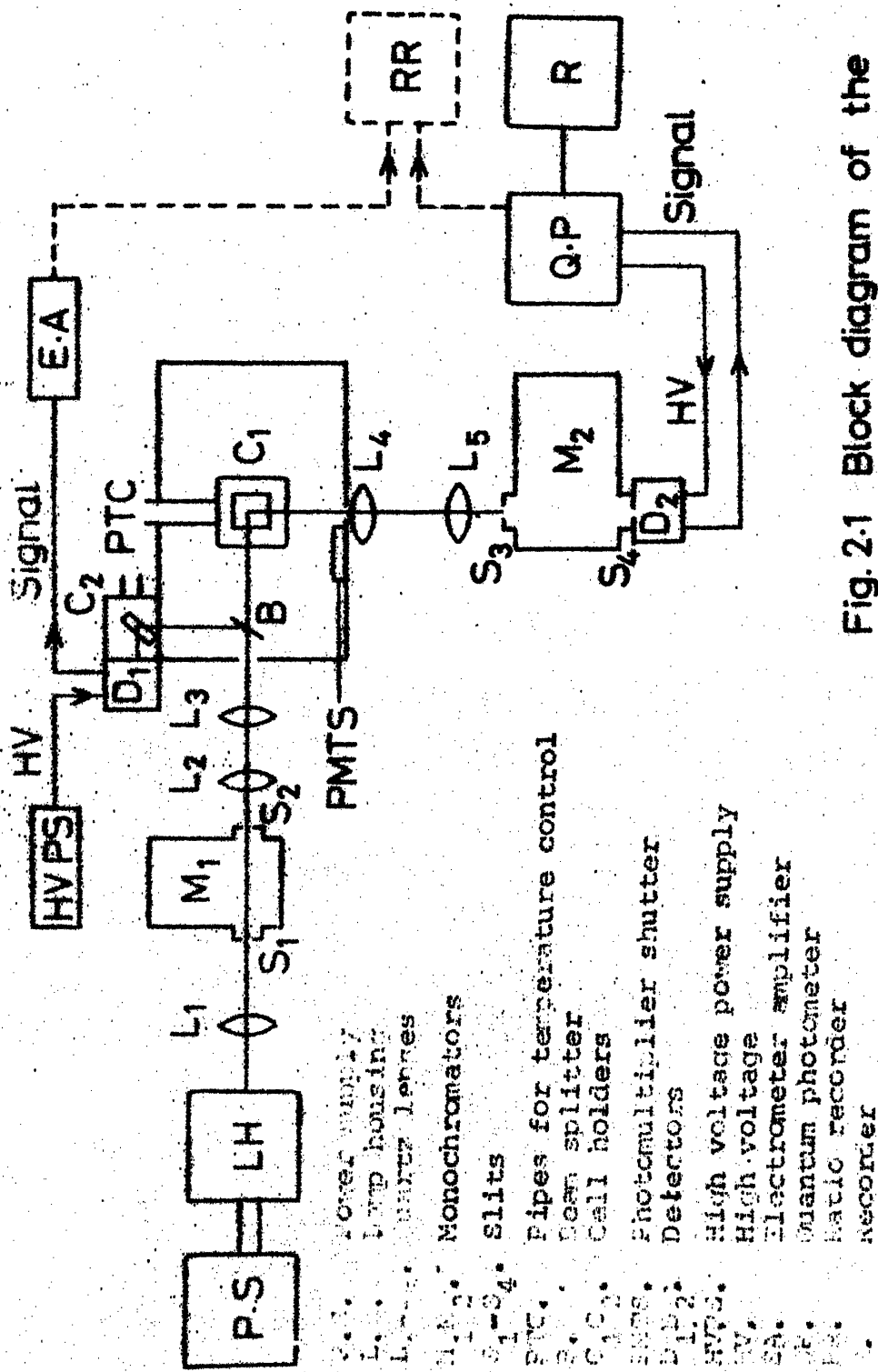
Fig. 2.1   Block diagram of the
Spectroflourimeter

Liq. N$_2$

Quartz cell

Quartz window

Liq. N$_2$

Air inlet

Motor
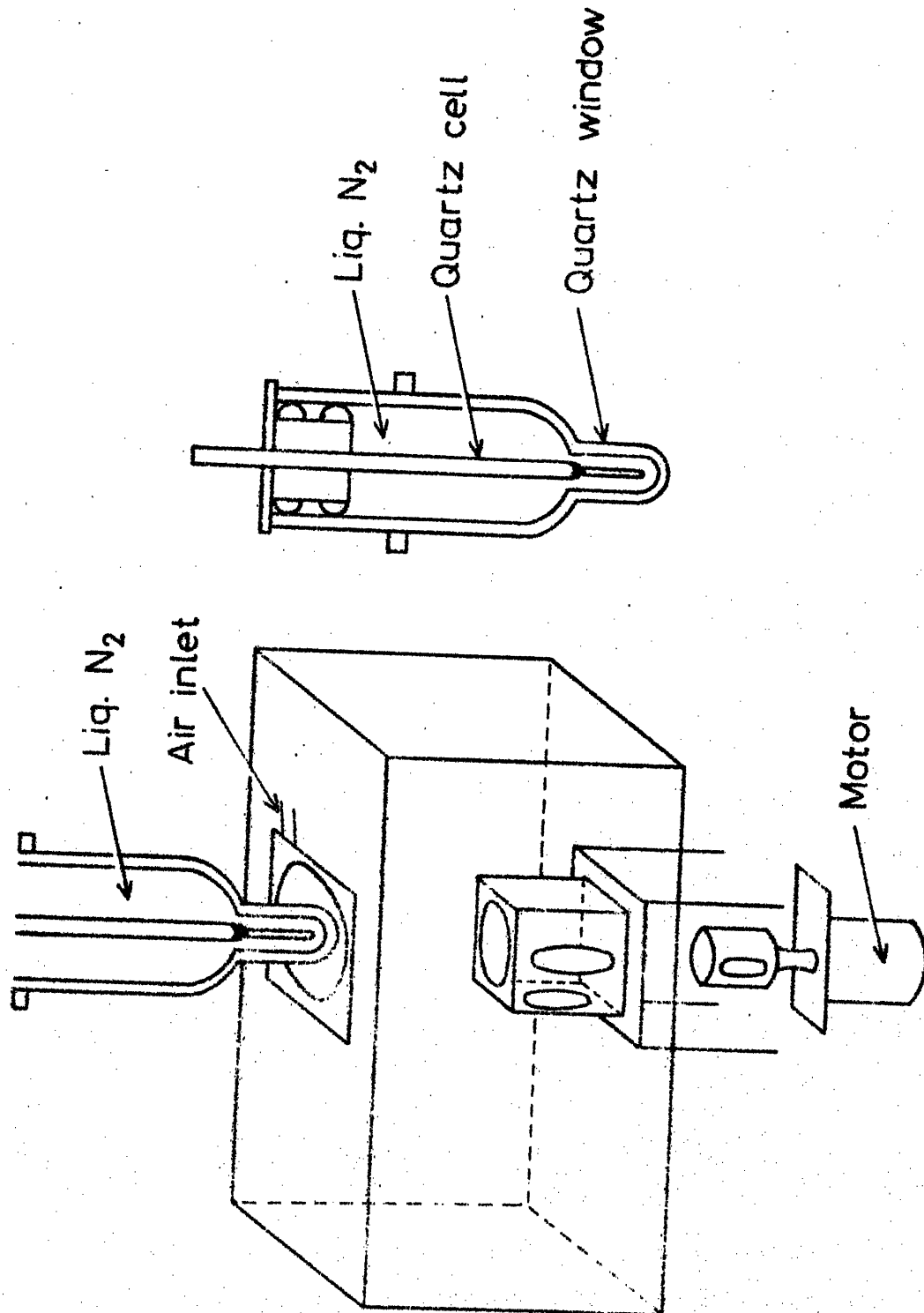
Fig. 2·2 Diagram of low temperature set up for fluorescence and phosphorescence.

blazed at 300 nm (2360 grooves/mm) with reciprocal linear disper-
sion of 1.65 nm/mm and the other blazed at 500 nm (1180 grooves/
mm) with reciprocal linear dispersion of 3.3 nm/mm was used for
the resolution of emission spectra. The focal lengths of the
quartz lenses (L_1-L_5) were chosen to suit the aperture ratios of
monochromators and to have maximum collection of the exciting as
well as the emitting light.

The cell compartment is designed for both room temperature
and low temperature measurements and is anodized black to minimize
scattering. The cell holder (C_1) is double walled with thermo-
statting arrangements to maintain a constant temperature. For low
temperature (77K) measurements, Aminco-Bowman's low temperature
fluorescence and phosphorescence accessory could be fitted in the
cell compartment by replacing the normal cell holder C_1 (Fig.2.2).
Provision is there to pass dry air to remove the condensed moisture
from the walls of the Dewar flask, used for low temperature measure-
ments. If necessary a beam splitter B could be fitted in the cell
compartment. This is a 1 mm thick quartz plate, placed at an angle
of 45° in the path of the exciting light to reflect 10% of it to
another cell holder C_2. This is used to calibrate the light source
from time to time and to determine the relative intensities of the
excitation light emerging from M_1 at all wavelengths as described
later in this chapter.

Princeton Applied Research Quantum Photometer console (model 1140A) was used for detection and amplification of emission. It consists of a detector assembly, an amplifier/discriminator, an electrometer, a detector voltage supply and two rate meters, one with log and the other with linear scale. The detector assembly with a 1P28 photomultiplier tube (Hammatsu, Japan) was fixed at the exit slit of M_2. Very weak signals could be detected in the photon-counting mode of the quantum photometer. The detected and amplified signal was read from the rate-meter on the front panel. A multirange and multispeed digital recorder (Fischer Recordall Series 5000) was used to record the signal output from the Quantum Photometer. The emission monochromator M_2 was scanned by a digital drive system specifically made for Jarrell-Ash Monochromators (Jarrell-Ash Omnidrive 82-462) which is coupled to the recorder. From time to time, both the monochromators were calibrated with alow pressure mercury lamp.

2.2 Experimental Procedure

A sample in the quartz cell is placed in the cell holder. The light of excitation wavelength selected by M_1 is focussed on the sample and the emission from the sample at a right angle is directed to M_2. The emission intensities at wavelengths selected by M_2 are measured from the quantum photometer display. The complete emission spectrum is recorded by scanning M_2. The total

energy output of the lamp is always kept constant by the suitable combination of current and voltage in the lamp power supply.

For a low temperature run, the cell compartment is fitted with low temperature accessary. The sample in the proper cell is placed in liquid nitrogen kept in a quartz Dewar flask for some time till the bubbling of nitrogen gets reduced. Then after removing the moisture condensed, the Dewar flask with the sample is placed in the cell compartment (Fig. 2.2). During scanning dry air is passed through the compartment to remove any moisture condensed.

The fluorescence excitation spectrum at room temperature or at low temperature can be obtained by setting M_2 at the fluorescence maximum and scanning M_1.

The excitation and emission spectra thus obtained are uncorrected. The corrected spectra have been obtained by determining the correction factors and by dividing the observed emission intensities by these factors at any specified wavelength. Automatic recording of the corrected excitation spectra is possible in this instrument if the signal from the sample cell and the signal from the reference cell are fed into a recorder which can record the ratio of the two signals (ratio recorder). This part is indicated by dotted lines in the block diagram (Fig. 2.1).

2.3 Correction Factors Determination

In a spectrofluorimeter, the intensity of the lamp, efficiency of the monochromator and the response of the photomultiplier tube are wavelength dependent. So all spectrofluorimeters record only an 'apparent emission spectrum' or an 'apparent excitation spectrum' in the absence of an automatic correction accessory.

Such spectra, in some regions are grossly distorted versions of the true spectra. Even though the uncorrected emission spectra can be used for some experiments like fluorimetric titrations, which are done at a particular wavelength, they are not useful in calculating quantum efficiencies and for reporting the fluorescence spectra of new compounds. Several methods have been described and used for the determination of correction factors.[62-67] The principles of Melhuish's[65] method for the calculation of correction factors $\Omega(\lambda)$ for the light source (150W Xe lamp) - Excitation monochromator combination have been followed in this study. The correction factors for the emission monochromator-1P28 photomultiplier tube combination have been determined by following the procedure of Chen.[66] All calibrations were done with 150W xenon lamp.

2.3.1 Correction factors for the light source (150W Xe lamp) - Excitation Monochromator Combination

A concentrated solution of Rhodamine-B (3gm/litre in

ethyleneglycol) was taken in a quartz cell of size 1 cmx0.5 cm and was placed in C_2 at an angle of 45°. The emission was viewed from the back of the cell (Fig. 2.1). The advantage of this arrangement[68] is that if the incident radiation contains a small portion of "impure wavelengths" not absorbed by the quantum counter (Rhodamine-B solution), they are not registered by the detector (D_2). The emission from this solution was passed through a narrow band metal interference filter placed before D_2. It has a maximum transmission at 620 nm with a band width of 10 nm. The intensity of the fluorescence signal at 620 nm is proportional to the intensity of the excitation light. This signal amplified by the electrometer amplifier, was recorded by scanning the M_1 from 230 to 600 nm, during which the slits of M_1 were kept at 1 mm (11 nm band width). The spectrum recorded is called the excitation system calibration curve and it is shown in Fig. 2.3. This curve gives the relative intensities of the excitation light emerging from M_1 at all wavelengths. These are the correction factors at different wavelengths i.e. $\Omega(\lambda)$. This $\Omega(\lambda)$ was used for the calibration of emission system.

2.3.2 Correction factors for the Emission Monochromator-1P28 photomultiplier tube combination

The calibration factors for M_2 were calculated from 230 to 450 nm for the low blaze grating (300 nm) and 350 to 550 nm for the high blaze grating (500 nm).
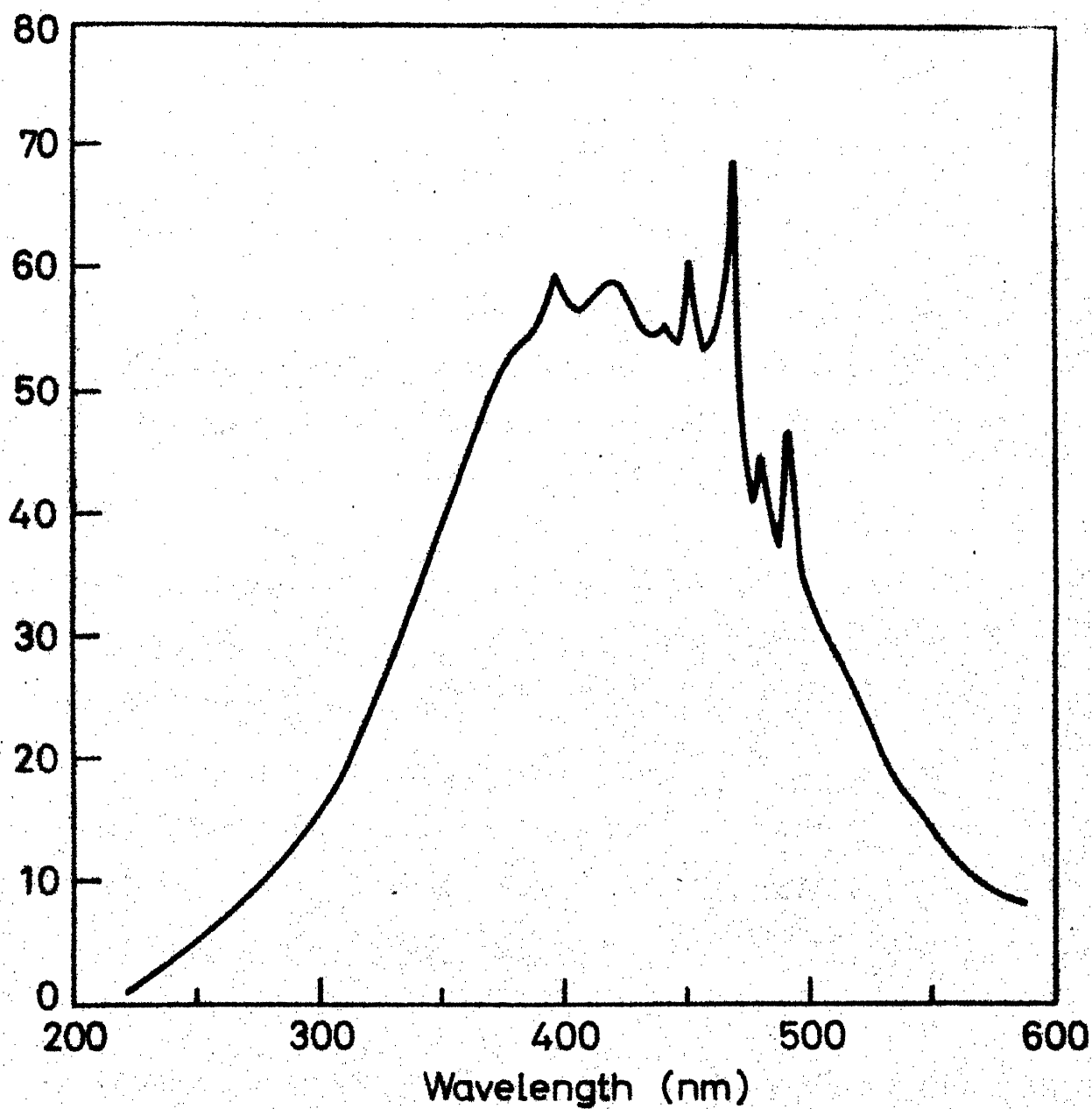
2.3 Relative intensity distribution of excitation source.

A quartz plate at 45° to the incident light was placed in C_1. The intensity of the incident light was reduced by adjusting the slit of M_1. The slit of M_2 was set at 1 mm.

One selected wavelength was set at M_1, the output of which was reflected by the quartz plate to M_2. M_2 was adjusted manually to give the maximum reading at the wavelength set in M_1. This maximum reading at this wavelength is the relative response of the emission monochromator-photomultiplier combination and is denoted by $R(\lambda)$. The maximum readings were obtained for each wavelength set at M_1. This $R(\lambda)$ when divided by $Q(\lambda)$ determined earlier, gave $S(\lambda)$, the emission correction factor at λ. A plot of $S(\lambda)$ vs λ gives the emission spectral sensitivity curve or the correction curve, as shown in Fig. 2.4, for the low blaze and the high blaze gratings.

These correction factors were used to correct the fluorescence spectrum of anthracene (1×10^{-5}M in ethanol), recorded using the low blaze grating and quinine sulphate (1×10^{-5}M in 0.1N H_2SO_4) recorded using high blaze grating. The corrected spectra thus obtained are shown in Figs 2.5 and 2.6. They match exactly with the spectra reported in the literature.[65]

2.4 Other Instruments

All absorption spectra were recorded in a Cary 17D spectrophotometer. pH of various solutions were measured using a
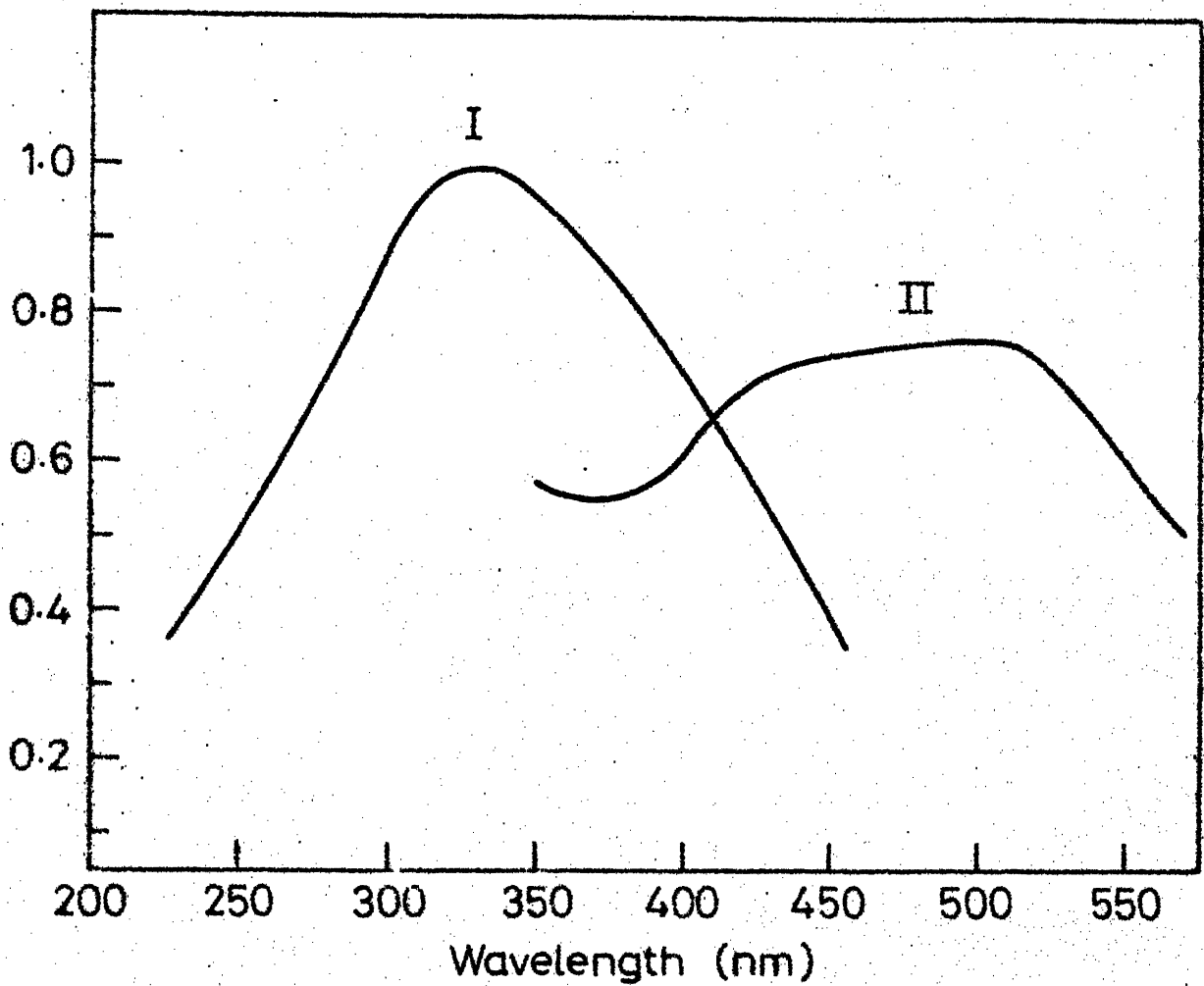
2.4 Emission calibration curves : I 300 nm blaze grating
II 500 nm blaze grating.
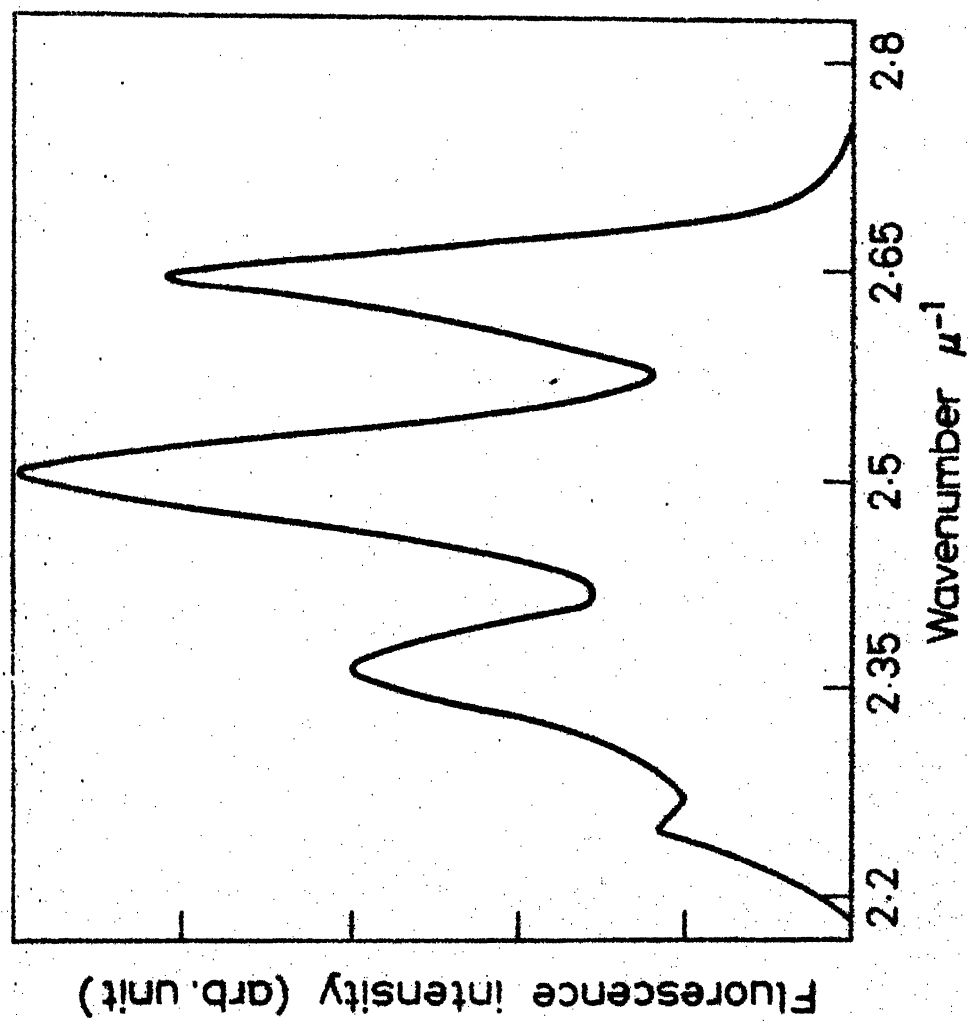
Fig. 2·5 Corrected Fluorescence spectrum of Anthracene (1×10^{-5} M in ethanol)
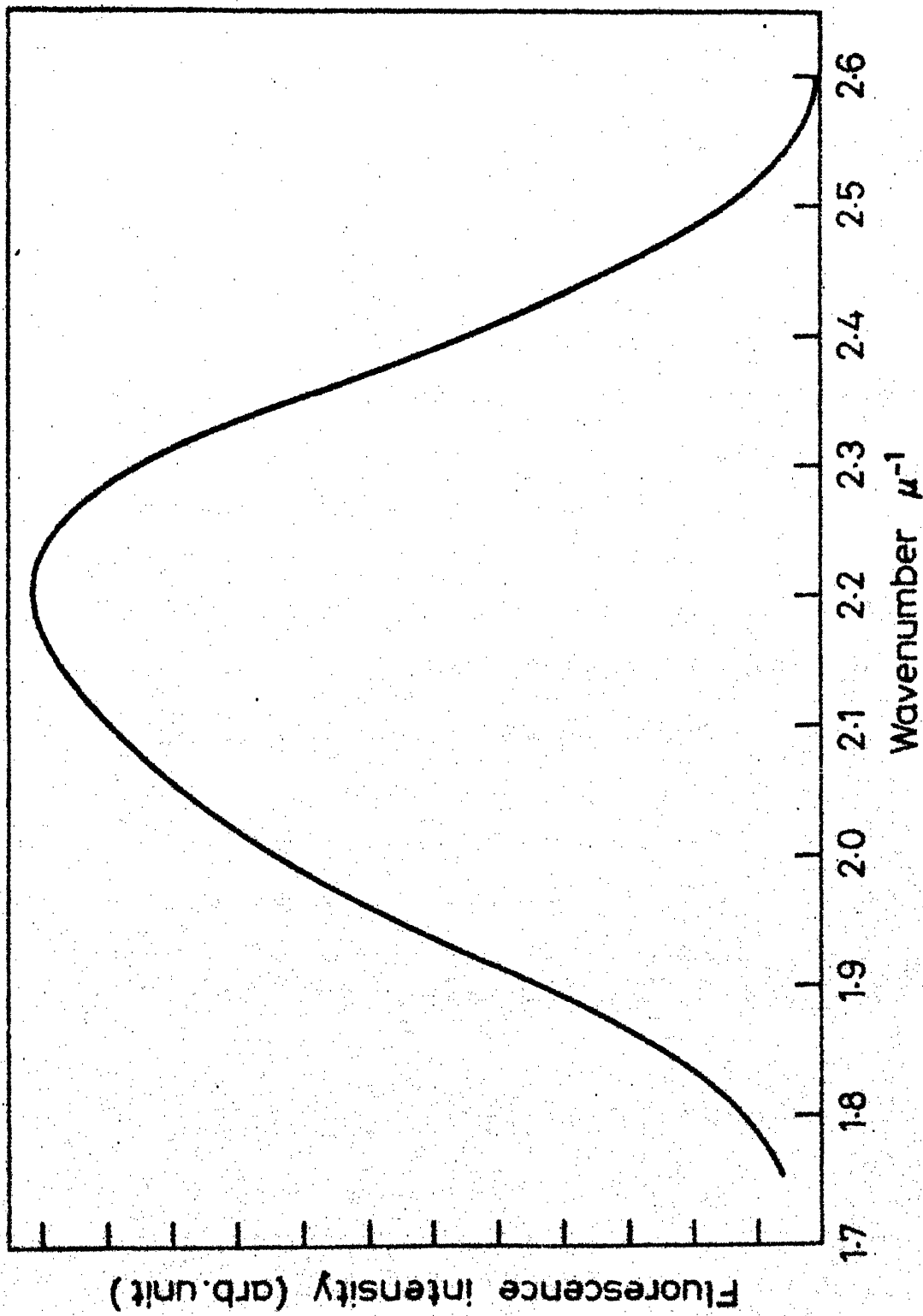
Fig. 2.6 Corrected Fluorescence spectrum of Quinine Sulphate (1×10^{-5}M in 0.1N H_2SO_4)

Fluorescence intensity (arb.unit)

Wavenumber μ^{-1}

Toshniwal pH meter model C144A. Standard buffer solutions were used for the calibration of the pH meter. Absorptiometric titrations were performed by a Toshniwal Spectrophotometer.

2.5 MATERIALS

2-Phenylbenzimidazole, 2-aminobenzimidazole, 2-hydroxybenzimidazole, 2-(o-aminophenyl)benzimidazole, 6-aminoindazole, 6-aminochrysine and 6-aminofluoranthene were obtained from Aldrich Chemical Company. These compounds were purified by repeated crystallisation from suitable solvents. O-Phenylenediamine was obtained from E-Merck, O-aminobenzoic acid, m-aminobenzoic acid and p-aminobenzoic acid were obtained from Sisco Research Laboratories.

AnalR grade sodium hydroxide, sulphuric acid, perchloric acid, hydrochloric acid and phosphoric acid were used as such. Spectrograde methanol from SD's, BDH and SD's spectrograde chloroform were used as such. GR grade Acetonitrile (E. Merck), ether, dioxane, heptene and cyclohexane (obtained from BDH) were purified as suggested in literature[69] and brief description of the method is given.

Cyclohexane was passed twice through an 11 mm diameter, 50 ml column fitted with 40g silica gel (60-120 mesh) to remove benzene, paraffinic hydrocarbons and carbonyl compounds. This was fractionally distilled over sodium at 80°C.

n-Heptane was mechanically shaken twice with conc. H_2SO_4 (12 hr each time), then for 1 hr each time with water, dil KOH and again with water. After standing over KOH for 24 hours, it was fractionally distilled.

Acetonitrile was further purified by fractional distillation over P_2O_5 at $81.5^{O}C$.

Ether was refluxed over $CaCl_2$, distilled, refluxed over sodium and fractionally distilled.

Dioxane was let stand over $FeSO_4$ for two days followed by refluxing for 6-8 hours with 1% HCl by bubbling nitrogen. It was made alkaline with KOH pellets, decanted the aqueous layer, refluxed over sodium and fractionally distilled under nitrogen atmosphere.

1-Methyl-2-benzimidazolinone was prepared[71] by refluxing equimolar ammounts of sodium carbonate, dimethyl sulphate and 2(3H)-benzimidazolone in acetone medium for 12 hours. It was extracted from heptane and recrystallised (m.p. $116^{O}C$) from methanol.

<u>2-(m-Aminophenyl)benzimidazole</u> was prepared[70] by heating at $250^{O}C$, an equimolar mixture of o-phenylenediamine and m-amino-benzoic acid in polyphosphoric acid medium for 6 hours. The resulting mixture was poured after cooling, in to large volume of water. The separated solid was washed throughly in an excess of 10% Na_2CO_3 solution and then by water. The dried crude product was recrystallised from alcohol (m.p. $256^{O}C$).

2-(p-Aminophenyl)benzimidazole was prepared by a similar
method by taking p-aminobenzoic acid and o-phenylenediamine
(m.p. 239°C).

2.5.1 Purity of Materials

All the compounds were checked for their purity by thin
layer chromatography and by taking u.v. spectra, in addition to
their sharp melting points which were in agreement with the
reported values.   IR spectra were taken for the compounds prepared
and these matched with literature spectra.[77] The fluorescent
compounds were further tested by their same emission maxima with
different excitation wavelengths.   The purity and transparency of
all the solvents were checked by their u.v. spectra taken using
triple-distilled water as reference.

2.6   Adjustment of H_o/pH/H_- values

pH of the solutions within the range 1-13 were adjusted by
small concentrations of phosphate buffer (10^{-3}M) as it was found
that they do not quench the fluorescence of the compounds and also do
not   alter the prototropic equilibrium under study.   Acetate
buffers were found to quench the fluorescence.   The total analyti-
cal concentration of buffers i.e. ($[H_2PO_4^-]$ + $[HPO_4^{2-}]$) was
maintained constant for each pH solution.

Hammett's acidity scale (H_o)[72] was used for the solutions with pH below 1. The Hammett's acidity and basicity scales represent the actual (or free) amount of protons or hydroxyl ions present which is found by their reaction with a weak base or a weak acid (indicator) respectively. Hammett's acidity scale modified by Jorgenson and Hartter[73] was used in this study. H_2SO_4 was used to obtain these H_o values.

A similar scale known as 'H_' scale for aqueous basic solutions constructed by Yagil[74] was used for measurements above pH 13.

2.7 Quantum yield calculations

The quantum yields of fluorescence $(\emptyset_f)$ of different compounds in different solvents were calculated relative to the commonly used fluorescence standards. Quinine sulphate[75] $(\emptyset_f = 0.55)$ in 0.1N H_2SO_4 having a λ_{max}(fluo) of 440 nm was used as a standard for compounds having a longer wavelength (~ 400 nm) fluorescence maxima. The excitation wavelength chosen was 313 nm. Anthracene $(\emptyset_f = 0.31)$ in ethanol was used for compounds having fluorescence maxima below 400 nm. The excitation wavelength chosen was 366 nm.

To avoid the absorption effects like concentration quenching, self absorption, attenuation of absorbance through the path length of light inside solution, dilute solutions were used for quantum yield measurements such that the absorbance was always about or

less than 0.1. Suitable wavelength was chosen for excitation where the absorption spectra had a flat region (maxima) to avoid errors due to a sharply varying absorbance in the finite band width of excitation. The optical densities of reference and test samples were always adjusted to the same or comparable values.

The formula used for the relative fluorescence quantum yield measurement is[76]

$$\emptyset_{(unknown)} = \emptyset_{(standard)} \times \frac{F_{(unknown)}}{F_{(standard)}} \times \frac{q_{(standard)}}{q_{(unknown)}} \times \frac{A_{(standard)}}{A_{(unknown)}}$$

where $\emptyset$ = Fluorescence quantum yield

F = Area under the fluorescence curve

q = Excitation light intensity at the excitation wavelength taken from the curve (Fig. 2.3)

A = Absorbance at the excitation wavelength.

EFFECT OF SOLVENTS ON ABSORPTION

AND FLUORESCENCE SPECTRA

3.1 Introduction

Platt's notation[78] is commonly used for specifying the electronic states of the condensed ring system and it uses the free electron model for classification of the spectra of cata-condensed hydrocarbons. According to his classification the two forbidden transitions A $\longrightarrow$ L_a and A $\longrightarrow$ L_b occur at the longest wavelengths. The state L_b is polarised along the longer axis of the molecule and L_a is polarised along the shorter axis and where A,B.....L,M correspond to the change in the orbital angular momentum, obtained from the orbital angular momentum quantum numbers based on above model. Although Platt's classification is not strictly applicable for the heterocyclic systems, like benzi-midazoles and indazoles, it has been observed that the spectrum of the heterocyclics have a general resemblance to the spectra of the corresponding fused-ring hydrocarbons, with the same number and disposition of rings (all six membered and aromatic),[79] hence a similar assignment has been made for these classes of molecules. It has been established that the ^1L_b band which is polarised along

the longer axis is almost localised on the carbocyclic ring of benzimidazole[80-82] and the ^1L_a band, which is polarised along the shorter axis, is localised along the heterocyclic ring. It has also been found that ^1L_b is the longest wavelength transition band in both the molecules and in general is less polarised than the ^1L_a band system.

3.2 Effect of solvent on absorption and fluorescence spectra

Electronic transitions in organic molecules in presence of a solvent are energetically different from those in isolated molecules because the dipole forces and the hydrogen bond interactions are operative between the solute and the solvent molecules, both in ground and in the excited states. Depending upon the nature and the extent of solute-solvent interactions, the spectral shape, maxima and intensities of these transitions change. The nonequal solvent stabilization of the ground and of excited states cause shifts in the absorption and emission band maxima. The spectra in a nonpolar solvent, in which the intermolecular interactions are minimal, approximate the vapour phase spectra. In this chapter absorption and fluorescence spectra of various compounds in a series of solvents, with increasing polarity, are presented. The nature of spectral transitions and shifts in the band maxima are discussed in terms of various kinds of solute-solvent interactions. Frank-Condon principle is the most important and valid assumption in any discussion of electronic transitions. Representative

energy level diagrams of the ground and excited states are shown

in the figure 3.1. These figures illustrate the relative
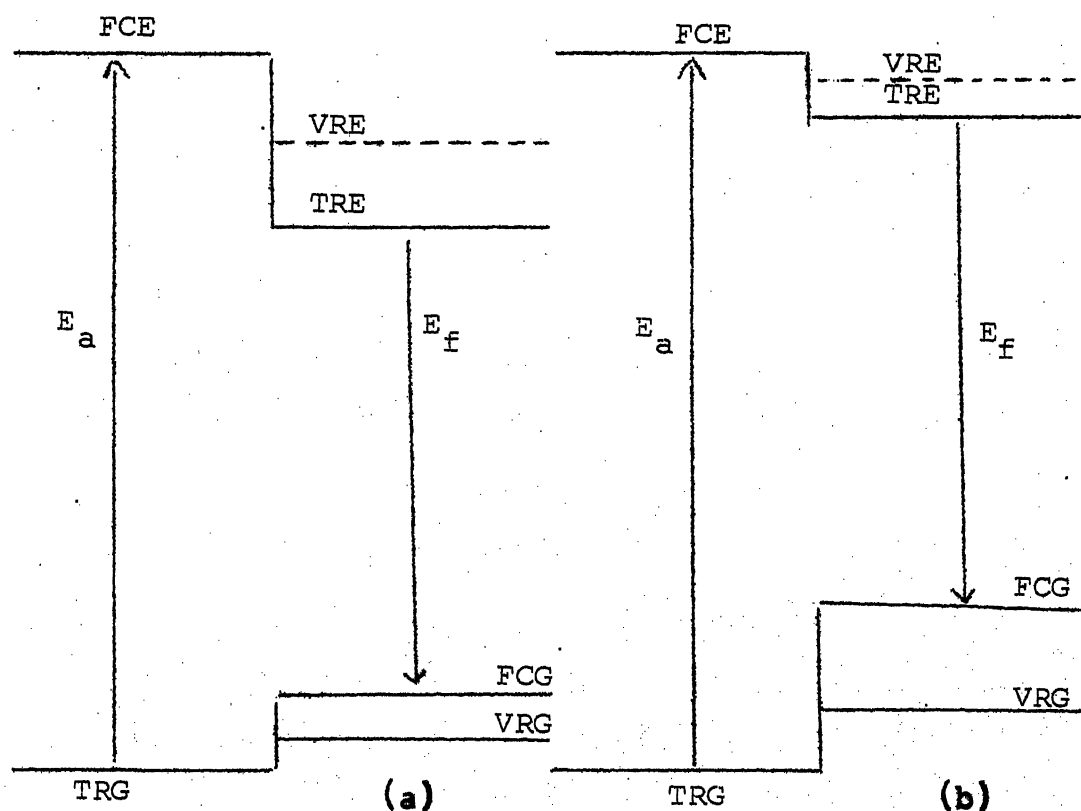
Fig. 3.1. Energy level diagram

magnitude of different kinds of relaxations in the ground and

electronically excited states. Fig. 3.1(a) represents a molecule

in which dipole moment increases and Fig. 3.1 (b) a molecule in

which the dipole moment decreases, upon excitation. In the above

diagram, E_a and E_f are the spectral absorption and fluorescence

energies, FCE and TRE, the energies of the Frank-Condon and

thermally relaxed excited states respectively, FCG and TRG are the

corresponding energies for the ground states, VRE and VRG are the

energies of thermally relaxed FC excited states and ground states when vibrational relaxation is the only thermal relaxation mechanism (i.e. if the fluorescence is measured in a rigid matrix so that solvent relaxation is impossible in the excited state). Thermal relaxation include vibrational, solvent and geometry relaxation.

Fig. 3.1(a) closely resembles the behaviour of the compounds selected in this study, because in all the compounds $\pi \to \pi*$ is the lowest energy transition, which is accompanied by a large increase in dipole moment. Before electronic excitation, the molecule is in a thermally equilibrated ground state solvent cage (TRG). On excitation, due to rapidity of electronic transition, the molecule in the excited state with a consequent different charge distribution, finds itself in the ground state solvent environment (FCE). Reorientation of solvent cage, or making and breaking of solvent bonds takes place within a time period of $10^{-14} - 10^{-12}$ seconds to bring the molecule to TRE. As normal lifetime of the excited state is much longer ($\sim 10^{-8}$ sec), fluorescence normally occurs from TRE. Upon fluorescence, the molecule comes to FCG where the molecule in the ground state has an environment of excited state solvent cage. Subsequent thermal relaxation brings the molecule back to TRG. The FCE is higher in energy than the TRE, and TRG is lower than FCG. Therefore, fluorescence occurs often at considerably longer wavelengths than expected purely on the basis of vibrational relaxation in polar solvents or on the basis of excitation wavelength.

Solvent interactions with solute molecules are predominantly electrostatic and may be of dispersive or hydrogen bonding type. Dispersive interaction includes induced dipole-induced dipole, dipole-induced dipole or dipole-dipole type. All these interactions lead to a net stabilization of the ground and excited states. As has been said earlier, there is an increase in dipole moment of a molecule under investigation, $\pi \rightarrow \pi*$ being the lowest energy excited singlet state, there will be a greater lowering of the energy of F.C. excited state, relative to ground state and thus, the fluorescence spectra of the molecules tend to show a greater wavelength dependence on solvent polarity than the absorption spectra. Due to this, larger redshift will be observed in fluorescence spectrum than in absorption under the above condition. The converse is true if the polarity of the solvent decreases upon excitation.

Hydrogen bonding interactions can be of hydrogen bond donor or hydrogen bond acceptor type. In hydrogen bond donor interaction there is an electrostatic interaction of a positively polarised hydrogen atom of the solvent with the lone pair of electrons on a basic atom in the solute and this results in lowering of energy. If in an electronic excitation process, there is a charge migration towards this basic center, hydrogen bond donor interaction will stabilize the electronic state and this will result in a red shift in absorption and fluorescence spectra with increasing hydrogen bond donor capacity of solvents. Conversly, if during excitation,

the electron density migrates away from the basic center, a blue shift is expected.

Hydrogen bond acceptor interaction is an electrostatic interaction between the lone pair of the solvent with the positively polarised hydrogen atom of the solute molecule. Hydrogen bond acceptor solvents cause red shift when solvating solutes at atomic sites which lose electron density in the FC excited state, and cause blue shift when solvating solutes at atomic sites which gain electron density in the FC excited state. Normally the trend in the shifts of absorbance and fluorescence band maxima with increasing solvent polarity are the same as long as the transition state involved are same. If an opposite trend is observed it may be due to the interaction of solvents at different sites of the solute molecule.

A combination of all kinds of interactions i.e. dispersive, hydrogen bond donor and hydrogen bond acceptor, may be present at the same time and their effects may be similar or opposite to one another. Hence a careful observation of absorption and fluorescence spectra in different solvents is necessary in order to obtain information about the redistribution of charge densities at different centers of the molecule in the excited state as well as to ascertain the presence of specific kind of interaction although it is not simple.

In this chapter an analysis of the shapes and the shifts in absorption and fluorescence spectra of a set of ten compounds, consisting of two amino hydrocarbons, 6-aminoindazole and seven substituted benzimidazoles, in a series of solvents with varying polarity and hydrogen bond donor/acceptor ability, have been carried out. All the molecules except the amino hydrocarbons have more than one basic center and one partially positive pyrrolic hydrogen which can have electrostatic interactions (both dispersive and hydrogen bonding type) with the solvent molecules. It has been tried to determine the nature and the site of the more predominant interactions from absorption and fluorescence spectral shifts. Protonation and deprotonation are extreme cases of hydrogen bonding. The nature of the spectral shifts in hydrogen bonding solvents can also throw some light on the site of protonation, discussed in Chapter 4.

3.3 Results and Discussion

3.3.1 6-Aminochrysene(CNH$_2$)[147]

---
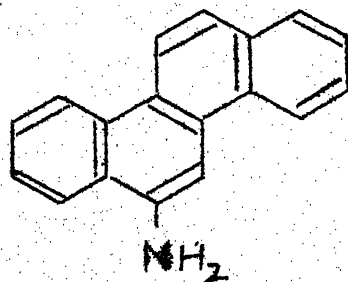
147. A.K. Mishra and S.K. Dogra, J. Photochem., <u>23</u>, 163 (1983).

Fig. 3.2 Absorption spectra of 6-aminochrysene in various solvents.

6×10^{-6} M, 298 K
— Cyclohexane
— Acetonitrile
— Methanol
— Ethanol
— Water (satd.)

Wavelength (nm) →

Absorbance

Fig. 3.3 Fluorescence spectra of 6-aminochrysene in various solvents.

6×10^{-6} M, 298 K

✕	Hexane
⊗	Acetonitrile
□	Methanol
△	Ethanol
●	Water (satd.)
○	Ho –5H$_2$So$_4$

λ (nm)
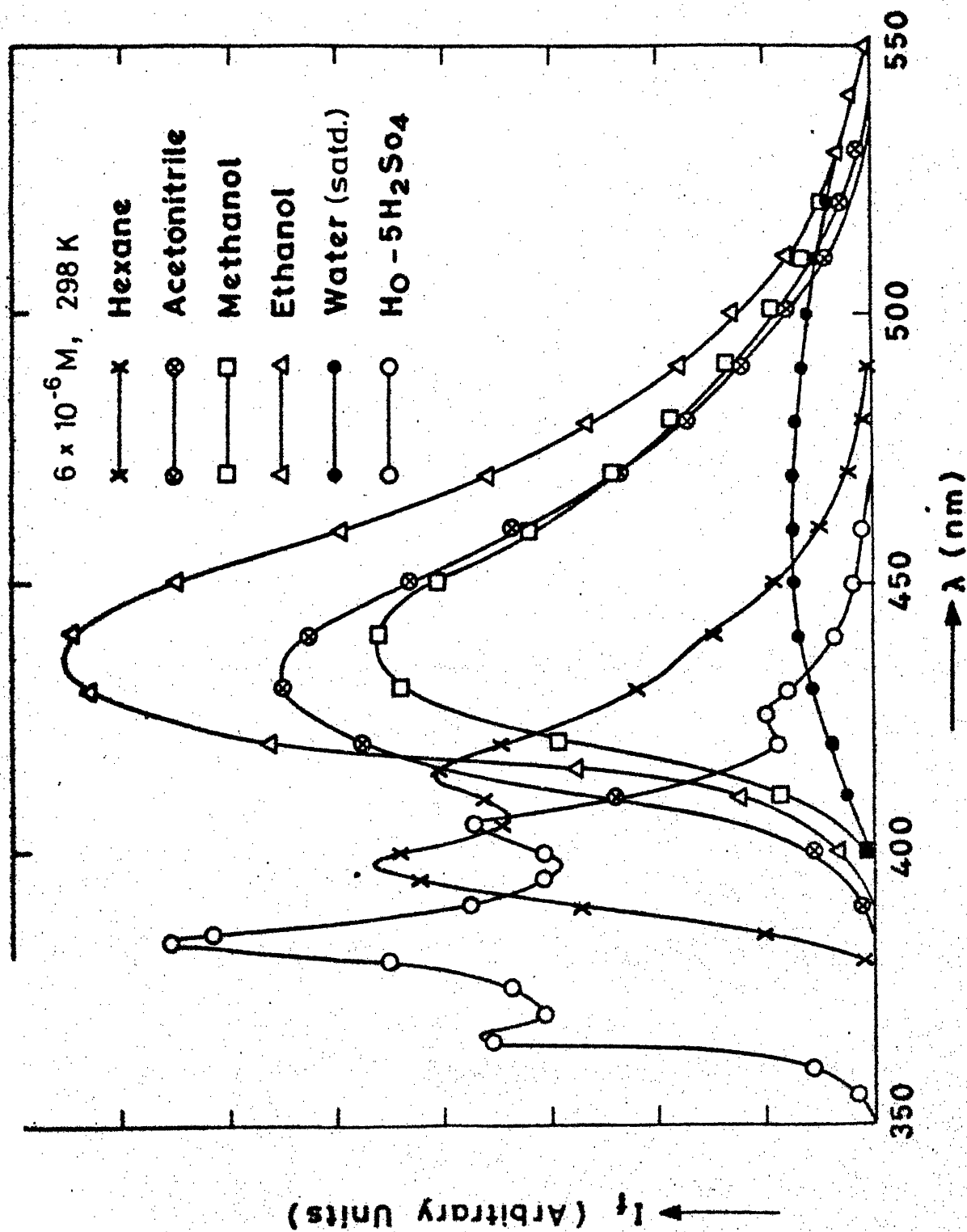
I$_f$ (Arbitrary Units)

Table 3.1.A. Absorption maxima and log ε_{max} of 6-aminochrysene in various solvents.

Solvent	λ_{max}(nm) (log ε_{max})			
Cyclohexane	228 (4.77)	242 (4.39)	276 (5.28)	338 (4.34)
Acetonitrile	228 (4.71)	242.5 (4.59)	276 (4.96)	341 (4.29)
Methanol	227 (4.72)	242 (4.59)	273 (4.96)	339 (4.29)
Ethanol	227 (4.71)	242 (4.58)	273.5 (4.96)	339 (4.28)
Water	–	233	273	340

Table 3.1.B. Fluorescence maxima and $\emptyset_f$ values of
6-aminochrysene in various solvents.

Solvent	λ_{max}(nm)			$\emptyset_f$ (λ_{exc}=340 nm)
Cyclohexane	398	414	440	0.28
Acetonitrile		430		0.20
Methanol		440		0.18
Ethanol		436		0.25
Water		470		0.16

The absorption spectra of CNH_2 in different solvents are presented in Fig. 3.2. The values of absorption maxima in different solvents alongwith molar extinction coefficients are listed in Table 3.1. Owing to the low solubility of CNH_2 in water, the absorption spectrum was taken in a saturated solution. The fluorescence spectra in different solvents are given in Fig. 3.3 and the values of fluorescence maxima ($\lambda_{max}^{(flu)}$) with quantum yields ($\emptyset_f$) are given in Table 3.1. The long wavelength absorption band is broad in all the solvents as compared to the structured spectrum of chrysene.[83] In particular it is very broad in water and accurate estimation of $\lambda_{max}^{(abs)}$ is difficult. The fluorescence spectrum in hexane is structured, but the structure is lost as the polarity and hydrogen bonding ability of the solvent increases. This loss of structure in the absorption and fluorescence spectra of the parent molecule is due to the perturbation of the π cloud of the ring by the lone pair of the nitrogen atom of the amino group. This is confirmed by the absorption and fluorescence spectra of CNH_3^+ (where the lone pair of the amino group is hindered), which are structured and blue shifted as compared to the spectra of CNH_2 and resembles those of the parent chrysene[83] molecule.

Owing to the broadness of the 338 nm absorption band there is no observable effect on $\lambda_{max}^{(abs)}$, but the 276 and 242 nm absorption bonds are slightly blue shifted with increasing polarity and hydrogen bonding ability of the solvents. However a continuous red shift in the fluorescence maxima and a decrease in the

fluorescence quantum yield was observed under the above conditions. The fluorescence spectra of CNH_2 in water is much broader and more red shifted than that in the other solvents.

The amino group attached to the chrysene ring possesses bi-functional characteristics. It can accept a proton from hydrogen donating solvents to form a hydrogen bond with the lone pair, thus producing a blue shift compared with cyclohexane, and it can also donate a proton to the hydrogen acceptor solvents, which results in a red shift compared with cyclohexane. Although it is very difficult to draw any conclusion regarding the solvent interaction with the solute molecule from the effect of solvents on the 338 nm absorption band, the effects on the 276 and 242 nm bands as well as on the absorption spectra of the protonated species (Ch.4, Fig. 4.1), which is an extreme case of hydrogen bond formation, clearly show that only the hydrogen bond donor interaction of the solvent with the lone pair are predominant in the ground state. However, the red shift observed in the fluorescence spectra, on changing the solvent from cyclohexane to water, shows that in the excited state, the availability of the lone pair for hydrogen bond formation is markedly reduced by a greater charge transfer interaction of the lone pair of the amino group with the ring i.e. the amino group acts as a hydrogen atom donor group. The decrease in the quantum yield of fluorescence under the above conditions can be explained by a similar mechanism.

3.3.2 3-Aminofluoranthene (FNH_2)[148]
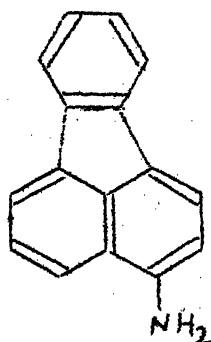
Fluoranthene molecule belongs to the nonalternant class of hydrocarbons with 1-, 2-, 3-, 7-, and 8- positions being non-equivalent. But it can be visualised as two alternant hydrocarbons joined by two essentially single bonds and thus the electronic transitions can also be regarded as arising from naphthalene and benzene moieties.

The $\lambda_{max}^{(abs)}$ along with log ε_{max} in each solvent have been listed in Table 3.2 and the spectra are given in Fig. 3.4. The ε_{max} in water could not be calculated as the absorption spectrum was observed in saturated solution due to less solubility. The $\lambda_{max}^{(abs)}$ and ε_{max} in cyclohexane and ethanol agree nicely with the literature values.[84]

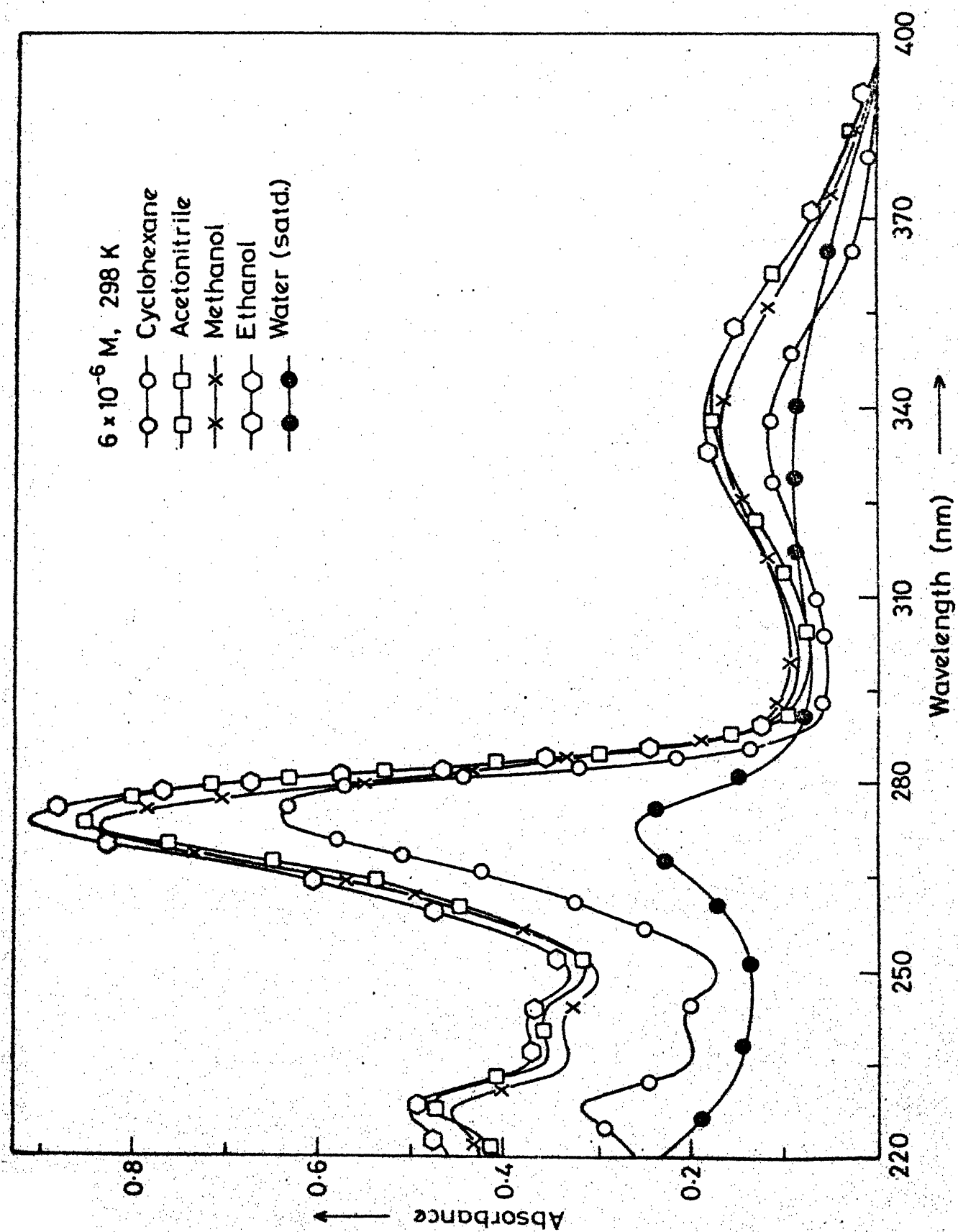148. A.K. Mishra and S.K. Dogra, J. Chem. Soc. Perkin Trans.II, in press.
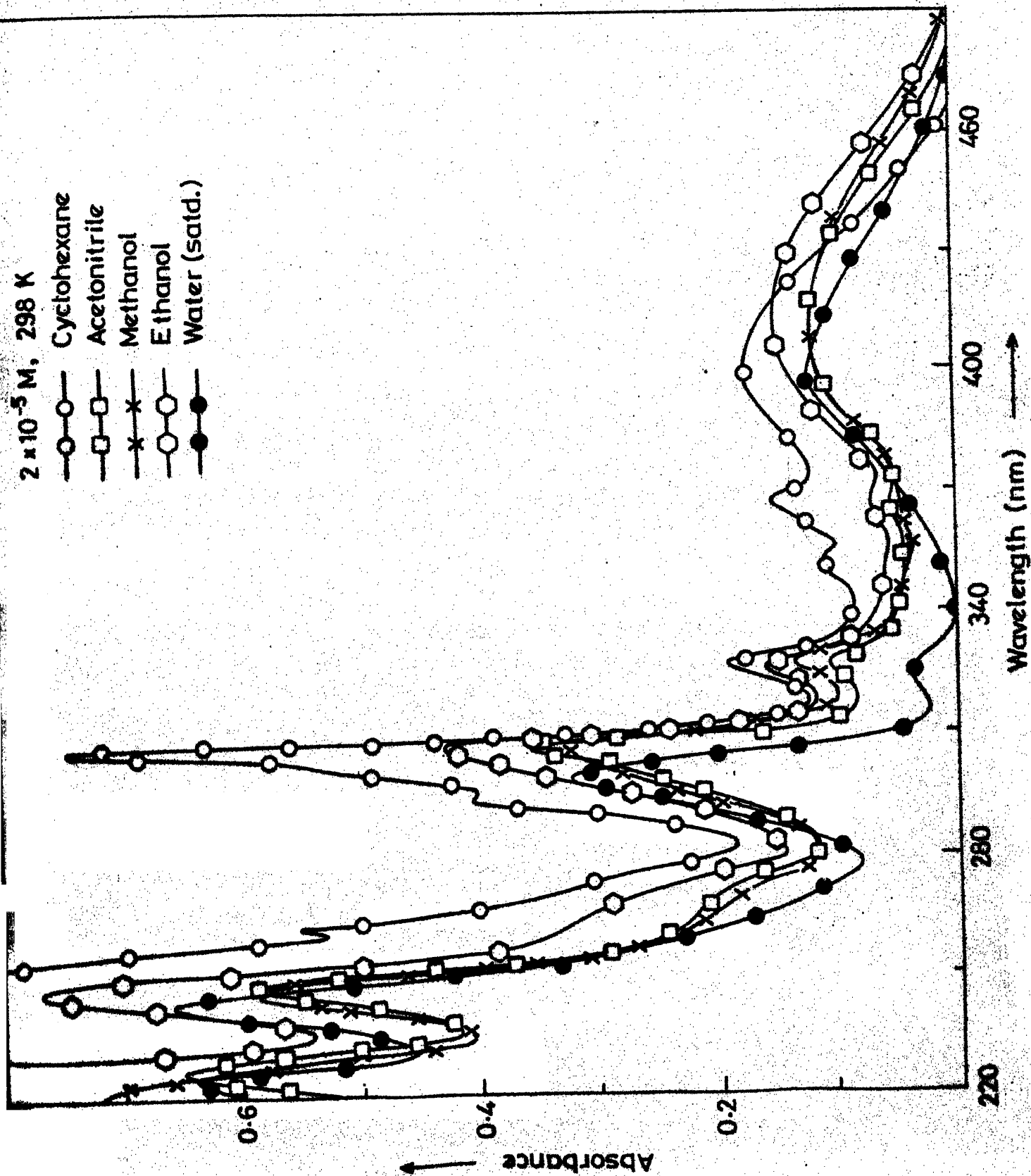
Fig.3.4 Absorption spectra of 3-aminofluoranthene in various solvents.
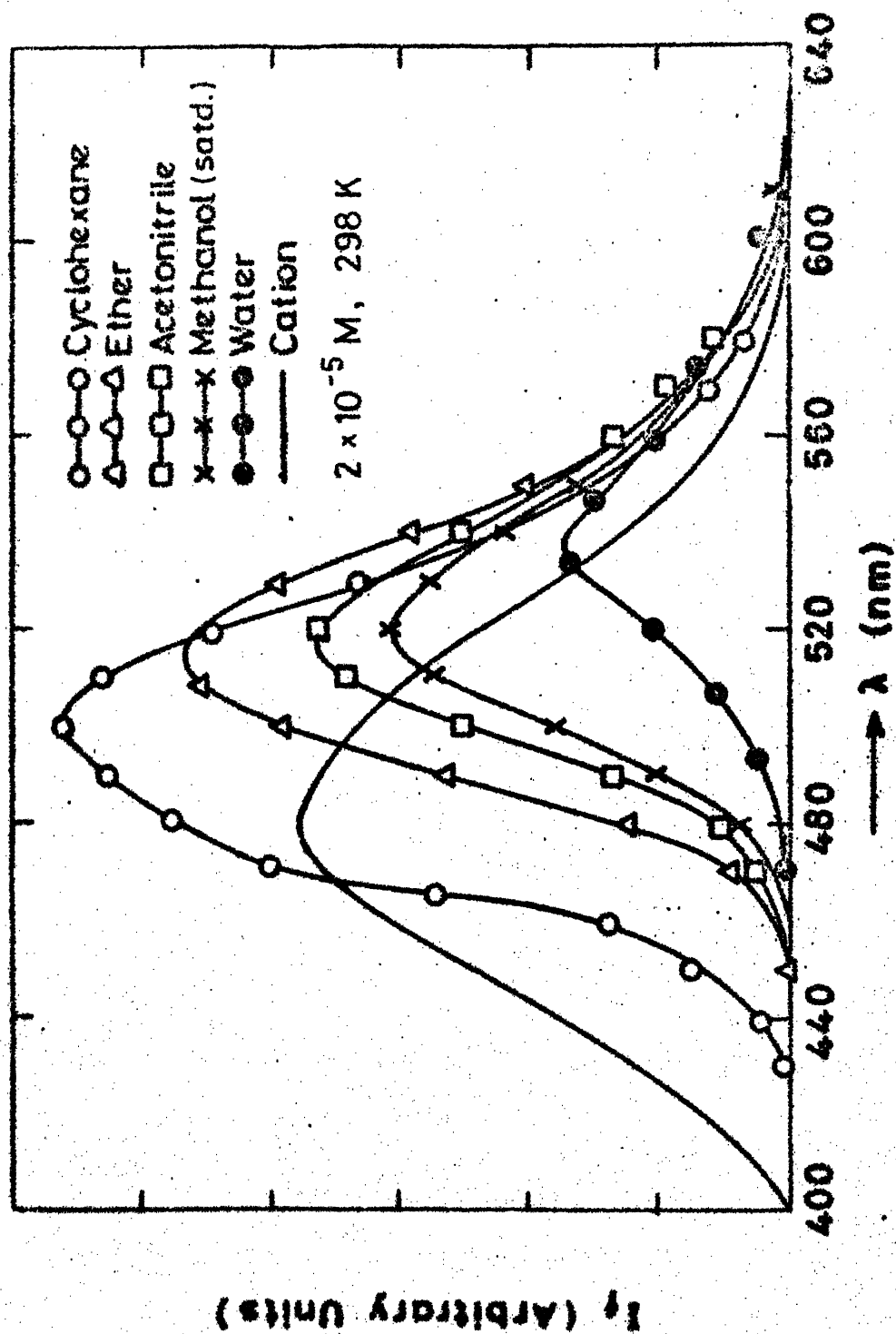
Fig.3.5 Fluorescence spectra of 3-aminofluoranthene in various
solvents.

Table 3.2.A. Absorption maxima and log ε_{max} of 3-amino-
fluoranthene in various solvents.

Solvent	λ_{max} (nm) (log ε_{max})						
Cyclohexane	225 (4.74)	245 (4.72)	292.5 (4.29)	305 (4.58)	327.5 (3.97)	368 (3.87)	398.5 (3.93)
Acetonitrile	225 (4.56)	245.5 (4.52)	293 (4.09)	305 (4.30)	326 (3.79)	368 (3.44)	414 (3.78)
Ether	227 (4.53)	246 (4.52)	293 (4.09)	307 (4.32)	327 (3.85)	368 (3.40)	420 (3.78)
Methanol	225 (4.54)	245 (4.50)		306 (4.25)	325 (3.84)	368 (3.50)	414 (3.81)
Ethanol	225 (4.60)	245 (4.59)		306.5 (4.34)	325 (3.91)	368 (3.55)	410 (3.88)
Water	220	244		300	325	366	406

Table 3.2.B. Fluorescence maxima and $\emptyset_f$ of 3-amino-
fluoranthene in various solvents.

Solvent	λ_{max}(nm)	$\emptyset_f$(λ_{exc}=410 nm)
Cyclohexane	500	0.222
Ether	515	0.218
Acetonitrile	518	0.170
Methanol	520	0.145
Ethanol	520	0.155
Water	535	0.150

The data of Table 3.2 indicate that except for the first transition, the other transitions are hardly affected by the change in the polarity or the change in the hydrogen bond interaction of the solvents. The first transition is red shifted in all the solvents as compared to the cyclohexane one. This red shift is maximum in ether i.e. hydrogen bond accepting solvent and decreases as the hydrogen bond donating character of the solvent increases.

Table 3.2 gives the $\lambda_{max}^{(flu)}$ of FNH_2 along with the fluorescence quantum yield $(\emptyset_f)$ and the spectra are given in Fig. 3.5. The spectra in ethanol agrees with the literature value.[85] Unlike absorption spectra, there is a regular bathochromic shift in $\lambda_{max}^{(flu)}$ and decrease $\emptyset_f$ as the polarity and the hydrogen bond formation tendency of the solvent increases, whereas on protonation, the fluorescence maxima is blue shifted. As has been stated earlier, the amino group can act as hydrogen acceptor as well as hydrogen donor. Thus a blue shift in the former and a red shift in the latter should be observed in the spectral properties. It has been shown by Thulstrup et al.[85] that the first transition in FNH_2 is long axis polarised whereas the second and third are short axis polarised. In FNH_2, the amino group is substituted along the longer axis of fluoranthene, it is quite expected that only the longer axis polarised transition will be affected more. The results indicate a similar behaviour. Acetonitrile and ether are only hydrogen accepting whereas methanol, ethanol and water can

behave both ways. Thus the red shift in absorption maxima in ether is quite expected. In methanol, ethanol and water, hydrogen bond donor effect also becomes operative which opposes the hydrogen bond acceptor and the dispersive interaction effect and thus a combined effect is expected to be observed. From the results in Table 3.2, it is clear that water is acting as a better hydrogen bond donating than hydrogen bond accepting solvent. On the other hand, the regular red shift in the fluorescence band maxima clearly shows that the amino group is behaving like a hydrogen donor species and this is in agreement with existing results that due to greater charge migration from the amino group to the aromatic ring in S_1 state, it behaves as a stronger acid in S_1 state than in S_0 state (see Chapter 4). The decrease in fluorescence quantum yield from cyclohexane to water can be explained on the same lines as has been done for 6-aminochrysene.

3.3.3   6-Aminoindazole (INH$_2$)
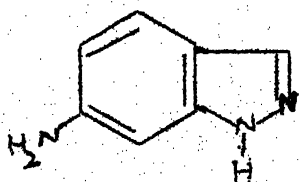
The absorption and fluorescence spectra of INH_2 are given in Fig. 3.6 and 3.7 respectively and the values of $\lambda_{max}^{(abs)}$, log ε_{max}, $\lambda_{max}^{(flu)}$, ϕ_f are listed in Table 3.3. The values of $\lambda_{max}^{(abs)}$ and ε_{max} in ethanol agree nicely with the literature value.[85a]

The absorption spectrum of INH_2 in each solvent is broader than that of parent molecule (indazole)[86] and each peak is slightly red shifted. Also unlike parent molecule $\lambda_{max}^{(abs)}$ is very slightly red shifted in hydrogen bond accepting but increasing polarity solvents, and blue shifted in solvents where hydrogen bond donor interaction is also there. The fluorescence spectrum of INH_2 is regularly red shifted with the increase in the polarity and hydrogen bonding ability of solvents as compared to cyclohexane or n-heptane. The bathochromic shift is more in the latter than in the former solvents. Similar to the explanation given before for aminohydrocarbons, it can be concluded from this spectral behaviour that the amino group acts as both proton acceptor and proton donor in the ground state (S_o) but only proton donor in S_1 state. Also, due to charge migration from amino group to the ring, the amino group becomes more acidic in S_1 than in S_o state.

From the data of Table 3.3 it can be seen that bathochromic shift in fluorescence maximum in methanol relative to n-heptane is quite large, indicating that the hydrogen bond between the solvent and solute is very strong and may actually result in a stoichiometric complex between the excited solute and solvent molecule. To supplement this idea, the fluorescence spectrum of
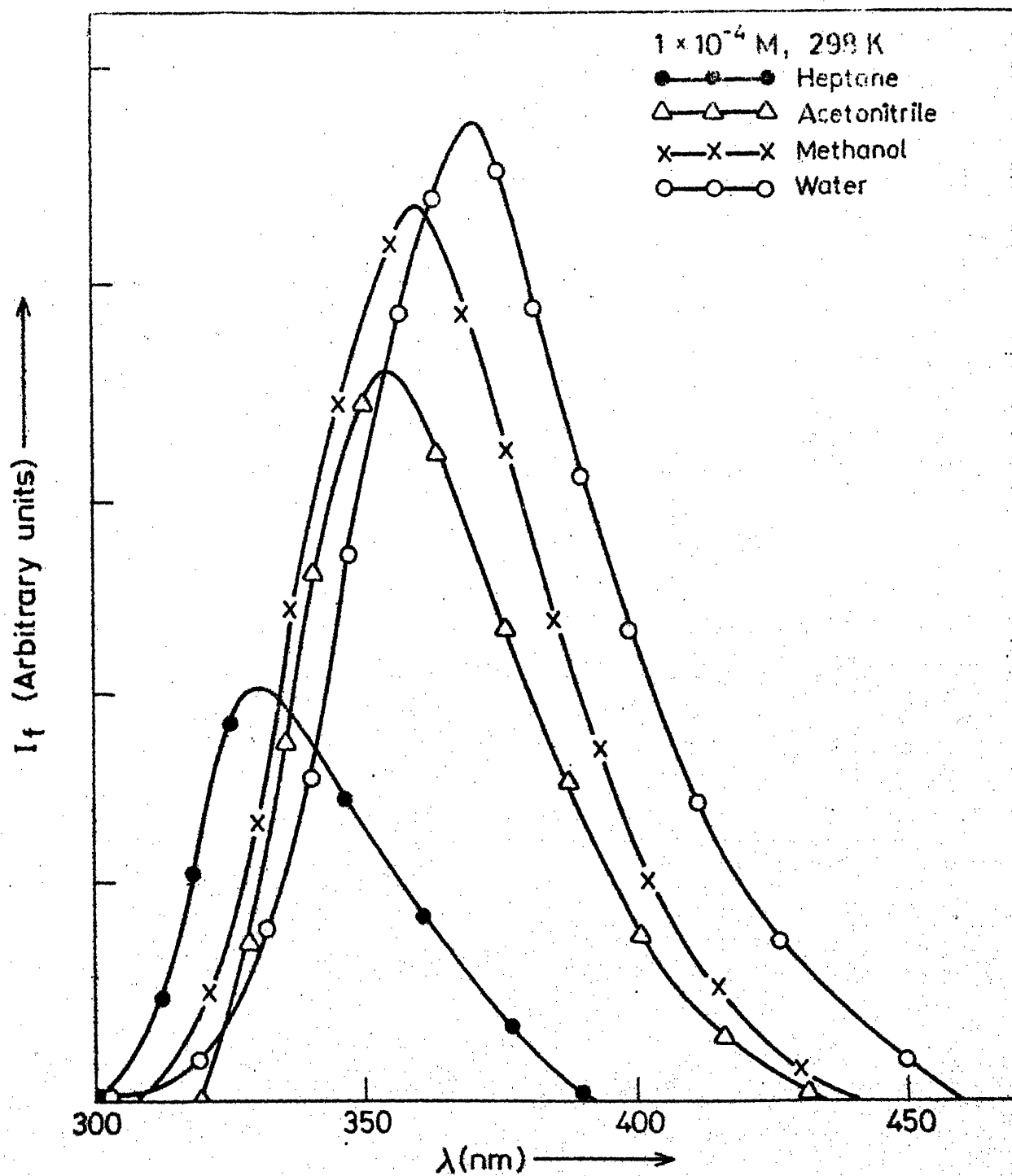
Fig.3.7 Fluorescence spectra of 6-aminoindazole in various solvents.

Table 3.3.A. Absorption maxima and log ε_{max} of 6-aminoindazole in various solvents.

Solvent	λ_{max}(nm) (log ε_{max})				
n-Heptane	216	230	255	274	295
Cyclohexane		230			295
Ether		230 (4.05)	268 (3.72)	276 (3.73)	298 (3.84)
Acetonitrile	217 (4.05)	229 (4.04)	267 (3.71)	275 (3.69)	300 (3.82)
Methanol		227 (3.91)	270 (3.71)	276 (3.71)	296.5 (3.82)
Ethanol		227 (3.84)	267 (3.71)	277 (3.71)	296 (3.82)
Water	210 (4.36)	225 (4.26)	275 (3.67)	289 (3.78)	294 (3.81)

Table 3.3.B. Fluorescence maxima and $\emptyset_f$ of 6-amino-
indazole in various solvents.

Solvent	λ_{max}(nm)	$\emptyset_f$(λ_{exc}=295 nm)
n-heptane	330	0.34
Cyclohexane	336	-
Ether	353	-
Acetonitrile	355	0.23
Methanol	360	0.27
Ethanol	365	0.32
Water	370	0.39

INH_2 in n-heptane, containing various proportions of methanol were recorded. The results indicated that addition of only 2% of methanol (v/v) to n-heptane produces a red shift in $\lambda_{max}^{(flu)}$ upto the extent of 2290 cm^{-1} whereas the fluorescence maximum shifted to 2530 cm^{-1} only, in 100% methanol.

3.3.4 2-Phenylbenzimidazole (PBI)[149]
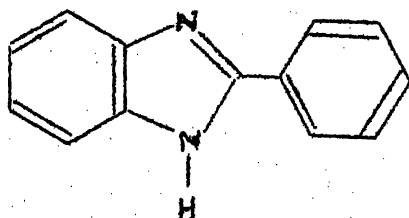
The absorption and fluorescence spectra in different solvents are shown in Fig. 3.8 and 3.9 respectively. The absorption and fluorescence maxima in ethanol match nicely with the literature value.[87,88] The absorption and fluorescence band maxima, log ε_{max} and $\emptyset_f$ are given in Table 3.4.

The absorption spectrum of PBI in cyclohexane is structured and the vibrational structure can be nicely explained with the vibrational frequency of 922 cm^{-1} in S_1 with the O-O band at 31545 cm^{-1} (317 nm). As expected, the structure is lost with the increase in the polarity or hydrogen bonding nature of the solvent.

149. A.K. Mishra and S.K. Dogra, Spectrochim Acta, 39A, 609 (1983).
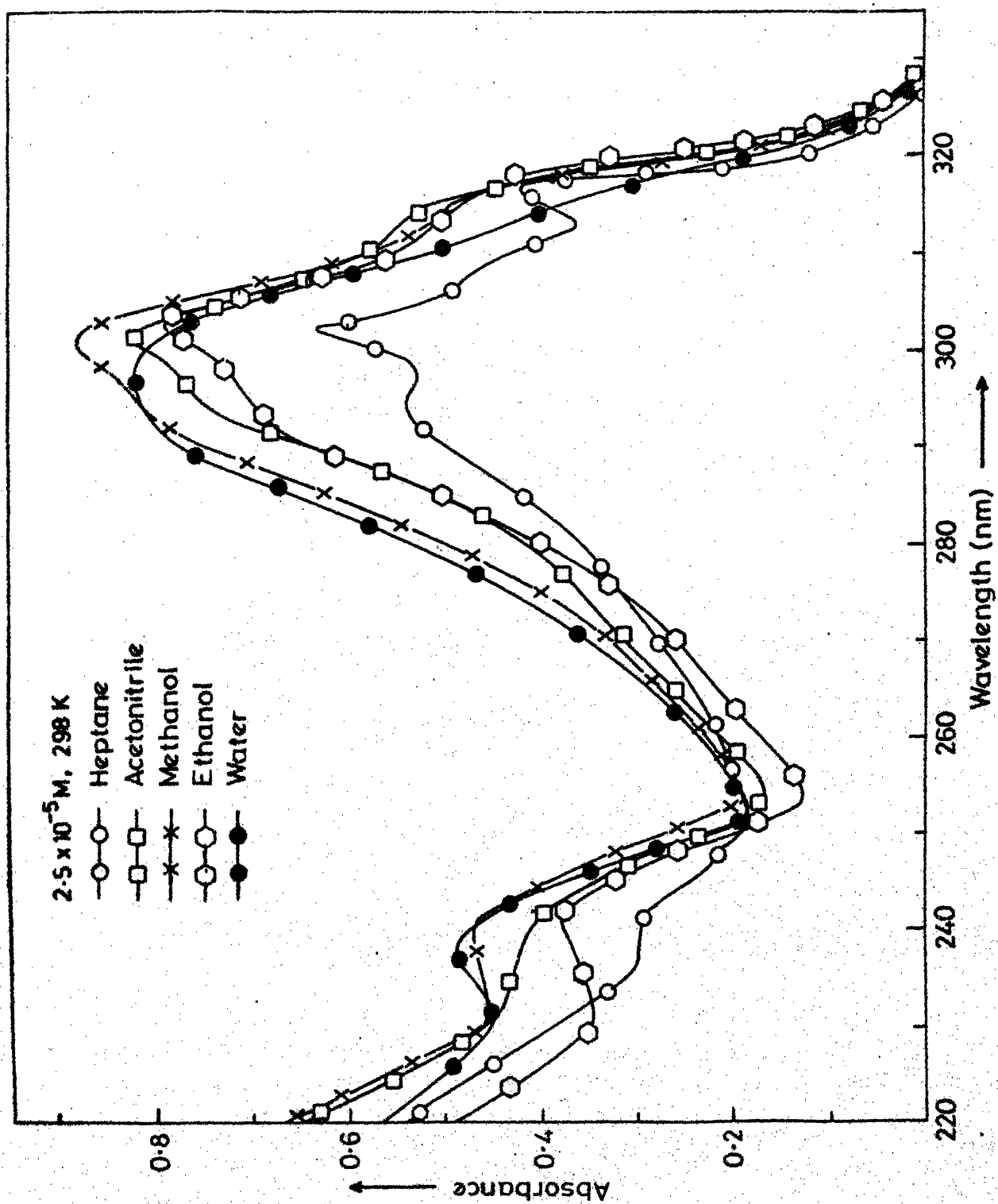
Fig.3.6 Absorption spectra of 2-phenylbenzimidazole in various solvents.
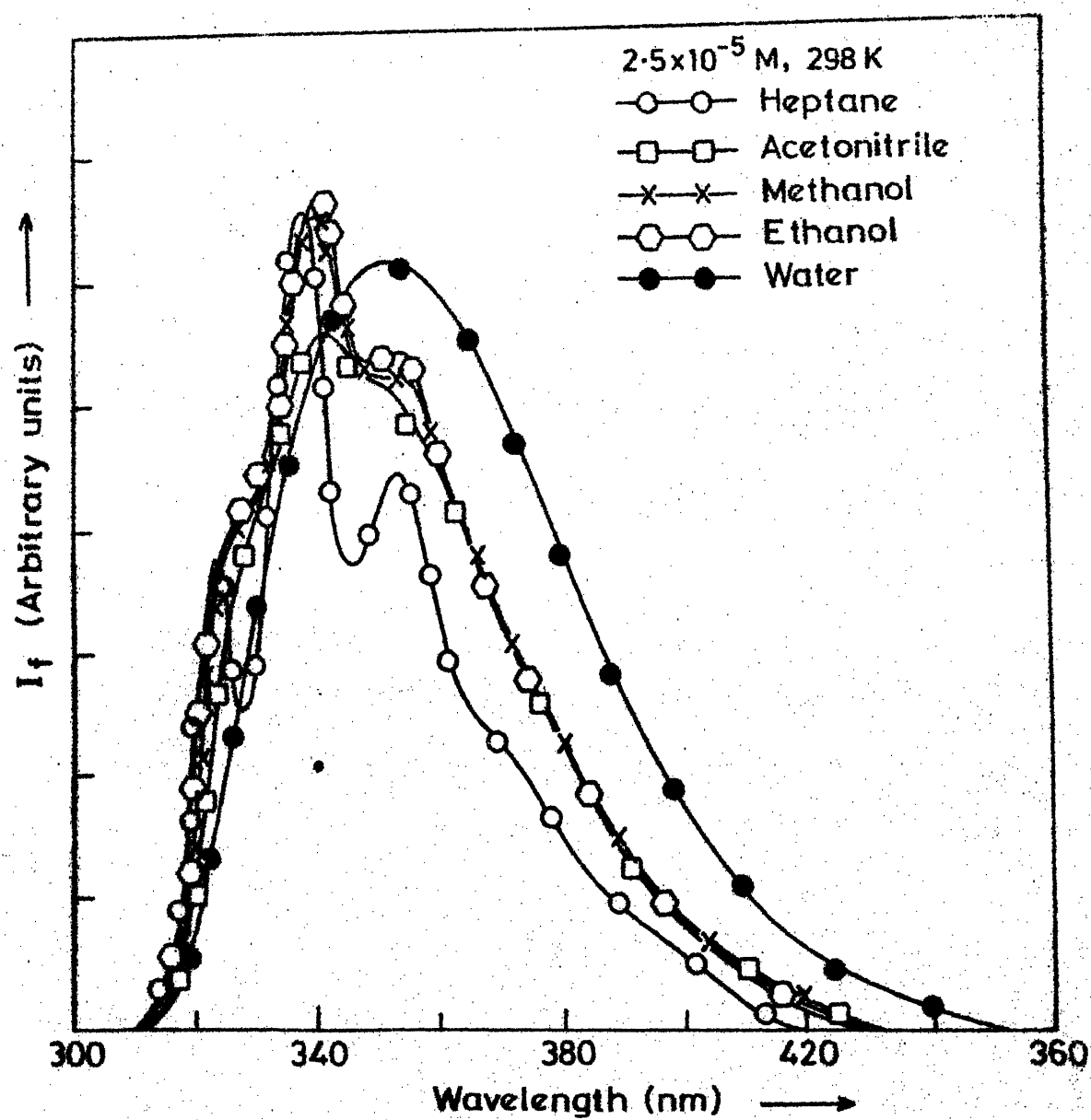
Fig.3.9 Fluorescence spectra of 2-phenylbenzimidazole in various solvents.

Table 3.4.A. Absorption maxima and log ε_{max} of 2-phenyl-benzimidazole in various solvents.

Solvent	λ_{max}(nm) (log ε_{max})							
Cyclohexane	230	240 (3.93)	248	291	295	302.5 (4.25)	308	317
Acetonitrile		240 (3.96)	248		294	301 (4.28)		314
Methanol		240 (4.10)	248		294	301 (4.39)		315
Ethanol		241 (4.04)	248		296	302.5 (4.36)		316.2
Water		238.2 (4.15)				299 (4.37)		

Table 3.4.B. Fluorescence maxima and $\emptyset_f$ of 2-phenyl-
benzimidazole in various solvents.

Solvent	λ_{max}(nm)					$\emptyset_f$ (λ_{exc}=300 nm)
Cyclohexane	321	336	352.5	367.5	387.5	0.11
Acetonitrile	327	342	357.5			0.11
Methanol	325	341	354.	375		0.10
Ethanol	324	341.5	360	372.5		0.11
Water			.360			0.13

The band maxima is slightly blue shifted on going from cyclohexane to water. This opposite behavior of the $\pi \to \pi^*$ transition in absorption spectrum with increase of polarity of solvent can be explained as follows. The solvent interaction is a kind of partial bond formation. Due to this, the phenyl ring rotates around the single bond and the conjugation with the BI ring decreases, thus resulting in a blue shift. Similar to absorption, the fluorescence spectrum in cyclohexane is nicely structured and can be explained by the vibrational frequency of 1391 cm^{-1} in S_0. The O-O band in cyclohexane is assigned to the shortest wavelength band of 31152 cm^{-1} (320 nm). This clearly indicates that the geometry of the molecule in S_0 state is retained in S_1. The coupling of vibrational frequencies with the electronic motion in S_0 and S_1 states respectively, are different because the electronic excitation can not change the vibrational frequency by such a large value of 468 cm^{-1}. The small red shift and the Stoke's shift (absorption maximum to fluorescence maximum) which shows an increase with increasing solvent polarity, can be due to a normal behaviour of $\pi \to \pi^*$ transitions. The quantum yields of PBI in different solvents, are nearly the same, indicating and as observed in fluorescence maxima shift that the given species does not have any specific interaction with any solvent.

3.3.5 2-Hydroxybenzimidazole(BIOH) (2(3H)-Benzimidazolone) and 1-Methyl-2-benzimidazolinone(NMeBI)
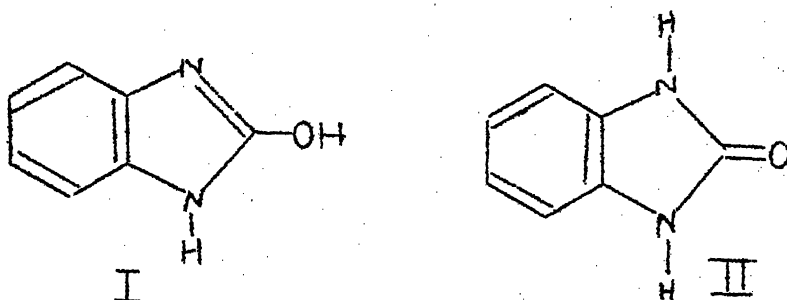
2-Hydroxybenzimidazole(I), due to tautomerism can also exist in the keto form i.e. 2(3H)-benzimidazolone(II) and it has been established from the following studies that it mainly exists in the latter form.[92-94,71] For example, alkylation or arylation by various procedures have always yielded N-methyl (or -aryl) rather than O-methyl (or -aryl) derivative,pK_a and absorption spectral study have clearly depicted the presence of keto form.[89,95] There are a couple of reactions,(e.g. chlorination by $POCl_3$ giving 2-chlorobenzimidazole etc.) which have indicated the presence of hydroxyl group in the molecule. Though there are some scattered studies carried out with absorption spectra in some solvents,[96,97] no systematic study has been carried out on the effect of solvents on the absorption and emission characteristics of the molecule.

The absorption and fluorescence spectra of BIOH in different solvents are given in Fig. 3.10 and 3.11 respectively. The absorption maxima with log ε_{max} and the fluorescence maxima with $\emptyset_f$ are
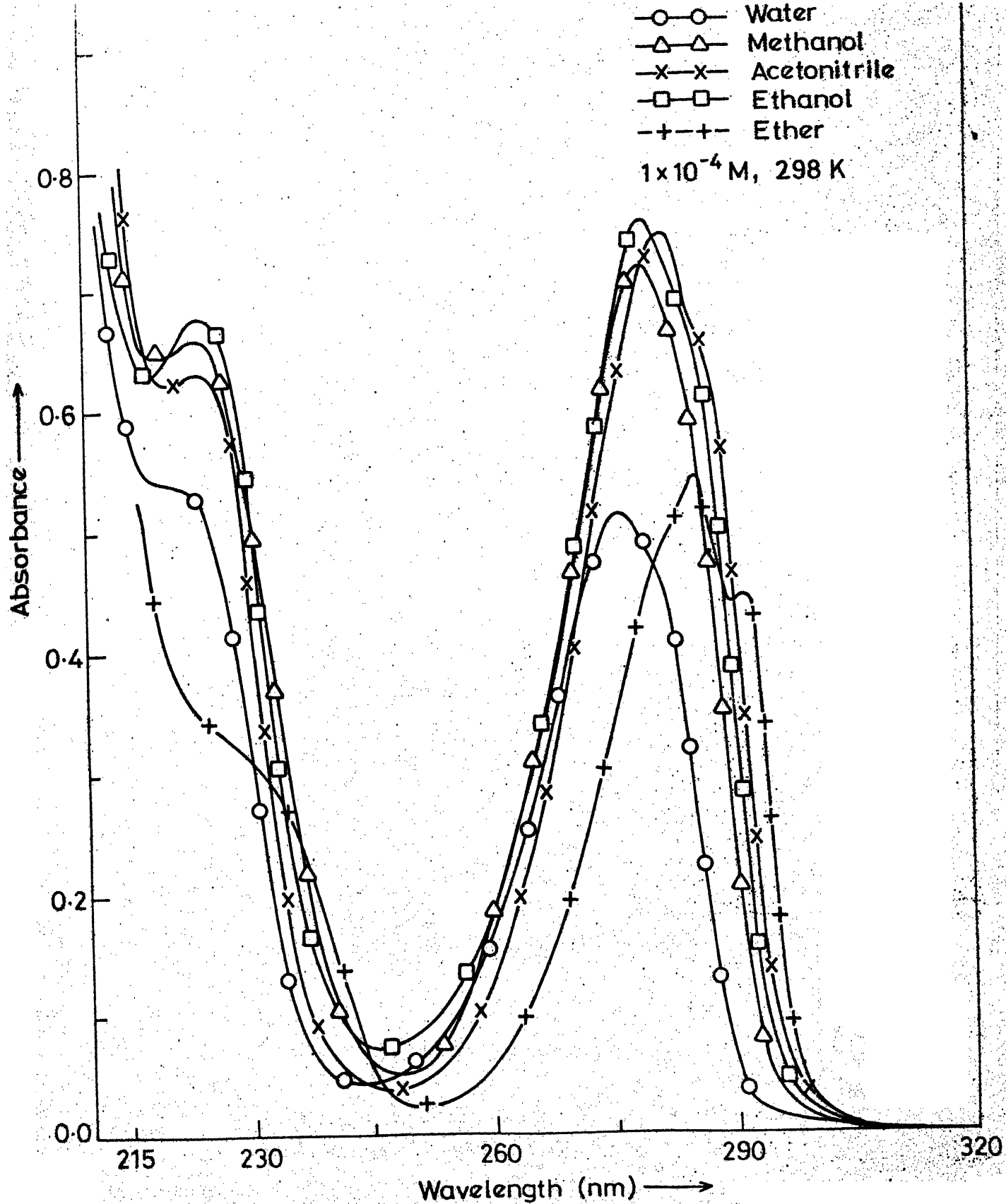
Fig. 3.1 Absorption spectra of 2-hydroxybenzimidazole in various solvents.
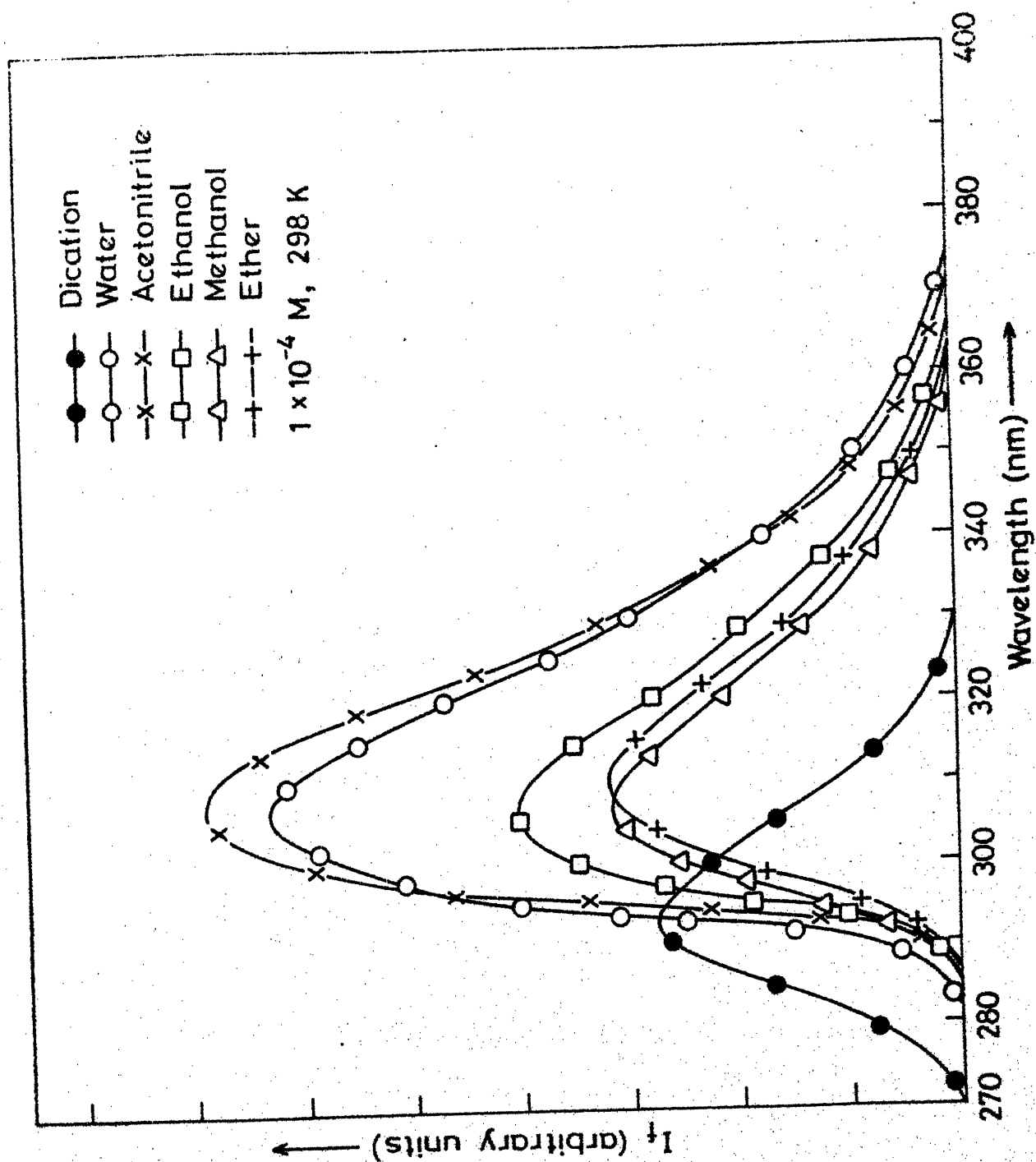
Fig. 3.11 Fluorescence spectra of 2-hydroxybenzimidazole in various solvents.

Table 3.5.A. Absorption maxima and log ε_{max} of 2-hydroxy-benzimidazole in various solvents.

Solvent	λ_{max}(nm) (log ε_{max})			
Ether	227 (3.70)	281	285 (3.73)	291
Acetonitrile	224 (3.83)		281.5 (3.89)	
Methanol	223 (3.85)		280 (3.90)	
Ethanol	223 (3.85)		281 (3.89)	
Water	222 (4.02)		275 (4.01)	

Table 3.5.B. Fluorescence maxima and $\emptyset_f$ of 2-hydroxy-
benzimidazole in various solvents.

Solvent	λ_{max}(nm)	$\emptyset_f$(λ_{exc}=280 nm)
Ether	310	-
Acetonitrile	307.5	0.36
Methanol	306.5	0.31
Ethanol	307.5	0.34
Water	305	0.44

given in Table 3.5. It has been reported by Efros et al[89] and Nuhn et al[90] that the ultraviolet spectra of benzimidazolone strongly resemble those of their N,N-dimethyl derivatives. The luminescence spectra of benzimidazolones show a fluorescence band at 300 to 350 nm.[91]

BIOH was completely insoluble in cyclohexane or n-heptane and hence the spectra could not be taken in a non-polar medium. Except in ether, the absorption spectra is broad and the long wavelength as well as the short wavelength band systems are slightlyblue shifted with increase in the polarity or hydrogen bond formation tendency of various solvents. The fluorescence spectrum, a broad band under the above circumstances also shows the same trend i.e. $\lambda_{max}^{(flu)}$ is blue shifted. The quantum yield and Stoke's shift [$\lambda_{max}^{(abs)}$ - $\lambda_{max}^{(flu)}$] increases slightly with the increase in hydrogen bond formation tendency of the solvents.

As said earlier, this molecule can be viewed as species I and II. In the former case, since hydroxyl group is an electron donating group, the L_a and L_b band systems of the benzimidazole molecule should be shifted bathochromically (predominantly the shorter wavelength L_a band) in comparison to parent molecule in any particular solvent. The results of Table 3.5 indicate that the longer wavelength band system is shifted bathochromically whereas the shorter wavelength one is shifted hypsochromically with respect to benzimidazole band systems in any one solvent.

The species II can be viewed as i) a benzene moiety with
two cyclic amino groups ortho to each other and (or) ii) a carbo-
nyl group with two amino groups similar to urea molecule. In the
former case, the two amino groups, being electron donors and
possessing charge transfer interaction property, will shift the
absorption band system localised on benzene molecule to longer
wavelength. The effects of these substitutions on 257 nm and
200 nm bands, originating from the benzene ring, can be calculated
with the relations given by Stevenson.[98] The values of these
absorption maxima are found to be roughly at 289 nm and 245 nm
respectively. Both the band systems agree with the experimental
values and the agreement would have been further better had the
BIOH molecule been soluble in nonpolar solvents, where the struct-
ure in the absorption spectrum (if there is any) is clearly noti-
ced. The absorption spectra of 1-methyl-2-benzimidazolinone in
different solvents is shown in Fig. 3.12 and the $\lambda_{max}^{(abs)}$ are
listed in Table 3.6. Fortunately, this derivative is soluble in
nonpolar solvents. Both the band systems show nice vibrational
pattern and is slightly red shifted with respect to BIOH(II), as
expected (methyl group being an electron donating group). The
vibrational frequencies taking part with the electronic motion
are 425 cm^{-1} and 770 cm^{-1} belonging to the benzene ring system,
thus confirming that both the bands are originating from the
benzene ring. This also helps in explaining theblue shift observed
in absorption spectra in the hydrogen donating solvent as compared
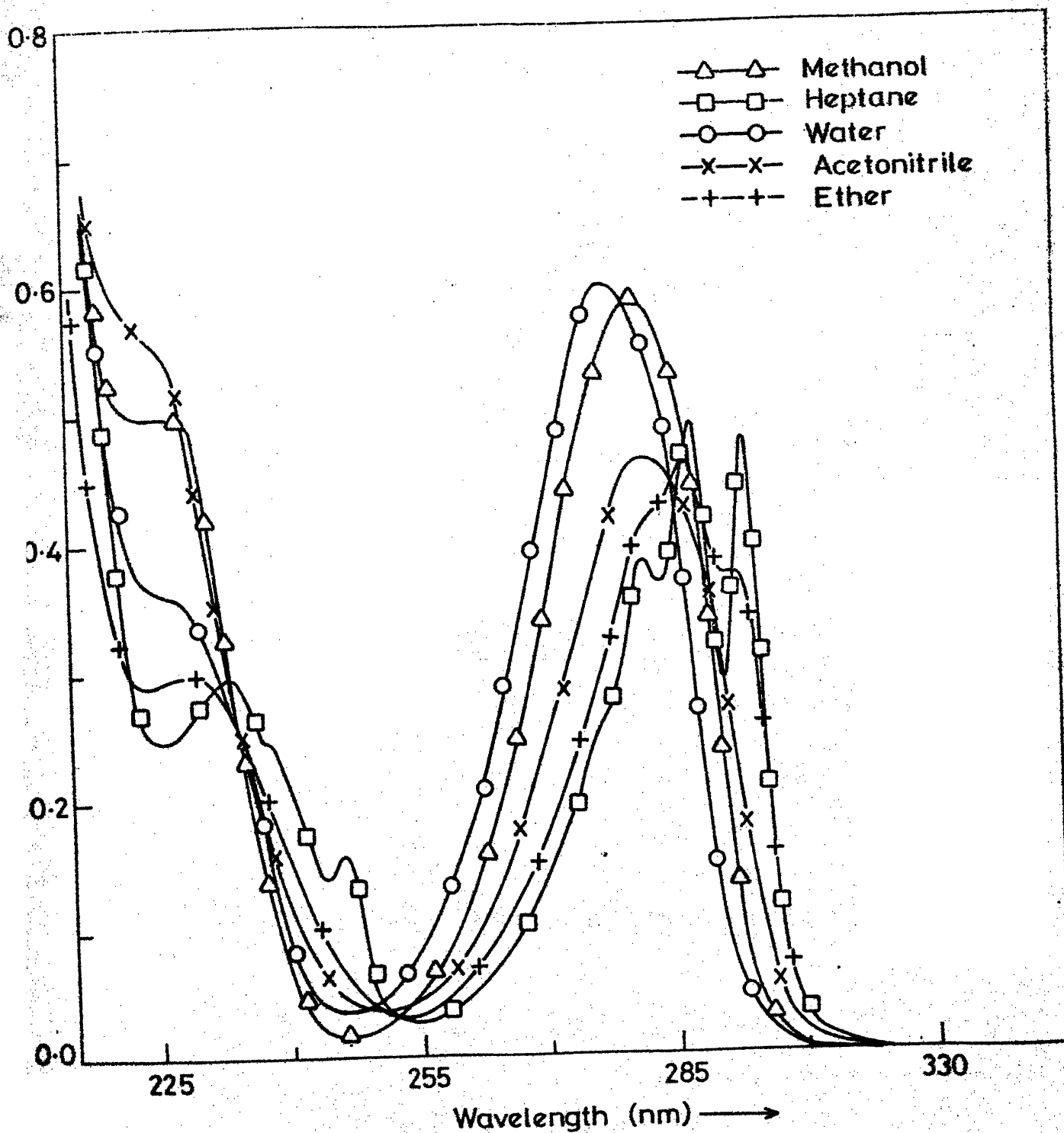
Fig.3.12 Absorption spectra of 1-methyl-2-benzimidazolinone in various solvents.

Table 3.6.A. Absorption maxima of 1-methyl-2-benzimidazolinone in various solvents.

Solvent	λ_{max}(nm)						
n-Heptane	233	237.5	246	276	281.5	287	293
Ether	228				283	287	292
Acetonitrile	227				282		
Methanol	226				280		
Water	224				278		

Table 3.6.B. Fluorescence maxima of 1-methyl-2-benzimida-zolinone in various solvents.

Solvent	λ_{max}(nm)
n-Heptane	312
Ether	308
Acetonitrile	312
Methanol	309
Water	310

to nonpolar one, because hydrogen bond forming solvents will stop the lone pairs of $\rangle\overset{..}{N}H$ groups in taking part in the charge transfer interaction as $\pi \to \pi^*$ is the lowest energy transition. If the species II is viewed as a second alternative, the origin of shorter wavelength band system can also be assigned to $n \to \pi^*$ transition of the carbonyl group having situation similar to urea to explain the observed blue shift in absorption spectra. But this band system in urea occurs at around 205 nm with much lower extinction coefficient. Thus the earlier conclusion seems more plausible.

The blue shift observed in the fluorescence spectra of BIOH in different solvents confirm the presence of species II in the first excited singlet state. Further, increase in the Stoke's shift, though not much with the increasing polarity and hydrogen bond formation tendency of solvents, indicates that the molecule is slightly more polar in S_1 than in S_0 state. The fluorescence spectrum of 1-methyl-2-benzimidazolinone in different solvents (Table 3.6) showing a similar trend and slightly red shifted as compared to BIOH in each solvent, also substantiate the earlier results.

All these results clearly show that: i) 2-hydroxybenzimidazole exists as species II, ii) both the absorption band systems originate from the benzene ring and iii) the cyclic $\rangle\overset{..}{N}H$ groups behave similar to amino group and affects the benzene transitions accordingly.

3.3.6 2-Aminobenzimidazole (BINH$_2$)
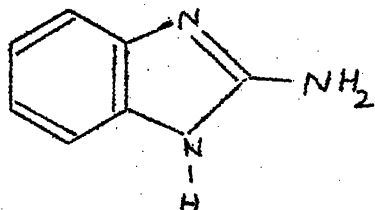
The absorption and fluorescence spectra of BINH$_2$ have been studied in different solvents except in heptane or cyclohexane where it was insoluble. The former have been shown in Fig. 3.13 and the latter in Fig. 3.14. $\lambda_{max}^{(abs)}$, log ε_{max}, $\lambda_{max}^{(flu)}$ and $\emptyset_f$ have been listed in Table 3.7. The doublet structure of long wavelength absorption band of benzimidazole[72] (271, 277 nm) molecule is lost in all the solvents and both the bands are red shifted as compared to the parent molecule. Both the band systems in absorption are blue shifted and the fluorescence band is red-shifted with increase in the polarity or hydrogen bonding ability of the solvents. The Stoke's shift increases under the above conditions, whereas the quantum yield decreases.

It has been shown by Tway and Love[61] that the transitions in benzimidazole molecule is of $\pi \longrightarrow \pi^*$ character and the absorption or fluorescence spectra is only slightly affected by the interactions of the solvent. Thus the effect of solvents on the

Fig.3.13 Absorption spectra of 2-aminobenzimidazole in various solvents.

Fig.3.14 Fluorescence spectra of 2-aminobenzimidazole in various solvents.

Table 3.7.A. Absorption maxima and log ε_{max} of 2-amino-
benzimidazole in various solvents.

Solvent	λ_{max} (nm) (log ε_{max})	
Ether	246 (4.07)	282.5 (4.06)
Acetonitrile	246.5 (4.00)	282.5 (4.01)
Methanol	242.5 (3.98)	281 (4.05)
Ethanol	245 (3.92)	281 (4.01)
Water (pH 7.5)	238 (3.92)	275 (4.02)

Table 3.7.B. Fluorescence maxima and $\emptyset_f$ of 2-amino-
benzimidazole in various solvents.

Solvent	λ_{max} (nm)	$\emptyset_f$ (λ_{exc}=280 nm)
Ether	310	–
Acetonitrile	312.5	0.31
Methanol	313.8	0.32
Ethanol	311.3	0.28
Water (pH 7.5)	319	0.025

spectra would be mainly due to their interaction with the amino group, which can act both as hydrogen bond acceptor and hydrogen bond donor. The results are quite similar to those observed for other arylamines as has been observed in CNH_2 and FNH_2.

It is known that in the substituted quinolines[38] excitation to the lowest excited singlet state results in the charge migration from the carbocyclic ring to the heterocyclic ring. Thus the presence of electron donating group ($-\ddot{N}H_2$) in the carbocyclic ring will substantially lower the energy of the excited state in comparison to that of the ground state. On the other hand, the electron donating group on the heterocyclic ring may raise, slightly lower or leave unchanged, the energy of the excited state, relative to the ground state, depending upon the magnitude of the stabilization energy from conjugation of the exocyclic amino group in the excited state in the aromatic system, relative to the magnitude of the stabilization energy resulting from repulsion of the lone pair of the amino group by the π cloud of the heterocyclic ring. The spectroscopic behaviour of $BINH_2$ can also be rationalized on the same lines because on comparing the absorption and fluorescence maxima of 2-aminobenzimidazole with those of 5-aminobenzimidazole,[61] the values of λ_{max} for the former are found to be lower than those of/the latter, thus establishing that the charge migration does take place in $BINH_2$ from carbocyclic ring to heterocyclic ring. Further, the results of the Table 3.7 also indicate that the amino group is acting as hydrogen bond acceptor in the ground state and hydrogen

bond donor in the first excited singlet state. The increase of Stoke's shift with the increase of polarity or hydrogen bonding capability of the solvents, confirms the finding of Tway and Love,[61] that $\pi \rightarrow \pi^*$ is the lowest energy transition in this molecule also.

3.3.7   2-(o-Aminophenyl)benzimidazole(oBNH$_2$)
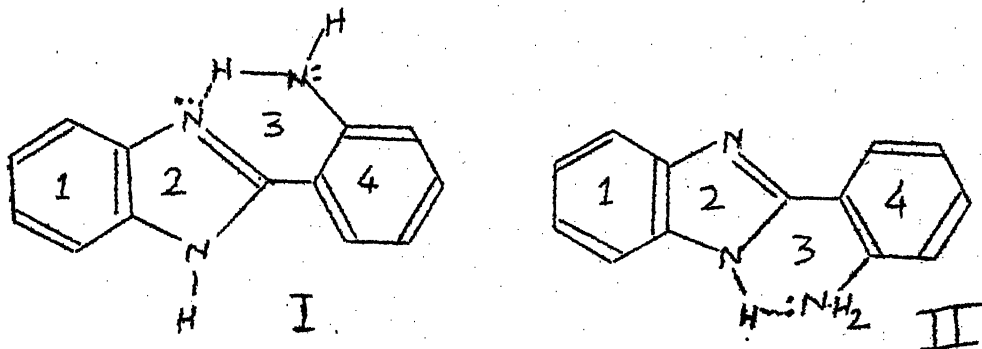
In this compound there can be a presence of intramolecular hydrogen bonding, leading to structure I (hydrogen atom of the amino group forming a bond with the pyridine nitrogen atom) or structure II (pyrrolic hydrogen atom forming a bond with the lone pair of the amino group), but both the structures form a sort of four membered condensed ring system. It does appear from the models that structure I is more stable than structure II. This could be due to the presence of lone pair of nitrogen atom and amino hydrogen atom in the same plane, thus the ring 3 formed is in the same plane as 1,2 and 4, whereas the ring 3 formed in the structure II may not be in the same plane as 1,2, and 4 because of

the steric hinderance of the amino hydrogen atoms from other

hydrogen atoms and the amino group may develop a tetrahedral

structure. From the nature and shifts of absorption and fluores-

cence spectra in different solvents it has been tried to ascertain

the presence of structures I and II and their stability in differ-

ent medium.

The absorption spectra of $OBNH_2$ have been recorded in differ-

ent solvents and shown in Fig. 3.15. The $\lambda_{max}^{(abs)}$ and ϵ_{max} of

various bands have been recorded in Table 3.8. Unlike other

substituted derivatives of benzimidazole (possess two band systems,

one at 277 nm and the other at 240 nm) this compound has three band

systems and this can be attributed to the presence of intramolecular

hydrogen bonding thereby resulting in either structure I or struct-

ure II (i.e. the formation of four rings). The absorption spect-

rum in cyclohexane or in n-heptane is structured, including the

longest wavelength band, which is broad in all other solvents,

whereas the structure of the other bands is lost as the polarity

or the hydrogen bond formation capacity of the solvents increases

and the hypsochromic shift is quite large in water specially in

the longest wavelength band.

Fig. 3.16 indicates that the fluorescence spectra of $OBNH_2$

in different solvents, except in water, shows two broad bands.

The $\lambda_{max}^{(flu)}$ and $\emptyset_f$ of the two bands are listed in Table 3.8. The

data of Table 3.8, show that the short wavelength band gets red

shifted, whereas the long wavelength band gets blue shifted with
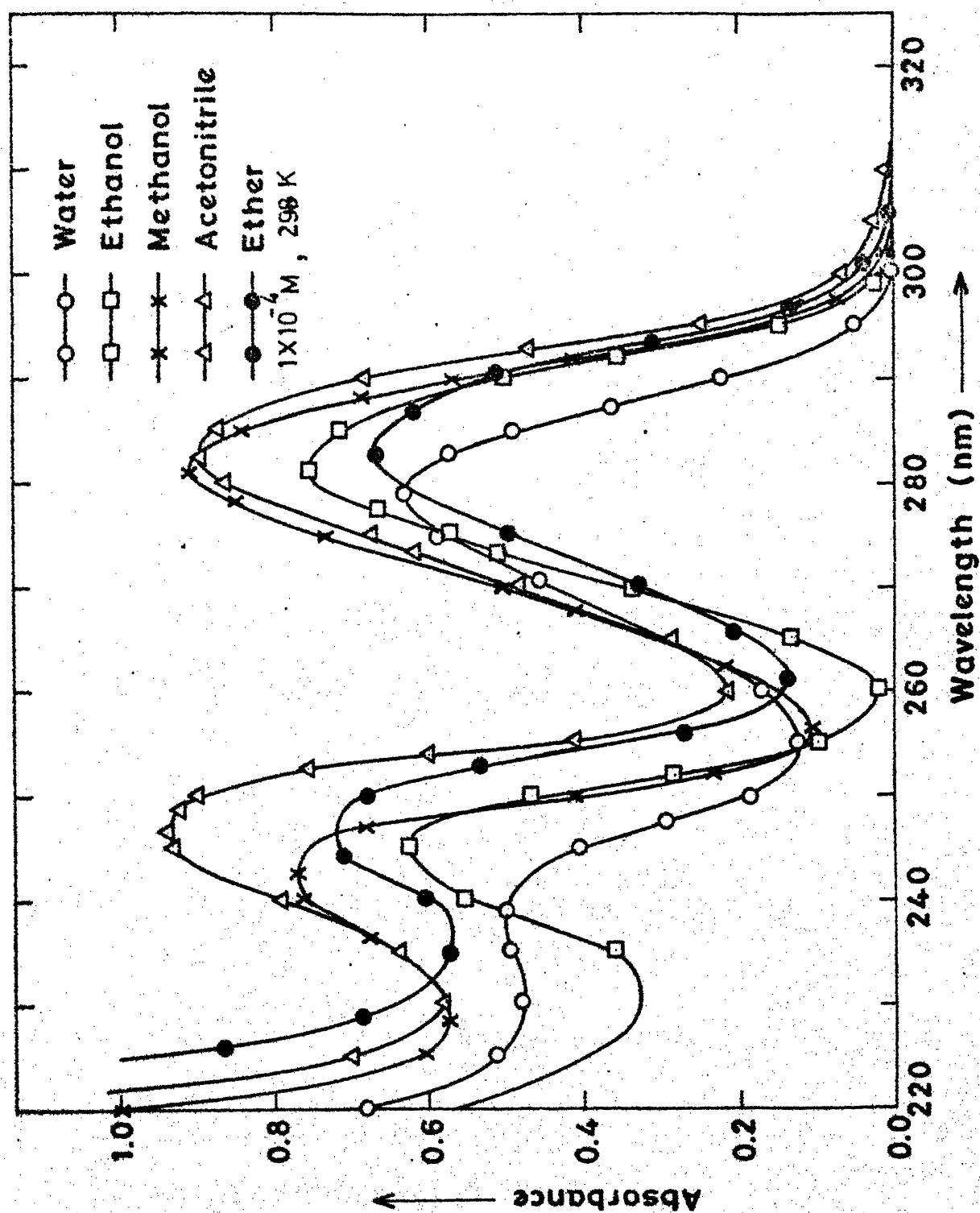
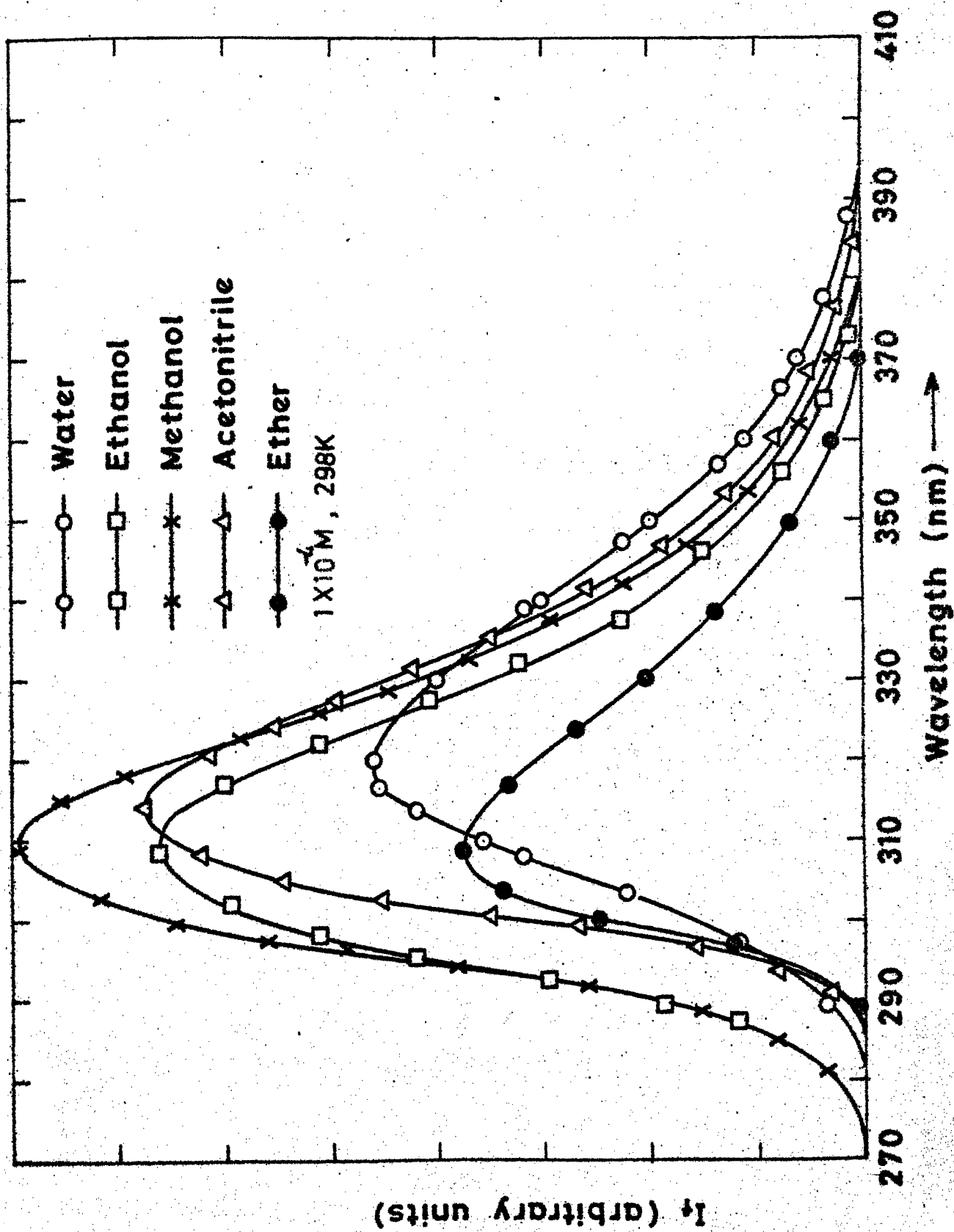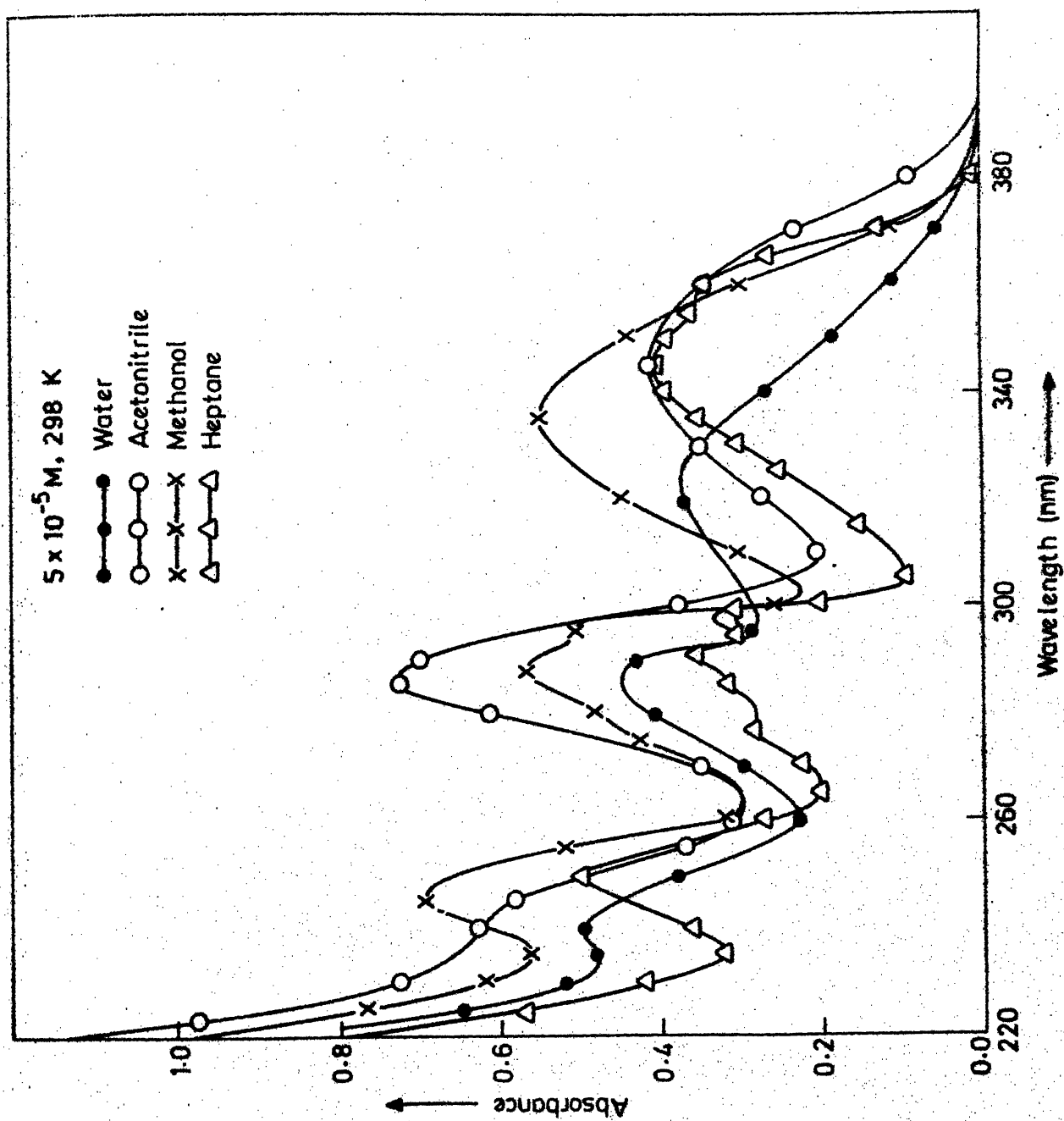Fig.3.15 Absorption spectra of 2-('o-aminophenyl)benzimidazole in various solvents.
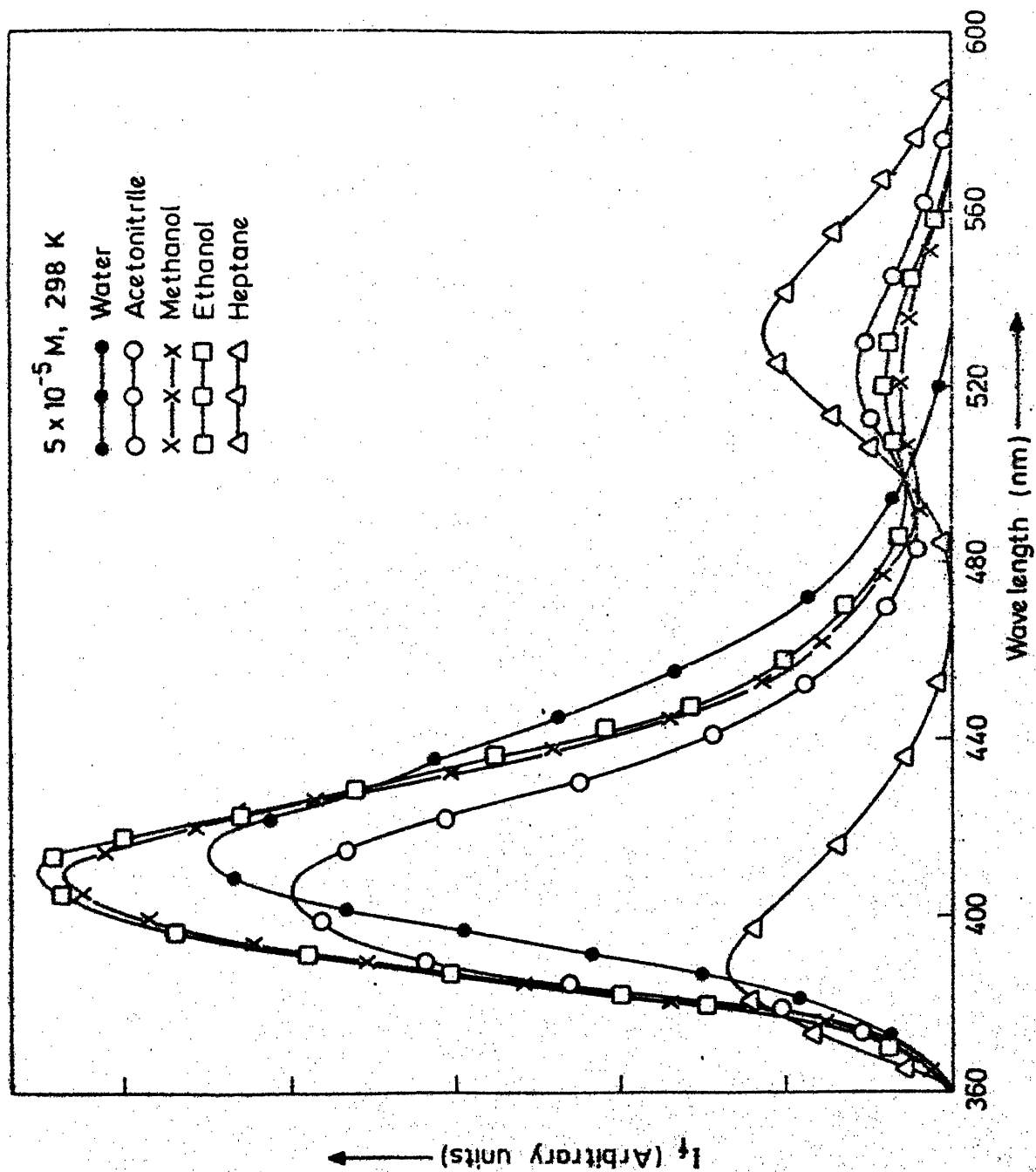
Fig.3.16 Fluorescence spectra of 2-(o-aminophenyl)benzimidazole in various solvents.

Table 3.8.A. Absorption maxima and log ε_{max} of 2-(o-aminophenyl)-
benzimidazole in various solvents.

Solvent	λ_{max} (nm) (log ε_{max})							
Cyclohexane	228 (4.64)	250 (4.01)	277 (4.05)	286	290 (4.13)	297 (4.16)	345 (4.19)	359
Ether	223 (4.70)	251 (4.32)	275		290 (4.20)	298 (4.30)	345 (4.17)	
Acetonitrile	222 (4.43)	242 (4.01)		286 (3.91)			344 (3.97)	
Methanol	222 (4.48)	246 (4.00)	270	287.5	294 (3.95)		335 (3.92)	
Ethanol	221 (4.45)	249 (3.99)	270	290	297 (3.95)		341 (3.95)	
Water	218 (4.70)	240 (4.33)			286 (4.27)		320 (4.18)	

Table 3.8.B. Fluorescence maxima and $\emptyset_f$ of 2-(o-aminophenyl)-benzimidazole in various solvents.

Solvent	λ_{max}(nm)	$\emptyset_f(\lambda_{exc}=345\text{ nm}^*)$	λ_{max}(nm)	$\emptyset_f(\lambda_{exc}=345\text{ nm}^*)$
Cyclohexane	390	0.014	530	0.013
n-Heptane	390	0.014	530	0.013
Ether	407	–	523	–
Acetonitrile	407	0.093	520	0.012
Methanol	410	0.125	520	0.008
Ethanol	413	0.126	520	0.008
Water	417	0.129	–	–

* Except water for which $\lambda_{exc}=320$ nm.

the increase in the polarity and hydrogen bond formation tendency
of the solvents. Further, under similar conditions, the fluores-
cence quantum yield of the former band increases whereas that of
the latter band decreases and the latter band in totally absent
in water. The fluorescence intensity ratio ($\frac{I_{530}}{I_{390}}$) of the two
bands is nearly equal in n-heptane and this ratio decreases in
going from n-heptane $\longrightarrow$ ether $\longrightarrow$ acetonitrile $\longrightarrow$ methanol (or
ethanol). Moreover the intensity ratio in methanol could be
achieved by adding only 2% methanol to n-heptane. It is also
observed that this intensity ratio of these bands in n-heptane
donot change within the concentration range 10^{-5} to 10^{-3}M of $OBNH_2$.
Whereas the intensity ratio (I_{530}/I_{390}) in n-heptane increases
(though small), with the increase in the wavelength of excitation
especially towards the red edge of the longest wavelength absor-
ption band.

The above results can be explained on the following lines:
The intramolecular hydrogen bond formation can take place either
between the pyridinic nitrogen atom and the hydrogen atom of the
amino group or between the lone pair of the amino group and the
pyrrolic hydrogen atom (structures I and II) as mentioned earlier.
Possibly the additional ring formation at the pyridinic center(I)
will be more stable due to somewhat increased planarity of this
ring as compared to structure(II), in which the hydrogen bonded
amino group will tend to develop a tetrahedral structure. In non-
polar medium both these structures are equally probable, being

present in a state of dynamic equilibrium (one can imagine only a small activation barrier between the two structures). Thus both the forms are present in ground as well as in the excited state. Relatively broad, slightly structured (showing two distinct peaks) longest wavelength absorption band in cyclohexane and n-heptane, actually is due to a superimposition of two bands, belonging to different forms of $OBNH_2$ because the uncorrected excitation spectra in n-heptane (Fig. 3.17) taken at emission wavelengths of 390 nm and 525 nm respectively, showed the presence of only one maxima in each case, agreeing with the respective long wavelength maxima in the absorption spectrum in n-heptane (345 nm and 359 nm), whereas the other short wavelength bands appeared at the same wavelength in both the cases (this confirm the earlier conclusion that species I is relatively more stable than species II). With the increase of hydrogen bonding ability of the solvents, the lone pair on the amino group of the structure I, gets progressively blocked due to hydrogen bonding with the solvent and it will be maximum with water. Thus the lone pair of the amino group is stopped from the participation of change transfer interaction of amino group and ring. This explains the large blue shift in the longest wavelength absorption band (which is due to the extra ring) as compared to the other absorption bands[99] (which are due to the benzimidazole moiety) in water as compared to other solvents. Further, the loss in the structure of the long wavelength band could be due to large hypsochromic shift of one band relative to other and thus the two bands mix with each other.
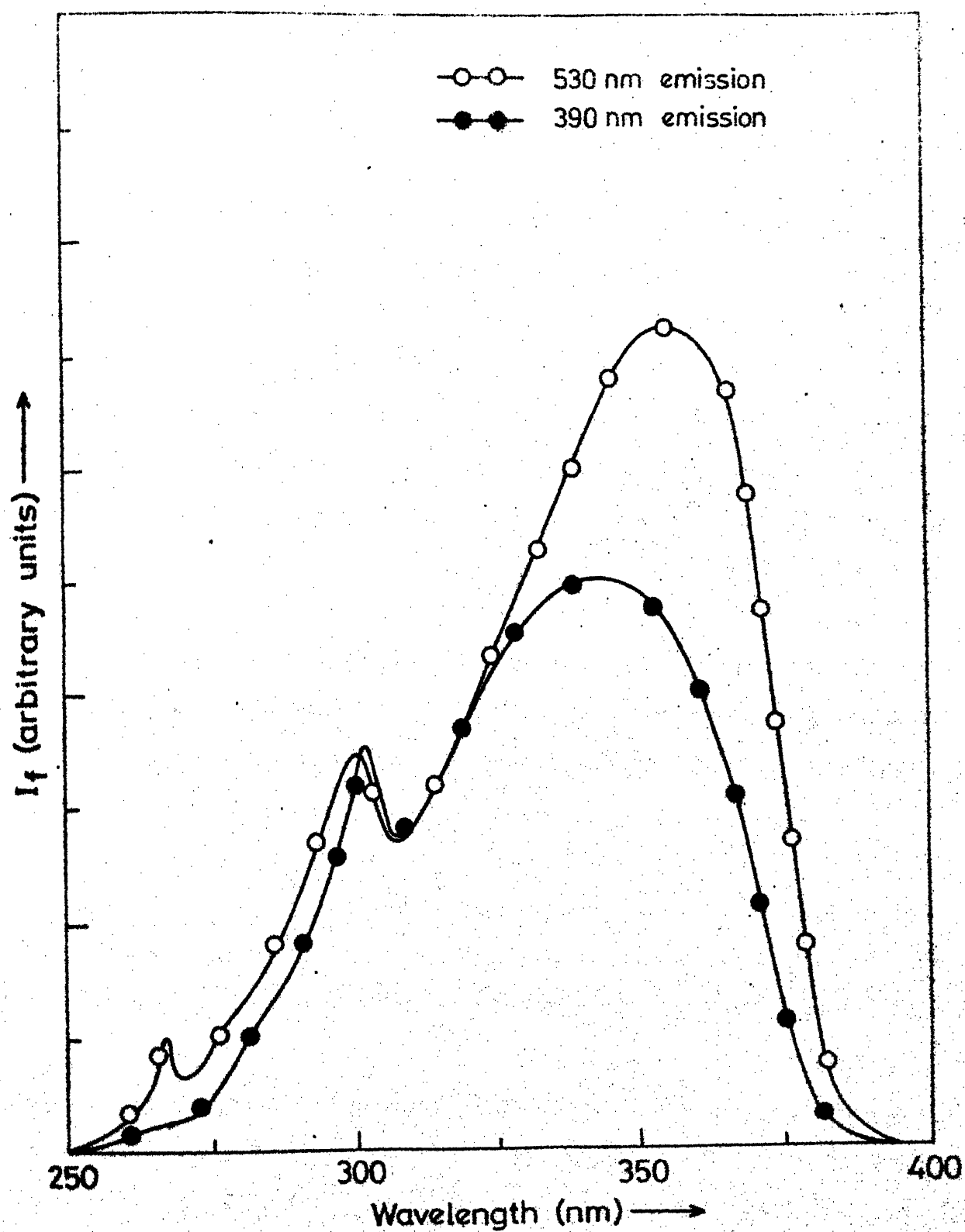
Fig.3.17 Excitation spectra of 2-(o-aminophenyl)benzimidazole.

The above hypothesis can also explain the behaviour of fluorescence spectra quite nicely in different solvents. In n-heptane and cyclohexane, two distinct band systems are observed due to forms I and II, with equal intensity. The longer wavelength band which is due to I, progressively decreases in intensity as we go from n-heptane ——> acetonitrile ——> methanol ——> water and the shorter wavelength band, due to structure II, increases in intensity. This could be due to the increase in population of molecules in structure II in polar solvents because of the progressive blocking of lone pair on pyridine nitrogen atom or due to stronger interaction of the solvent with the amino group of I and thus quenching the fluorescence, as observed in other arylamines.[57] Under the above conditions, the blue shift in the long wavelength band is due to the interaction of the solvent with the lone pair of the amino group and the red shift in the shorter wavelength band is due to interaction of the solvent with the lone pair of the pyridinic nitrogen atom. It may be noted that the lone pair of the amino group is not available for the solvent interaction in structure II. As said earlier, this behavior is self-explanatory in case of $\pi \longrightarrow \pi^*$ as the lowest energy transition. This, as well as the effect of pH (see Chapter 4) which is an extreme case of intermolecular hydrogen bonding, supports the above assignments to structures I and II.

The relatively small increase in the intensity ratio (I_{530}/I_{390}) in n-heptane with the increase in the excitation

wavelength (structure II has small absorption and increase in the above ratio should be more) could be due to the fast dynamic equilibrium between the two structures even in the excited state but a definite conclusion cannot be drawn from this study as the absorption spectra of the two structures are overlapping each other in this region.

3.3.8   2-(m-Aminophenyl)benzimidazole (mBNH$_2$)
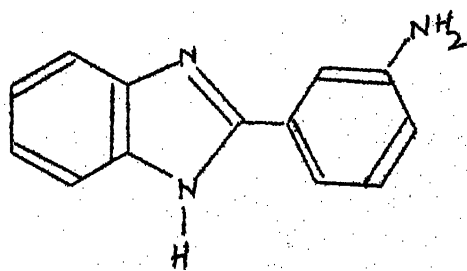
The absorption maxima ($\lambda_{max}^{(abs)}$), log ε_{max}, fluorescence maxima and ϕ_f in different solvents are listed in Table 3.9; the former is shown in Fig. 3.18 and the latter in Fig. 3.19. The data of Table 3.9 shows a small redshift of the longest wavelength absorption maxima on going from heptane ——➤ chloroform ——➤ ether ——➤ acetonitrile and then nearly remains steady with protic solvents. Also there is a loss of absorption band structure in highly polar solvents. The fluorescence spectrum is a broad band and largely red shifted on going from heptane to water. Under the above conditions the quantum yield decreases, except in water

Fig.3.18 Absorption spectra of 2-(m-aminophenyl)benzimidazole
in various solvents.

Table 3.9.A. Absorption maxima and log ε_{max} of 2-(m-aminophenyl)-benzimidazole in various solvents.

Solvent	λ_{max} (nm) (log ε_{max})					
n-Heptane	225	237	254	293	303	320
Dioxane		247 (4.17)	255 (4.13)		302 (4.35)	322 (4.06)
Ether		247 (4.26)	255 (4.15)	297.5 (4.39)	304 (4.40)	322 (4.06)
Acetonitrile	225 (4.50)	241 (4.26)	255 (4.06)	295.5 (4.32)	302 (4.32)	323 (3.95)
Methanol	224 (4.52)	241 (4.27)	255 (4.09)	295.5 (4.34)	303 (4.31)	323 (3.96)
Ethanol	225 (4.49)	241 (4.24)	255 (4.07)	295 (4.32)	303 (4.31)	323 (3.96)
Water	220 (4.52)	242 (4.25)		295 (4.34)		322.5 (3.96)

Table 3.9.B. Fluorescence maxima and $\emptyset_f$ of 2-(m-aminophenyl)-benzimidazole in various solvents.

Solvent	λ_{max}(nm)	$\emptyset_f(\lambda_{exc}=320$ nm)
n-Heptane	360	0.146
Dioxane	388	0.088
Ether	388	0.124
Acetonitrile	387	0.128
Methanol	408	0.068
Ethanol	408	0.072
Water	420	0.132

where it is more than methanol and ethanol but less than heptane. The Stoke's shift also increases under these conditions.

The above behaviour closely resembles the behaviour of other arylamines like CNH_2, FNH_2, INH_2 and $BINH_2$. Thus it can be argued on the same lines that $mBNH_2$ also behaves like an arylamine in its solvent dependence study and acts as a hydrogen bond acceptor in S_0 state and hydrogen bond donor in S_1 state. The very large red shift in fluorescence band maxima can again be attributed to the formation of a 1:1 solute-solvent complex in the first excited singlet state. This hypothesis was tested by adding different proportions of methanol to n-heptane and it was found that addition of 1.5% (volume/volume) methanol shifts the fluorescence maxima from 360 nm to 390 nm, whereas 100% methanol further shifts it only to 408 nm. Thus it can be deduced that although the amino group acts almost independently as a pure amino group in the ground state it is affecting the fluorescence behaviour through an increased interaction of the π cloud of the phenyl ring. The relatively low quantum yield for $mBNH_2$ in different solvents could be due to increased modes of vibrational deactivation introduced by phenyl ring. Thus benzimidazole in methanol has a quantum yield of 0.67,[53] PBI 0.10 and $mBNH_2$ 0.07. The relative aloofness of the amino group in $mBNH_2$ has been further substantiated in the discussion of its acid-base properties.

3.3.9   2-(p-Aminophenyl)benzimidazole(pBNH$_2$)

The structure of the molecule is given on P.100. The

absorption spectra and the fluorescence spectra in different sol-

vents are given in Fig. 3.20 and 3.21 respectively, the λ_{max}(abs),

log ε_{max} and λ_{max}(flu), $\emptyset_f$ are given in Table 3.10. The two nor-

mal absorption band systems of benzimidazole molecule are kept

intact except that both are red shifted but the third band system

(λ_{max}(abs) ~ 207 nm) is also observed. The long wavelength band

is a doublet, like that in benzimidazole, but the structure is

lost and also it is red shifted as the polarity of the solvent

increases except in water where the broad band is red shifted with

respect to n-heptane but blue shifted relative to methanol and

acetonitrile. The structure of the second band system undergoes

a similar change of structure loss but the band maxima is regularly

blue shifted. The fluorescence spectrum is nicely structured in

less polar solvents (n-heptane, dioxane and ether) and can be

explained by the vibrational frequency of 1390 cm^{-1} in S$_0$ and this

is similar to that observed in 2-phenylbenzimidazole (P.56). This

at least proves that the origin and nature of this particular

transition band is the same in PBI and pBNH$_2$. To substantiate

it even further, low temperature fluorescence spectra of pBNH$_2$ was

taken in water. Again the vibrational structure could be nicely

explained by a vibrational spacing of 1397 cm^{-1}. Another long

wavelength fluorescence band (maxima at ~500 nm) is observed

whose intensity is much less than that of the short wavelength

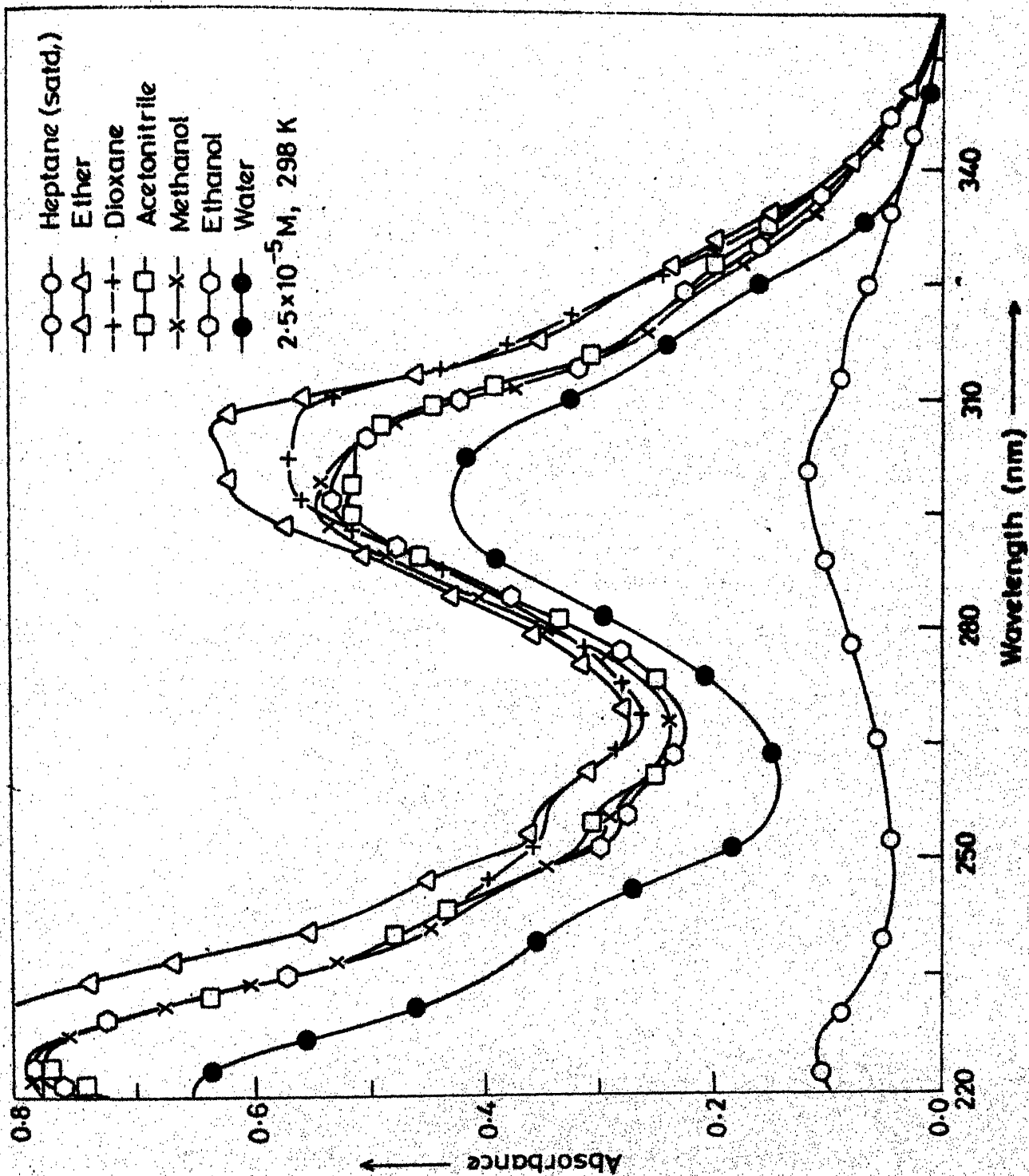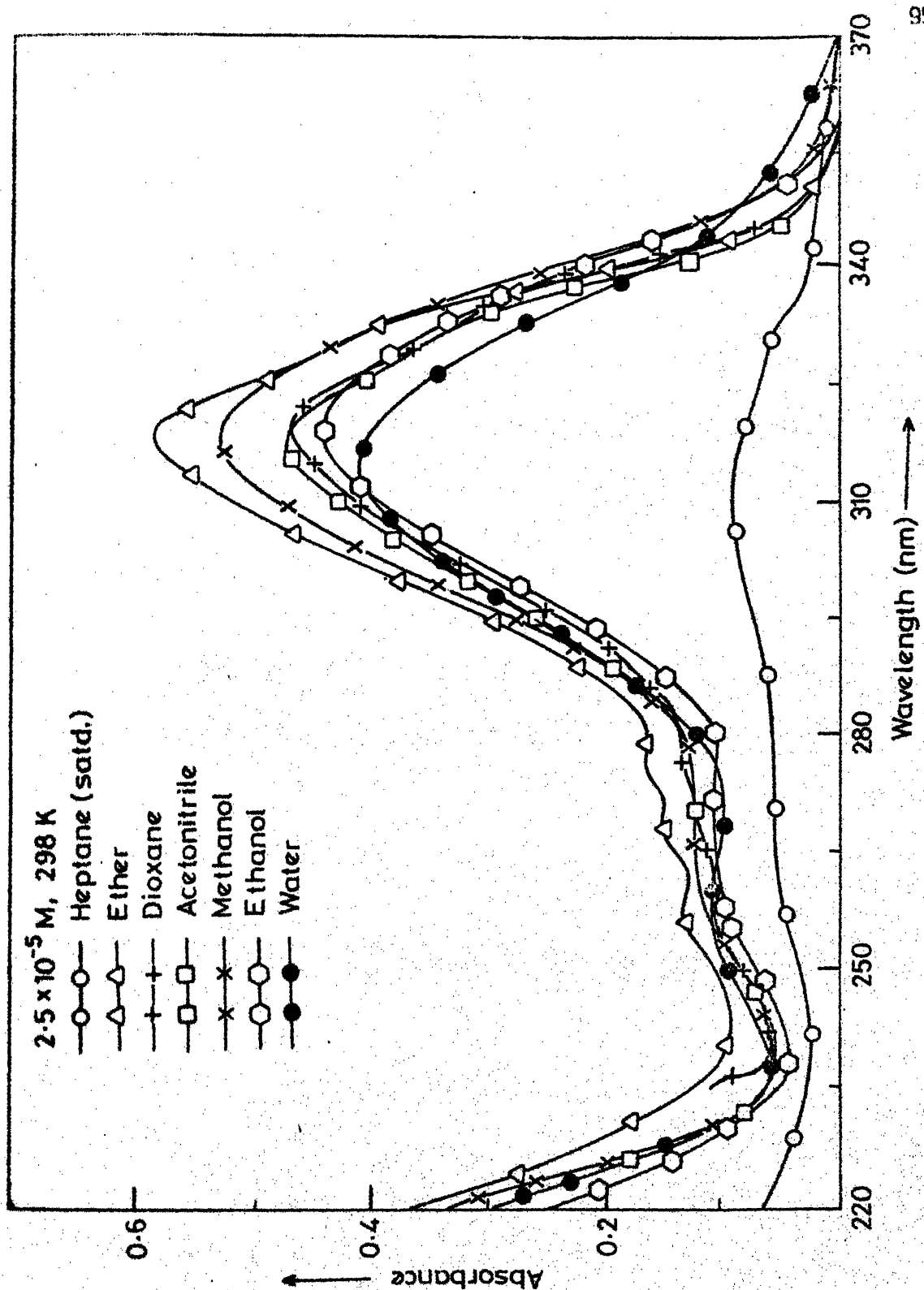Fig.3.20 Absorption spectra of 2-(p-aminophenyl)benzimidazole in various solvents.
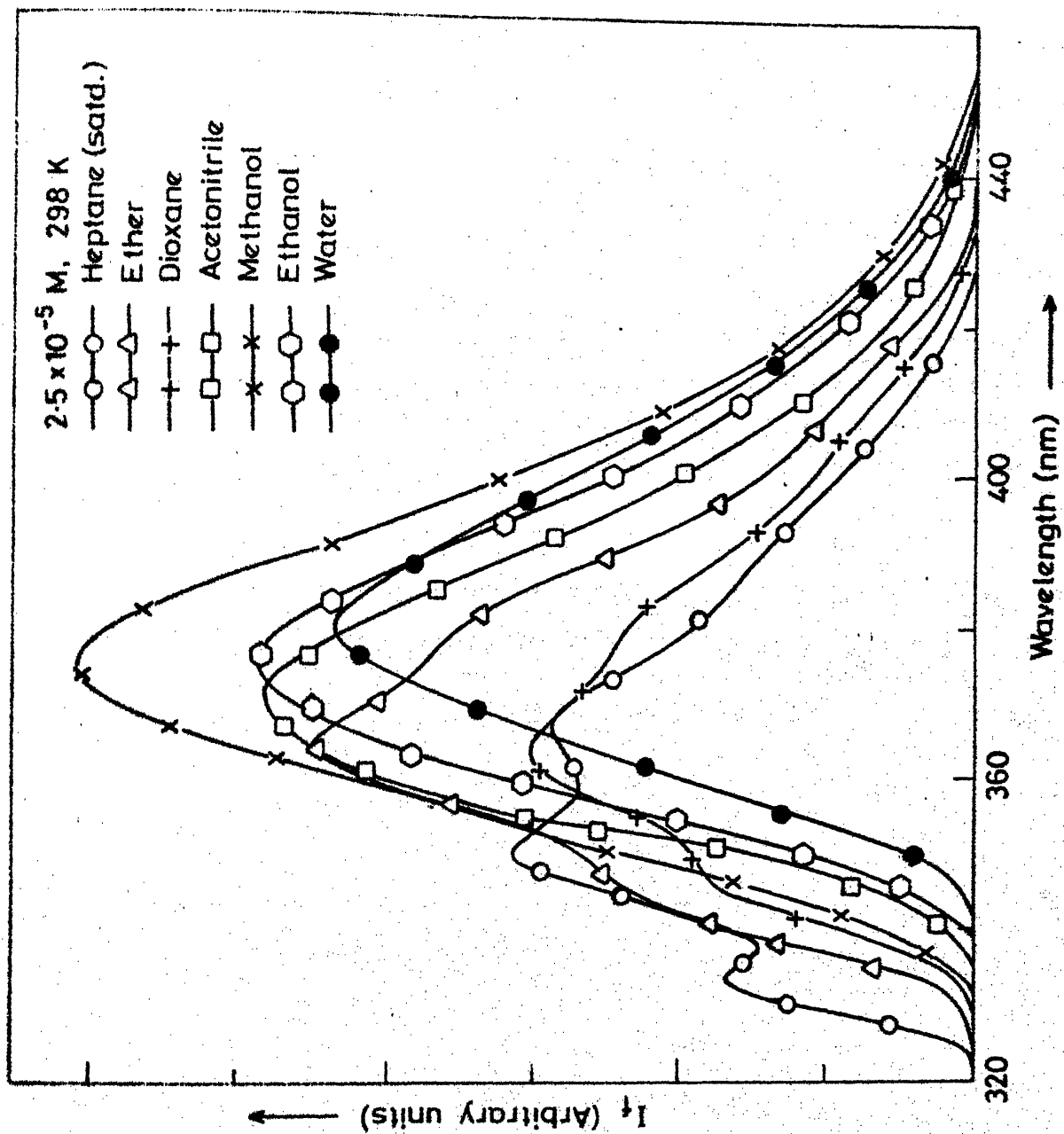
Fig.3.21 Fluorescence spectra of 2-(p-aminophenyl)benzimidazole in various solvents.

Table 3.10.A. Absorption maxima and log ε_{max} of 2-(p-amino-phenyl)benzimidazole in various solvents.

Solvent	λ_{max} (nm) (log ε_{max})					
n-Heptane	207	~270			310	330
Dioxane	–	258 (3.64)	268 (3.70)	277 (3.73)	318 (4.27)	333 (4.09)
Ether	210 (4.35)	257 (3.71)	268 (3.78)	276 (3.82)	316 (4.37)	331 (4.21)
Acetonitrile	211 (4.32)	257 (3.68)	267 (3.64)		316 (4.27)	
Methanol	210 (4.37)	~260(broad) (3.68)			317 (4.32)	
Ethanol	210 (4.38)	~260(broad) (3.62)			318 (4.27)	
Water	207 (4.39)	~255(broad) (3.73)			313 (4.30)	

Table 3.10.B. Fluorescence maxima and $\emptyset_f$ of 2-(p-aminophenyl)-benzimidazole in various solvents.

Solvent	λ_{max}(nm)				$\emptyset_f$(λ_{exc}=315 nm)
n-Heptane	334	350	368	384	0.485
Dioxane		348	363	380	0.453
Ether		348	363	380	0.775
Acetonitrile			370		0.822
Methanol			376		0.900
Ethanol			378		0.836
Water			382		0.852

fluorescence but their intensity ratio remains unchanged with the change in concentration (10^{-5} - 10^{-3}M), solvents and pH of the solution.

The very structure of pBNH$_2$ is suggestive of a direct conjugation of the lone pair of the amino group with the rest of the molecule, unlike mBNH$_2$, thus making the phenyl ring in the same plane as that of benzimidazole in the excited singlet state, probably by increasing the bond order between the two ring systems. The loss of band structure even in slightly polar solvents shows clearly that the amino group is interacting directly with the benzimidazole moiety. The red shift observed in the long wavelength maxima and the increased Stoke's shift confirms the $\pi\pi^*$ character of the transition and the small blue shift in absorption spectra in water, relative to methanol or other polar solvents could be due to the fact that water here is acting preferentially as a hydrogen donor solvent to the lone pair of amino group (following the explanation offered for other amino compounds).

The fluorescence does show a red shift on going from heptane to water, but it is only about 20 nm as compared to 60 nm for mBNH$_2$. This suggests that the formation of an 1:1 solute-solvent complex, which was responsible for a very large red shift in mBNH$_2$ is not taking place in this case, probably due to a reorganisation and delocalization of charges through conjugation. The small red shift is probably similar to that given in the case of 2-amino-

benzimidazole i.e. presence of electron donating group in the heterocyclic ring.

The quantum yield values for pBNH$_2$ are interestingly very high and show an increasing trend from nonpolar to polar solvents. An explanation for this very high quantum yield is difficult, but probably the other resonating structure II make the molecule more planar and somewhat rigid, thereby decreasing many vibrational deactivation modes and this could lead to an increased quantum efficiency.

The presence of long wavelength band could not be explained from this study and is still under investigation.
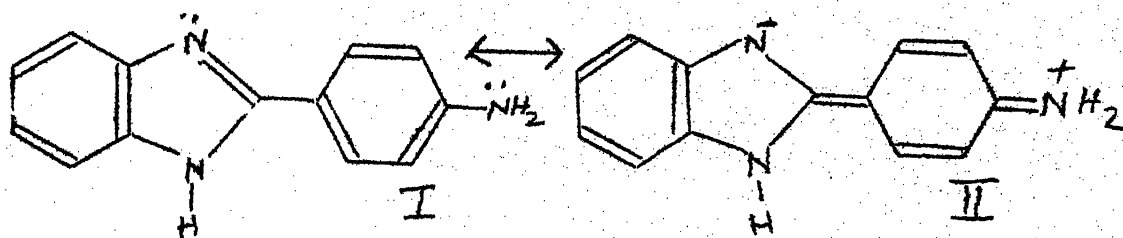
EFFECT OF pH ON ABSORPTION
AND FLUORESCENCE SPECTRA

4.1 Introduction

The basicity or acidity of a molecule is directly related

to its electronic structure. Since transitions are, in general,

accompanied by a reorganisation of the molecular electron density,

the basicity or acidity of such molecules may vary significantly

from one electronic state to another. The shift in equilibrium

position between the ground and the excited states is reflected

by the spectral shifts of the absorption and the fluorescence

spectra of both the acidic and the basic forms of the molecules.

A brief description and principle of each method which have been

used to determine the ground and excited state acidity constants

is discussed below.

4.2 Ground state equilibrium constants[100]

The dissociation reaction of any acid can be represented as

$$BH^+ + H_2O \rightleftharpoons B + H_3O^+ \qquad (4.1)$$
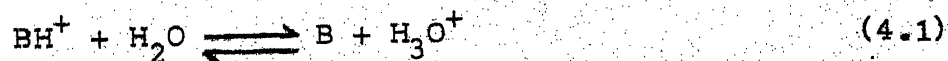
and the equilibrium constant by the relation

$$pH = pK_a + \log \frac{[B]}{[BH^+]} \qquad (4.2)$$

where $[B]$ and $[BH^+]$ are the concentrations of the base and its conjugate acid respectively. pH represents the hydrogen ion concentration at the above concentration of the species and pK_a, the equilibrium constant of the above reaction. Thus pK_a can be calculated if one knows the concentration of each species at the specific pH and these can be calculated spectrophotometrically as follows:

(i) If the absorption spectra of acid and its conjugate base do not overlap, one can choose the two wavelengths, which only represent the respective species, and measure the absorpances (A) as a function of pH. The concentration of each species can be calculated from the Beer-Lambert's law i.e.

$$A = \varepsilon cl \qquad (4.3)$$

where ε, is the extinction coefficient at the respective chosen wavelength; l, the pathlength and c, the concentration. ε can be calculated from the solution of known concentration which contains only the one specific form.

(ii) If the absorption spectra of both the species overlap each other, absorbances are measured at two chosen wavelengths λ_1 and λ_2 i.e.

$$A_{\lambda_1} = \varepsilon_{\lambda_1}(BH^+) \, c_{BH^+} \, 1 + \varepsilon_{\lambda_1}(B) c_B 1 \qquad (4.4)$$

$$A_{\lambda_2} = \varepsilon_{\lambda_2}(BH^+) \, c_{BH^+} \, 1 + \varepsilon_{\lambda_2}(B) \, c_B 1 \qquad (4.5)$$

The values of ε_{λ_i}'s of each form, at each analytical wavelength can be calculated as mentioned in (i) and the concentration of each species as

$$c_{BH^+} = \frac{A_{\lambda_1} \varepsilon_{\lambda_2}(B) - A_{\lambda_2} \varepsilon_{\lambda_1}(B)}{\varepsilon_{\lambda_1}(BH^+) \, \varepsilon_{\lambda_2}(B) - \varepsilon_{\lambda_2}(BH^+) \, \varepsilon_{\lambda_1}(B)} \qquad (4.6)$$

$$c_B = \frac{A_{\lambda_1} \varepsilon_{\lambda_2}(B) - A_{\lambda_2} \varepsilon_{\lambda_1}(BH^+)}{\varepsilon_{\lambda_1}(B) \, \varepsilon_{\lambda_2}(BH^+) - \varepsilon_{\lambda_2}(B) \, \varepsilon_{\lambda_1}(BH^+)} \qquad (4.7)$$

if pathlength is 1 cm.

4.3 Excited state acidity constants

Broadly there are two different methods to determine the excited state acidity constants apart from the dynamic method involving time dependent fluorescence spectroscopy.[112] One method uses Förster cycle to calculate the excited state acidity constants using spectral band maxima for the acid form and its conjugate base form. The other is fluorimetric titration method. Both the methods, with their merits and limitations are discussed below.

4.4 Förster Cycle Method

A thermodynamic cycle named after Förster,[24,25] is based upon the thermodynamic equivalence of all routes from the ground state of the acid to the thermally equilibrated S_1 state of the conjugate base. From the energy level diagram (Fig. 4.1) it can be seen that there are two mechanistically different but energetically equivalent pathways from the ground state and BH^+ to the excited state base B^*.
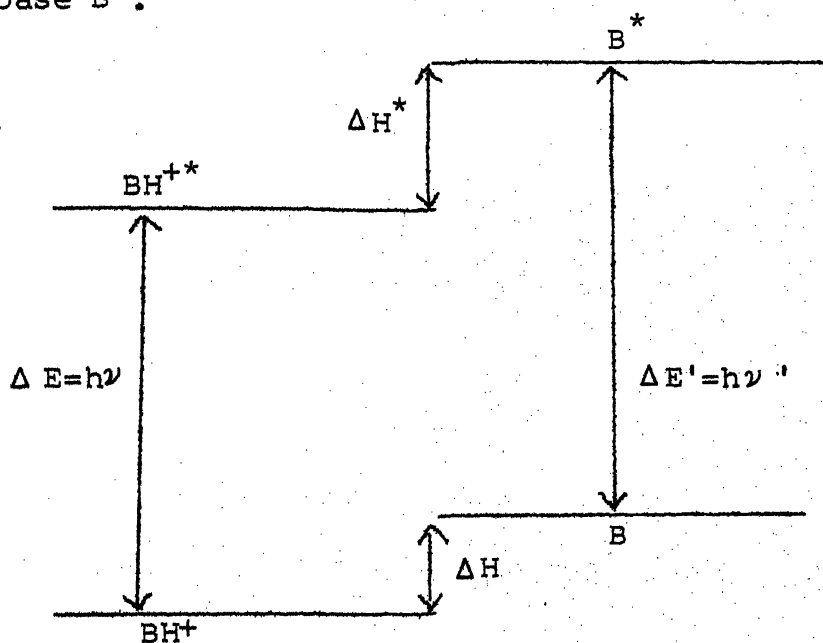
Fig. 4.1. The Förster Cycle

So it follows that

$$\Delta E + \Delta H^* = \Delta E' + \Delta H \qquad (4.8)$$

where ΔE and $\Delta E'$ are the energies of the 0-0 electronic transitions of acid and its conjugate base and ΔH and ΔH^* are

the enthalpies of acid ionization in the ground and excited states respectively.

From the above equation

$$\Delta E - \Delta E' = \Delta H - \Delta H^*$$

$$= (\Delta G + T \Delta S) - (\Delta G^* + T \Delta S^*) \qquad (4.9)$$

where ΔG and ΔS are the free energy and entropy changes respectively (excited state values are denoted by asterisks). Assuming $\Delta S = \Delta S^*$, it follows from (4.9)

$$\Delta E - \Delta E' = \Delta G - \Delta G^*$$

$$= -RT (\ln K_a - \ln K_a^*) \qquad (4.10)$$

or

$$pK_a - pK_a^* = \frac{\Delta E - \Delta E'}{2.303RT}$$

$$= \frac{NhC}{2.303RT}(\bar{\nu} - \bar{\nu}') \qquad (4.11)$$

At 25°C it becomes

$$pK_a - pK_a^* = 2.1 \times 10^{-3} (\bar{\nu} - \bar{\nu}') \qquad (4.11a)$$

where $\bar{\nu}$ and $\bar{\nu}'$ are the wave numbers of 0-0 transition from BH^+ to BH^{+*} and B to B^* respectively. These wave numbers can be determined from either absorption, fluorescence spectra or the average of absorption and fluorescence maxima. Knowing pK_a, pK_a^* can be calculated.

The accuracy and the limitations of this method have been reviewed in detail by many authors,[24,32,35,38,44,101] which in general are based on the following assumptions.

While measuring the values of $\bar{\nu}$ and $\bar{\nu}'$ from experiment, it has been assumed that the electronic states involved in the ground and excited states are the same. But if two different states are involved in fluorescence of BH^+ and B, the application of Förster cycle becomes meaningless. For example it is known[54] that ^1L_b is the lowest singlet state in benzimidazole and ^1L_a is the lowest state for its cation.

If there is a conformational change in the excited state or photo-tautomerism leading to a different geometry and structure of molecule, a large entropy error associated with the configurational change is introduced in the Förster cycle calculations.[24]

In aromatic molecules where there is not much change in molecular electronic structures subsequent to excitation, it is reasonable to assume that the entropy of protonation would be nearly equal in the ground and excited electronic states. For example in case of protolytic dissociation of β-naphthylammonium ion, it has been shown that the maximum error caused by the above assumption is not more than ± 0.2 units in the ΔpK_a.[102] By calculating pK_a^*'s at different temperatures, Weller[27] showed that there was practically no difference in ΔS^* for the ionization of β-naphthol in the S_o and S_1 states, despite a large change in

pK_a and obvious differences in solvation between the acid and its base. Similarly in aromatic acids it was found that $T \Delta S^*$ do not contribute more than 1 pK_a unit.[150]

Only the 0-0 vibronic transition frequency is to be used for calculation of pK_a^*'s by Förster cycle method. The spectra in aqueous solutions at room temperature are usually broad and structureless and the 0-0 band cannot be located easily. If the vibrational spacings in the ground and the excited states are same, there exists a mirror image relationship between the long wavelength absorption band and the fluorescence band.[103] In such cases, the point of intersection of the two bands can be approximated to 0-0 frequency.

In fact if this condition is valid and solvent relaxation is same for both species in the excited state, only absorption or only fluorescence band maxima can be used for calculation of pK_a^*. In general this is not the case and the average of absorption and emission band maxima can be used to approximate 0-0 transition frequency of the electronic transition. This is supposed to result in a cancellation of the energy discrepancies between the conjugate species due to unequal thermal relaxations. This technique often, but not always, yields good results. If the error introduced due to thermal relaxation in one of the methods (taking only absorption or only fluorescence) is unusually large, the error will be distributed while averaging.

The above discussion clearly shows that the accuracy of pK_a^* obtained by Förster cycle method depends upon the choice of the method employed which in turn depends upon the validity of the assumptions made.

The following formulas are used for calculating the pK_a^* values:

(i)   Absorption only:

$$pK_a - pK_a^* = 2.10 \times 10^{-3} (\bar{\nu}_{abs} - \bar{\nu}'_{abs}) \qquad (4.12)$$

(ii)   Fluorescence only:

$$pK_a - pK_a^* = 2.10 \times 10^{-3} (\bar{\nu}_{flu} - \bar{\nu}'_{flu}) \qquad (4.13)$$

(iii)   Average of absorption and fluorescence

$$pK_a - pK_a^* = 2.10 \times 10^{-3} (\bar{\nu}_{ave} - \bar{\nu}'_{ave}) \qquad (4.14)$$

where $$\bar{\nu}_{ave} = \frac{\bar{\nu}_{abs} + \bar{\nu}_{flu}}{2} \qquad (4.15)$$

$$\bar{\nu}'_{ave} = \frac{\bar{\nu}'_{abs} + \bar{\nu}'_{flu}}{2} \qquad (4.16)$$

$\bar{\nu}$ is the frequency maxima for the conjugate acid BH^{+*} and $\bar{\nu}'$ for the conjugate base B.

4.5 Fluorimetric Titration Method[27]

In this method fluorescence of a given sample is measured

at a selected wavelength for a series of proton concentrations.
The sample is excited at the isosbestic point to ensure equal
population of excited state species of the acid and its conjugate
base. If both the species involved in the equilibrium are fluores-
cent, the relative fluorescence intensity I/I_o can be plotted
against $H_o/pH/H_-$, similar to absorptiometric titration. If the
prototropic equilibrium is established within the lifetime of the
excited state, a plot of I/I_o against solution acidity will give
a sigmoid curve whose point of inflection is a measure of the
dissociation constant in the excited state. But if the rate of
fluorescence is relatively too fast, the prototropic equilibrium
is not established in the excited state before the emission takes
place, the curve will only give ground state equilibrium constant.
Generally this occurs if the lifetime of the excited species is
short and/or if there are insufficient number of protons in the
medium to establish equilibrium in the excited state, which may
occur in the mid-pH region. In the latter case the rate of proton-
transfer in the excited state can be increased by the addition of
buffers. It has been shown[105,104] that concentrated buffers help
in achieving the excited state equilibrium provided buffer ions
do not quench the fluorescence of the excited species.

4.6 Proton induced quenching of aromatic amines

It has been commonly observed in the fluorimetric titrations
of aromatic amines that there is no correspondence between the

quenching of aromatic amine fluorescence and the fluorescence intensity due to the formation of arylammonium ions at moderate hydrogen ion concentration.[106-113] This phenomenon was explained due to the formation of a nonfluorescent solute-solvent complex in the first excited singlet state. Recently Tsutsumi et al[112] and many others have shown that this behaviour at moderate hydrogen ion concentration is due to proton induced quenching of neutral amines. Isotopic and other studies[114] have indicated that this phenomenon is because of an electrostatic and covalent interaction between H^+ and a suitable carbon atom in the excited state. The introduction of electron donating groups in to the aromatic ring causes a charge migration from the substituents into the ring in the excited state. This tendency is enhanced by solvation of the excited state in polar media. Thus, the excited state has an intramolecular CT structure with an increase of the basicity of the aromatic ring. Thus (i) intramolecular charge transfer is responsible for the proton induced quenching and (ii) the proton induced quenching is caused by electrophilic protonation at one of the carbon atoms of the aromatic ring. Complete kinetic model for the proton transfer reaction of aromatic amines have been proposed by Tsutsumi et al[112] and the scheme is given below.

$$BNH_3^{+*} + H_2O \underset{k_1'}{\overset{k_1}{\rightleftharpoons}} BNH_2^* + H_3O^+ \tag{4.17}$$

$$k_f \diagup \quad \diagdown k_I \qquad\qquad k_f' \diagup \quad \downarrow k_I' \quad \diagdown k_q'[H^+]$$

$$BNH_3^+ + h\nu \qquad BNH_3^+ \qquad\qquad BNH_2 + h\nu' \qquad BNH_2 \qquad BNH_2$$
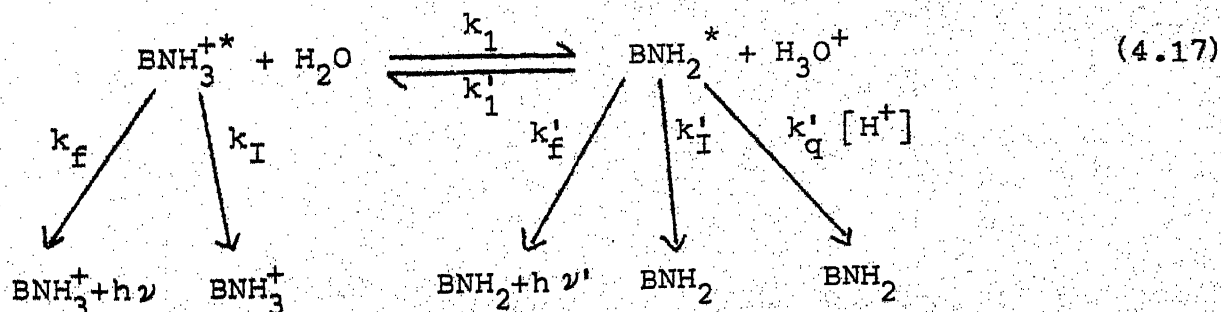
where k_f and k_I represent the rate constants for the fluorescence and radiationless quenching, k_1 and k_1' are the forward and reverse rate constants for the proton transfer reaction. Unprimed quantities refer to BNH_3^{+*} and primed quantities to BNH_2^*. If all the exciting radiation is absorbed only by the photodissociating acid, then applying steady state approximation, the following equations can be obtained:

$$\frac{\emptyset}{\emptyset_0} = \frac{1 + \left[k_1' \quad k_q' (1 + k_1 \tau_0) \right] \tau_0' [H^+]}{1 + k_1 \tau_0 + \left[k_1' + k_q' (1 + k_1 \tau_0) \right] \tau_0' [H^+]} \qquad (4.18)$$

$$\frac{\emptyset'}{\emptyset_0'} = \frac{k_1 \tau_0}{1 + k_1 \tau_0 + \left[k_1' + k_q' (1 + k_1 \tau_0) \right] \tau_0' [H^+]} \qquad (4.19)$$

where τ_0 and τ_0' are the lifetimes in S_1 states and $\emptyset_0$ and $\emptyset_0'$ are the quantum yields of the BH^+ and B respectively.

The quenching rate constant, k_q', can be estimated from equation (4.19) as follows: Writing equation (4.19) as

$$\frac{\emptyset_0'}{\emptyset'} = 1 + \frac{1}{k_1 \tau_0} + \frac{\left[k_1' + k_q' (1 + k_1 \tau_0) \right]}{k_1 \tau_0} \tau_0' [H^+] \qquad (4.20)$$

For large values of τ_0 and $k_1 > k_1' [H^+]$ at moderate $[H^+]$ $(< 0.5$ mol $dm^{-3})$ the following equations should hold:

$$k_1 \ \tau_o \ >> 1$$

and $\quad k_1'/k_1 \ \tau_o \ << \ k_q'$

and equation (4.20) can be simplified to

$$\frac{\phi_o'}{\phi'} = 1 + k_q' \ \tau_o' \ [H^+] \tag{4.21}$$

A stern-volmer plot of ϕ_o'/ϕ' against $[H^+]$ would give a linear relationship and from the slope of the plot, knowing the value of τ_o' the rate constants for proton induced quenching (k_q') can be found out. A deviation from linearity at higher proton concentrations may occur because of (i) a large variation in ionic strength at higher proton concentrations, (ii) a more specific short range interaction between BNH_2^* and H^+ may become dominant as reported by Weller[115] and (iii) the nonavailability of free water to accept protons from BNH_3^+ as the water molecule may have been protonated due to higher acid concentration.[110] Therefore, kinetic analyses involving proton induced quenching should be carried out at moderate acid concentration ($[H^+] < 0.5$ mol dm^{-3}).

4.7 Lifetime estimation

The lifetime τ_o or τ_o' used in the above kinetic model can only be accurately determined from lifetime measurements with a time dependence fluorimeter. To get an approximate estimation of lifetimes which can in turn provide an approximate idea of the order of proton-induced quenching rate constant, Strickler and Berg's[116]

formula has been used which was developed for aromatic hydrocarbons in a noninteracting medium. The formula gives reasonably accurate results if the mirror symmetry relation is valid. In its final form the equation is

$$k_f = \frac{1}{\tau_f} = \frac{8\pi \times 2303\, cn^2}{N}$$

$$\times \frac{\int F(\bar{\nu})\,d\bar{\nu}}{\int F(\bar{\nu})\frac{d\bar{\nu}}{\bar{\nu}^3}} \times \int \frac{\varepsilon(\bar{\nu})\,d\bar{\nu}}{\bar{\nu}}$$

$$= 2.88\times10^{-9}\, n^2 \times \frac{\int F(\bar{\nu})\,d\bar{\nu}}{\int F(\bar{\nu})\frac{d\bar{\nu}}{\bar{\nu}^3}} \times \int \frac{\varepsilon(\bar{\nu})\,d\bar{\nu}}{\bar{\nu}} \tag{4.22}$$

where k_f is the radiative transition probability related to radiative lifetime (τ_f). The molecular lifetime (τ_o) in any solvent can be calculated from the relation (4.23) where $\emptyset$ is the quantum yield of the species in that solvent.

$$\tau_o = \tau_f\, \emptyset \tag{4.23}$$

c is the velocity of light, 'N' is the Avogadro number and 'n' the refractive index. These relations assume a nondispersive molecular environment. If the refractive index $n = n_f$ in the fluorescence region and $n = n_a$ in the absorption region, then n^2 is replaced by n_f^3/n_a. These effects can be significant in pure aromatic liquids or in concentrated solutions. The integrals are taken over the $S_1 - S_o$ fluorescence spectrum and the S_o-S_1 absorption spectrum respectively.

4.8   Results and Discussions

4.8.1 6-Aminochrysene(CNH$_2$)[147]

The prototropic equilibria studied in the ground and excited states are

$$CNH_3^+ \xrightleftharpoons{\ \ 1\ \ } CNH_2 + H^+ \tag{4.24}$$

$$CNH_2 \xrightleftharpoons{\ \ 2\ \ } CNH^- + H^+ \tag{4.25}$$
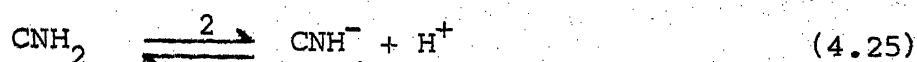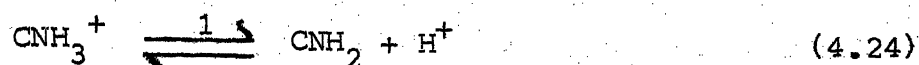
where CNH_3^+ and CNH^- are the cation and the anion of CNH_2 respectively. Because of the poor solubility of CNH_2 in water, the pH dependence study was carried out in 30% $MeOH-H_2O$. The absorption spectra of CNH_2 were investigated in the basicity-acidity range of H_o-8 to H_-16 and the absorption and fluorescence spectral maxima of different prototropic forms are listed in Table 4.1. The absorption spectrum of cation, as shown in Fig. 4.2, is structured, blue shifted and resembles that of Chrysene.[83]   The pK$_a$ for equilibrium 1 was calculated spectrophotometrically and found to be 3.15, which is in good agreement with the literature value.[84] The pK$_a$ of equilibrium 2 could not be calculated as there was no significant change in the absorption spectrum of CNH_2 even at H_-16 and this behaviour resembles with other aromatic amines.[119,120]

---

147. A.K. Mishra and S.K. Dogra, J. Photochem, 23, 163 (1983).
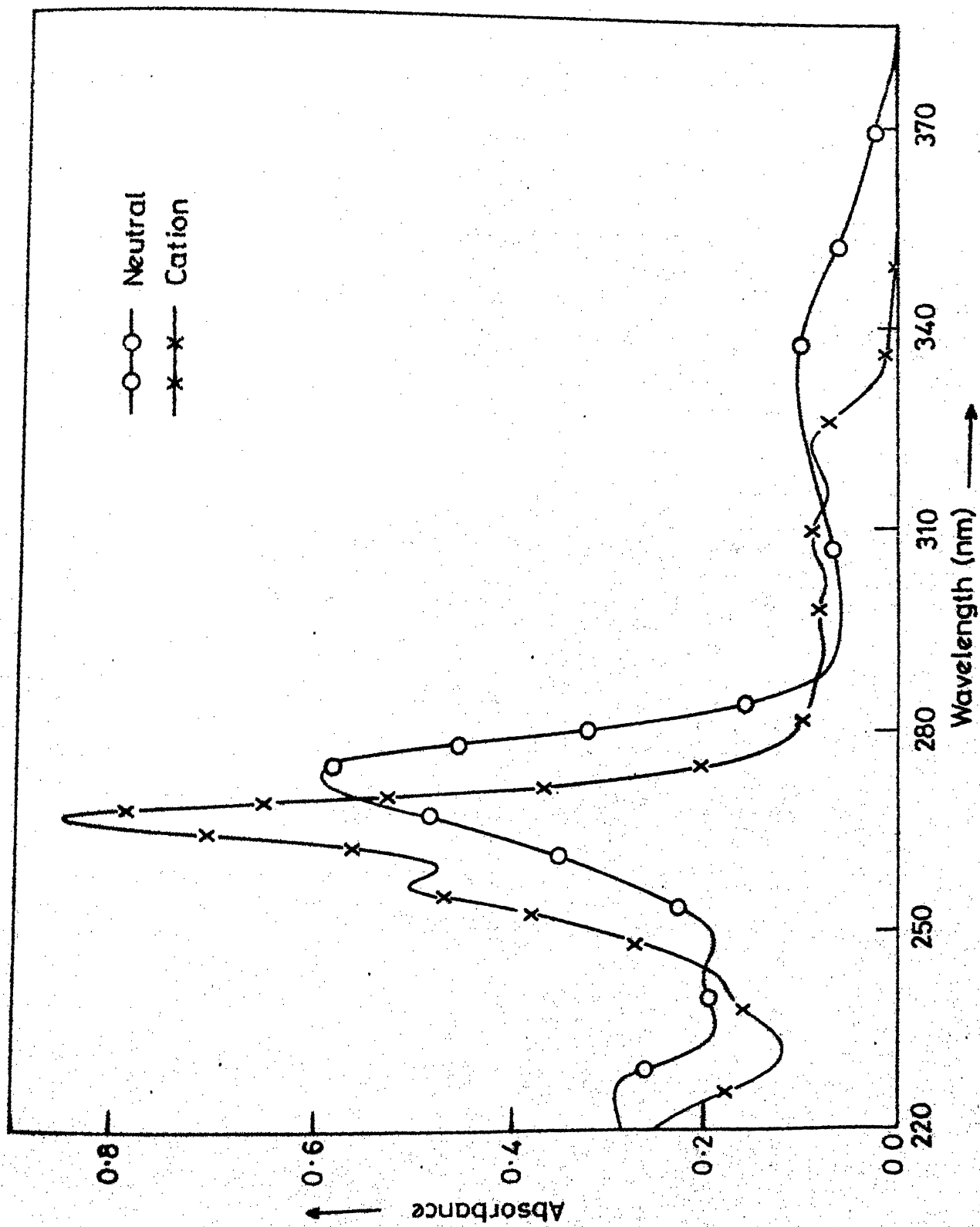
Fig.4.2   Absorption spectra of various prototropic forms of CNH_2 at 298K.

Table 4.1. Absorption maxima and fluorescence maxima ($\emptyset_f$) of different prototropic forms of CNH_2 at 298K.

Forms	abs(nm) λ_{max}				flu(nm) λ_{max}	$\emptyset_f$
Neutral	225 233	273	340		470	0.16
Cation	215 240	257 267 285 296 310 322			365 383 406 429	0.17

Table 4.2. Ground and excited state equilibria of CNH_2 at 298K

Equilibrium	pK_a	Förster cycle method			pK_a^* (F.T.)	λ isosbestic(nm)
		pK_a^* (abs)	pK_a^* (fl)	pK_a^* (av)		
Cation ⇌ Neutral	3.15	-2.35	-4.17	-3.26	-3.4	320
Neutral ⇌ Anion	>14	−	−	−	12.6	

The fluorescence spectra were studied in the range H_o-6 to H_-16. Only two species, the neutral molecule and the cation were observed to fluoresce. The spectra are reported in Fig. 3.3,p.39 As has been found for 9-phenanthrylamine,[120] the aminoquino-lines[57,58,60] and 5-aminoindazole,[49] the imino-anion does not emit in basic media and unlike 9-phenanthrylamine,[120] α-and β-naphthyl-amines,[121] no dianion emission is observed at 298K under highly basic conditions.

The pK_a^* of equilibrium 1 at 298K was calculated by using Förster Cycle method and absorption, fluorescence and average of the two band maxima. The values are listed in Table 4.2. The pK_a^* (1) and pK_a^*(2) were also calculated with the help of fluori-metric titration curves, shown in Fig. 4.3, and the pK_a^* values determined from these curves for the two equilibria are given in Table 4.2. It can be seen from Figure 4.3 that the fluorescence intensity of CNH_2 is quenched with decreasing pH and H_o. The mid point of the quenching is at pH 1.1, which cannot be the pK_a^* of equilibrium 1, as the fluorescence spectrum of CNH_3^+ is only observed below pH 0, and its intensity increases with increasing hydrogen ion concentration. The mid-point of this increase is at H_o-3.4, which is the pK_a^* of equilibrium 1. The sharp fluorimetric titration curves show that the formation of CNH_3^+ is completed within the lifetime of the excited neutral species.

The value of pK_a^* (1) obtained using Förster cycle and absorption data does not agree with that obtained by Tichy et al,[84]
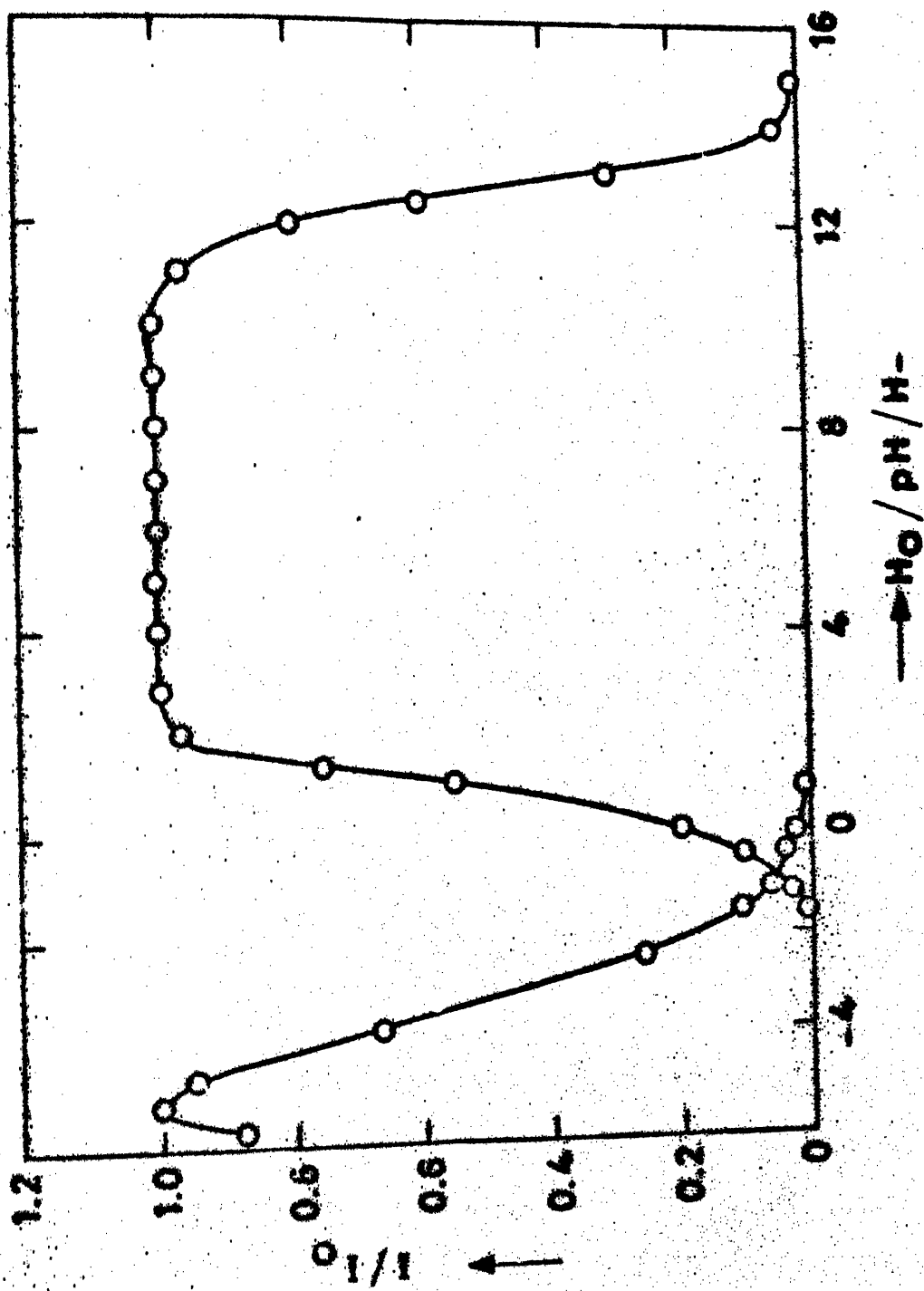
Fig. 4.3   Plot of I/I_o as a function of $H_o/pH/H_-$ of CNH_2 at 298K.

employing the same procedure. This difference could be due to a different assignment of $\bar{\nu}_{CNH_3^+}$ and $\bar{\nu}_{CNH_2}$ in absorption spectra. The absorption spectrum of the former is very sharp with three peaks of almost equal intensity whereas that of the latter is a very broad band. The fluorescence spectrum of two species are better behaved than the absorption one. The difference of 0.77 units between the pK_a^* (1) values, determined with the Förster cycle method using fluorescence band maxima and that calculated from fluorimetric titrations may be due to the difference in the solvent relaxation of the excited conjugate acid-base pair in highly concentrated acid solutions or use of band maxima rather than 0-0 transitions. The agreement between the pK_a^*(FT) and pK_a^*(ave) for equilibrium 1 may be due to the cancellation of solvent relaxation in the ground and excited states, acting in opposite directions.

The lack of correspondence between the onset of the fluorescence quenching of CNH_2 and the appearance of CNH_3^+ fluorescence clearly indicates that the fluorimetric titration curves do not describe a simple conjugate acid-base pair equilibrium in S_1 electronic state.[112] Rather, these curves indicate proton induced quenching of CNH_2 fluorescence at moderate $[H^+]$, and it has been shown that this process competes with the proton transfer reaction. Similar behaviour has been observed in many aromatic amino compounds.[106-112] Although under these circumstances an accurate value for the pK_a^* of equilibrium 1 can only be determined using

time dependence fluorimetry, the mid-point of CNH_3^+ fluorescence curve will not be far from the true value.

The kinetic model by Tsutsumi et al[112], has been discussed earlier (P.110). The lifetime of CNH_2 was calculated using the Strickler and Bergs[116] equation and was found to be 5.6 ns. The lifetime of CNH_3^+ is found to be 50 ns. Now under the conditions $\tau_o(CNH_3^+) > \tau_o'(CNH_2)$ and $[H^+]$ is quite small, the equation 4.21 (P.112) is valid. Accordingly $[(\phi_o/\phi)-1]$ has been plotted against $[H^+]$ in Fig. 4.4 and the value of $k_q \tau_o'$ obtained from the slope is 8.1 dm^3 mol^{-1}. The value of k_q thus obtained is 1.5 x 10^9 mol^{-1} $dm^3 s^{-1}$ which is of the same order of magnitude as that observed for other amino compounds (10^8-10^9 $dm^3 mol^{-1} s^{-1}$).[106-112]

The fluorescence of the neutral molecule is again quenched when the pH is increased above 10 and quenching is complete at pH 14.

This may be due to the formation of the CNH^- species as the imino-anions of aminopyridines,[122] aminoquinolines,[57-60] 9-phenanthrylamine,[120] and 5-aminoindazole[49] are known to be nonfluorescent. The mid point of this quenching occurs at pH 12.6, which is the pK_a^* for equilibrium (2) between the neutral molecule and CNH^-. This indicates that CNH_2 is more acidic in S_1 state than in S_o state, as has been found for other aromatic amines. Unlike 9-phenanthrylamine,[120] α- and β-naphthylamines,[121] the dianion of CNH_2 is not formed at all even at H_-16, or if it is formed under such conditions, it does not emit.
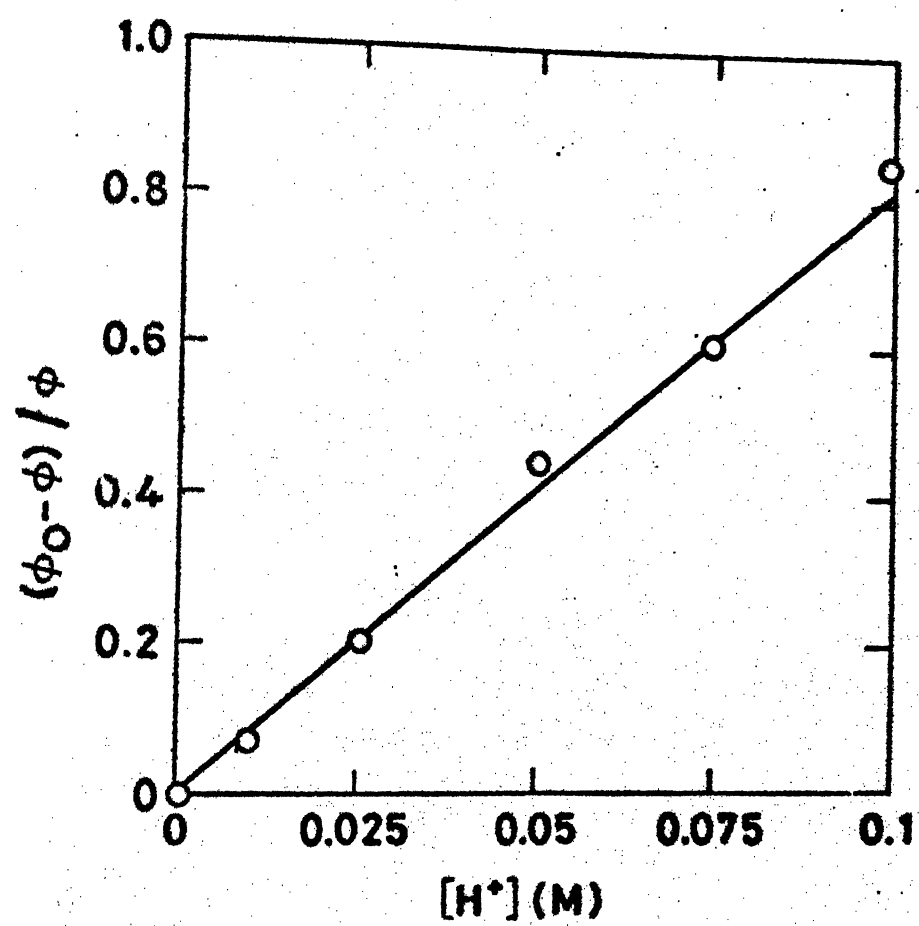
Fig.4.4   Plot of $(\phi_0-\phi)/\phi$ vs. $[H^+]$.

4.8.2   3-Aminofluoranthene(FNH$_2$)[148]

Due to the poor solubility of FNH$_2$ in water, the prototropic equilibria (1) and (2) have been studied in 30% methanol/water mixture.

$$FNH_3^+ \xrightleftharpoons{1} FNH_2 + H^+ \qquad (4.26)$$

$$FNH_2 \xrightleftharpoons{2} FNH^- + H^+ \qquad (4.27)$$
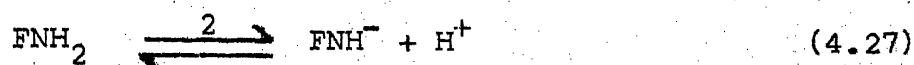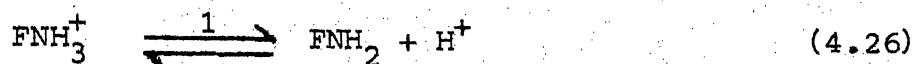
The absorption spectra of FNH$_2$ in this media have been recorded in the basicity/acidity range of H$_o$-6 to H_16. The absorption spectra of FNH$_3^+$ cation is blue shifted, structured and resembles that of fluoranthene,[123] as expected (Fig. 4.5). The pK$_a$ (1) is found spectrophotometrically to be 3.15. The agreement with the literature value of 2.85 (50% methanol/water) is quite good.[125] The pK$_a$ (2) could not be calculated as there was no significant change in the absorption spectra even upto H_16, indicating that pK$_a$(2), similar to other amino compounds and CNH$_2$, is greater than 16.[119-120]

The fluorescence spectra of FNH$_2$ have been studied in the range of H_-6 to H_16 in 30% methanol-water. Only the neutral and cation species were observed to fluoresce (Fig. 3.5, P.46). The absorption and fluorescence maxima of different prototropic forms are given in Table 4.3. The fluorescence of FNH$_2$ was quenched after H_14 and emission from no other species was detected even

148. A.K. Mishra and S.K. Dogra, J. Chem. Soc. Perkin Trans.II, in press.
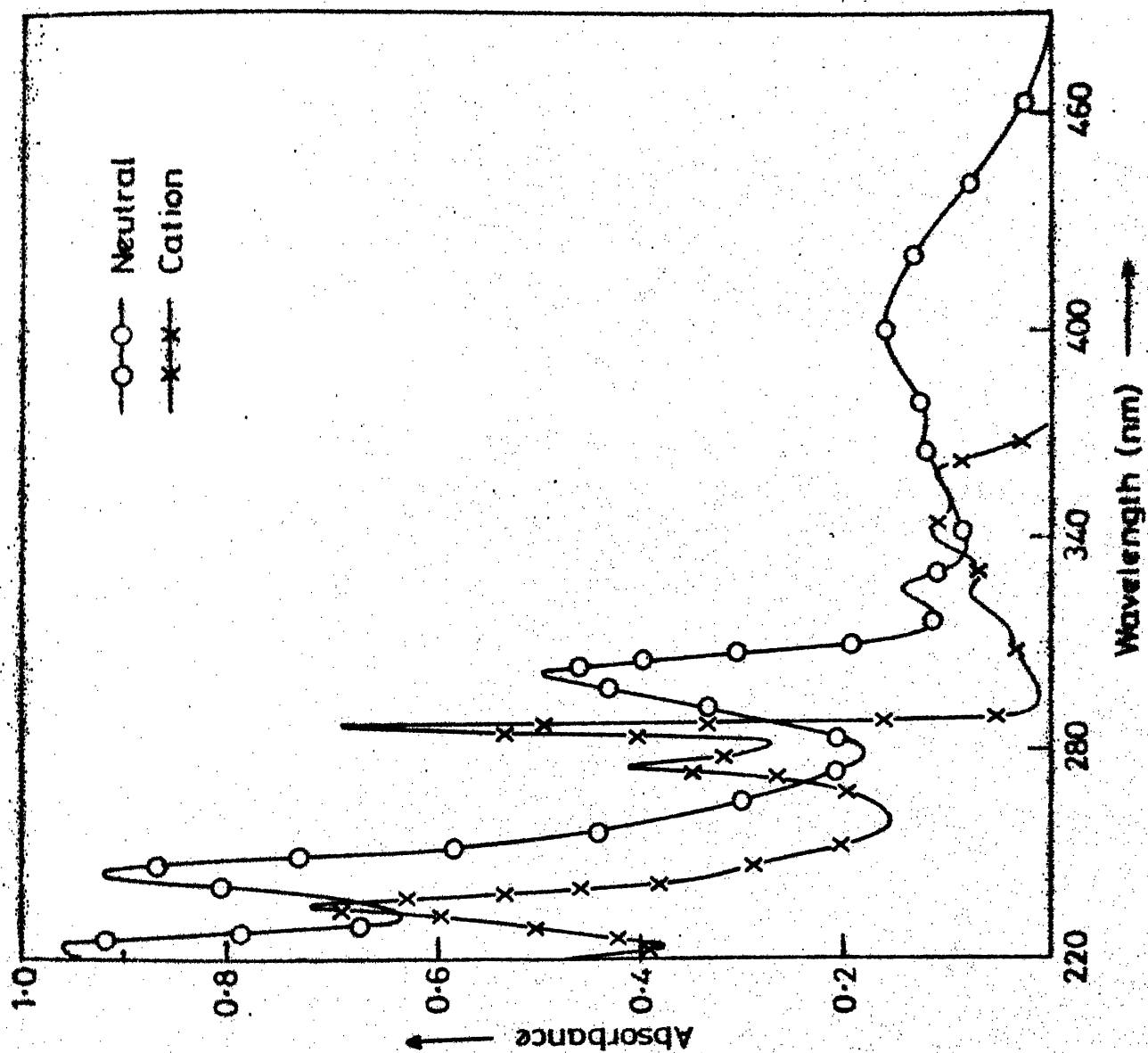
Fig.4.5   Absorption spectra of various prototropic forms of
FlH₂ at 298K

Table 4.3. Absorption maxima and fluorescence maxima $(\emptyset_f)$
of different prototropic forms of FNH_2 at 298K.

Forms	abs λ_{max} (nm)	flu λ_{max} (nm) $\emptyset_f$	
Neutral	220 244 325 366 300 406	535	0.150
Cation	207 234.5; 274.5 285.6; 310 323 342 357	475	0.224

Table 4.4. Ground and excited state equilibria of FNH_2 at 298K

Equilibrium	pK_a	Fostercycle method (approximate)	pK_a^*(FT)	$\lambda_{isosbestic}$ (nm)
		pK_a^*(FI) pK_a^*(DA)		
Cation ⇌ Neutral	3.15	-1.8 -1.5	-2.2	364
Neutral ⇌ Anion	>14	- -	13.8	

upto H_{-16}. As said earlier, the absorption spectrum of FNH_3^+ resembles that of fluoranthene very closely, and it has also been noted that band reversal takes place between the longest wavelength absorption bands of fluoranthene, when amino group is substituted at 3-position,[85] so FNH_3^+ emits from different electronic state than FNH_2. So, strictly speaking, Förster cycle method, employing absorption or fluorescence data, cannot be used with accuracy. Moreover even using high concentration ($\sim 10^{-3} M$), it was not possible to identify properly the much less intense longest wave-length absorption bands of FNH_3^+, which is buried under the relatively more intense second band. The ground and excited state equilibrium values are listed in Table 4.4.

The fluorimetric titration curve is shown in Fig. 4.6. The appearance of fluorescence intensity of the cation and the disappearance of fluorescence intensity of the neutral species do not exactly correspond each other i.e. the two curves do not intersect exactly at the middle (50%) but at $\sim 35\%$, indicating that a very slight proton induced quenching of the neutral species may be taking place. The $pK_a^*(1)$ has been calculated from the formation curve of FNH_3^+ and the value obtained is -2.2. This behaviour of FNH_2 is quite different from other aromatic amines, where there is no correspondence of the disappearance of neutral amines and the appearance of the respective ammonium ion. As stated in the case of CNH_2, appreciable proton induced quenching of neutral arylamines at moderate hydrogen ion concentrations[112] is observed. As has
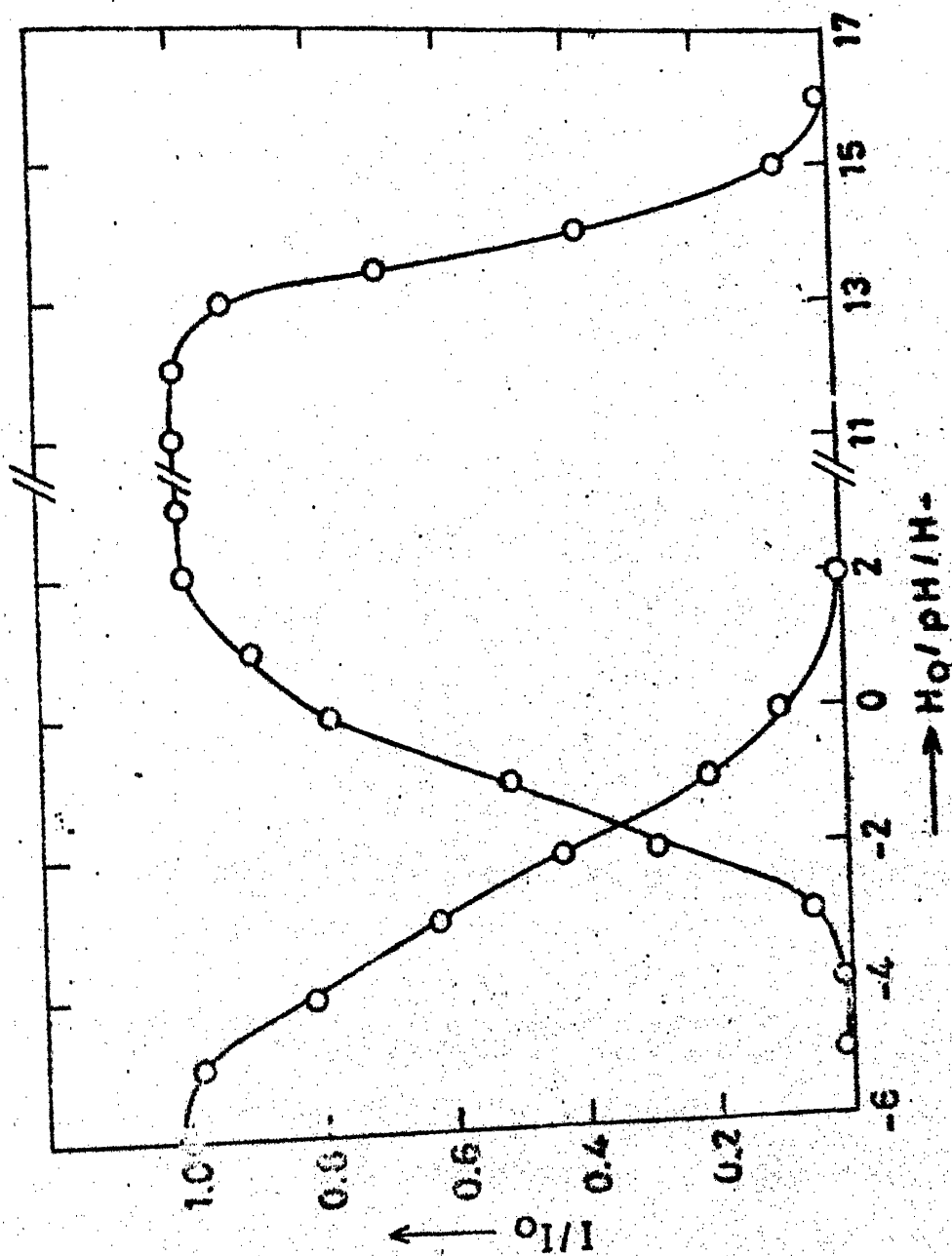
Fig.4.6 Plot of I/I_o as a function of $H_o/pH/H_-$ of FNH_2 at 298K.

been discussed earlier in this chapter this quenching has been
attributed to (i) intramolecular charge transfer and (ii) electro-
phillic protonation at one of the carbon atoms in the excited state.
In the present case, it has been shown, by theoretical calculati-
ons,[118] from infrared data[124] and the pK_a measurements[125] that the
conjugative power (i.e. charge transfer interaction) of amino
group in fluoranthene at position 3 is maximum, thus indicating
that fluoranthene differs from the usual benzenoid hydrocarbons
and behaves as non-alternant even in ground state. In other words
there is a significant interaction between the benzene and naphtha-
lene portions of the molecule. Though no data about the charge
densities at the nitrogen atom, at each carbon atom and the vibra-
tional frequencies in S_1 state, regarding FNH_2 molecule, are
available, the $pK_a^*(1)$ has shown that arylammonium ion is a stronger
acid in S_1 than in S_0. This means that charge migration will be
more in the excited singlet state, thereby fulfilling the first
condition. On the other hand, fluorimetric titrations have also
indicated that the rate of proton induced quenching of the fluores-
cence intensity of FNH_2 is much smaller than the rate of protonation,
depicting clearly that the interaction between the benzene and
naphthalene rings is also strong even in S_1. Due to this, the
charge density at the proper carbon atom of the fluoranthene will
not be large since the migrated charge will be widely distributed
on the carbon atoms of the ring. This means that the electrophillic
protonation at one of the carbon atom of FNH_2 will be locally
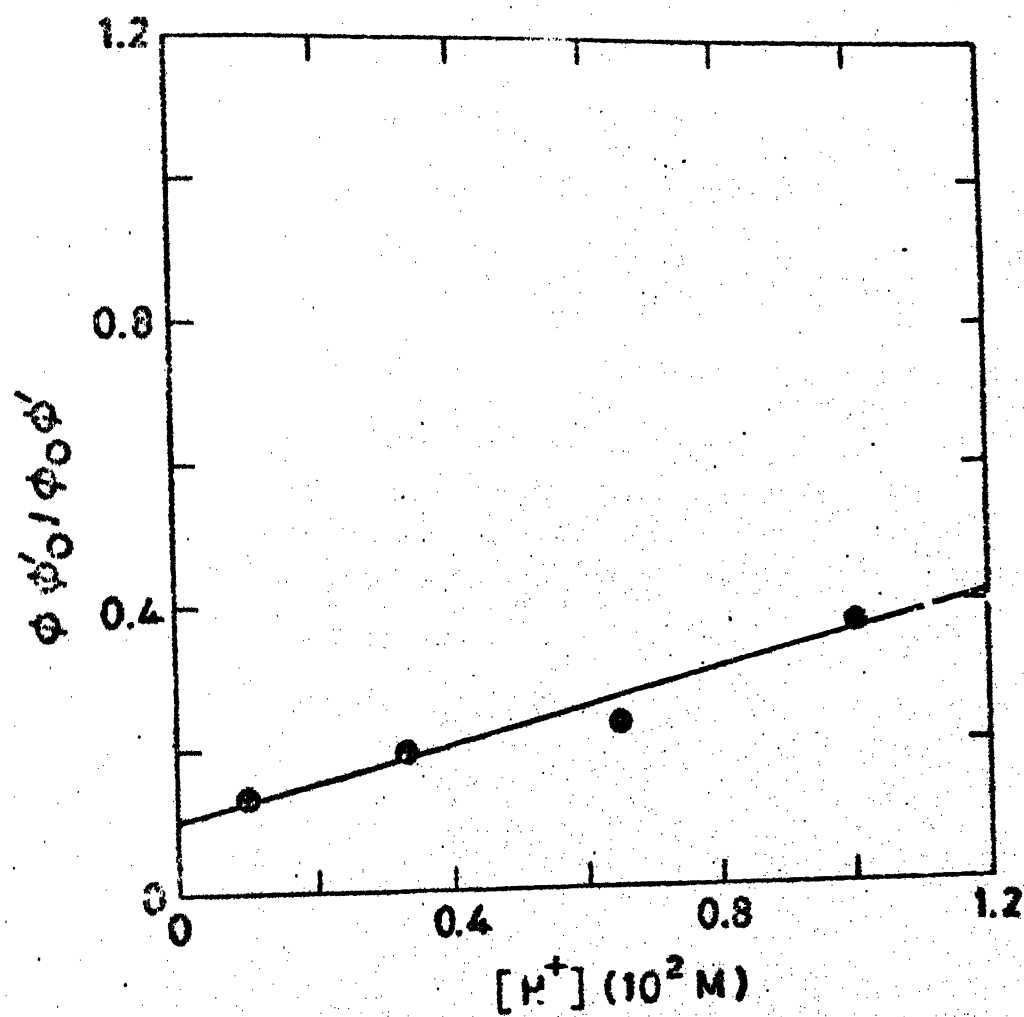
Fig.4.7   Plot of $\phi\phi_0'/\phi_0\phi'$ vs. $[H^+]$.

fluoranthene molecule is 210 ns.[127] Multiplying this by the fluorescence quantum yield of FNH_2 in water (0.15) gives an approximate molecular fluorescence lifetime of 35 ns. Taking τ_o' to be 35 ns and under first approximation, neglecting k_q', the value of k_1' obtained is $8.9 \times 10^6 Ms^{-1}$, whereas that of k_1 is $2.9 \times 10^8 s^{-1}$. The value of $pK_a^*(1) = -\log(k_1/k_1')$ thus calculated is -1.51. The agreement between the values of $pK_a^*(1)$ obtained by the later method and that obtained from the midpoint of the formation curve of FNH_3^+ is too good to believe, considering the inaccuracies in τ_o and τ_o', but one thing is certain that $k_q << k_1'$.

The fluorescence of the neutral molecule is again quenched when pH is increased above pH 13 and quenching is complete at H_16. The quenching is due to the formation of anion and $pK_a^*(2)$ obtained from the midpoint is at 13.8, indicating that FNH_2 is more acidic in S_1 than in S_o, as noticed for other arylamines.

4.8.3   6-Aminoindazole(INH_2)

Absorption spectra of INH_2 have been recorded in the basicity and acidity range of H_16 to H_o-10. Four ground state prototropic species, a dication(I), a monocation(II), the neutral molecule(III), and an anion(IV) have been observed. The absorption spectra of these four species have been depicted in Fig. 4.8, and the $\lambda_{max}^{(abs)}$ are listed in Table 4.5. The absorption spectral shifts due to the formation of various species at different H_o/pH/H_ values is

Fig. 4.8 Absorption spectra of various prototropic forms of
INH, at 298K.

Legend:
- Dication (I)
- Monocation (II)
- Monoanion (IV)
- Neutral (III)

Axes: Absorbance (vertical, 0.1 – 0.6), λ(nm) (horizontal, 240 – 360)

131
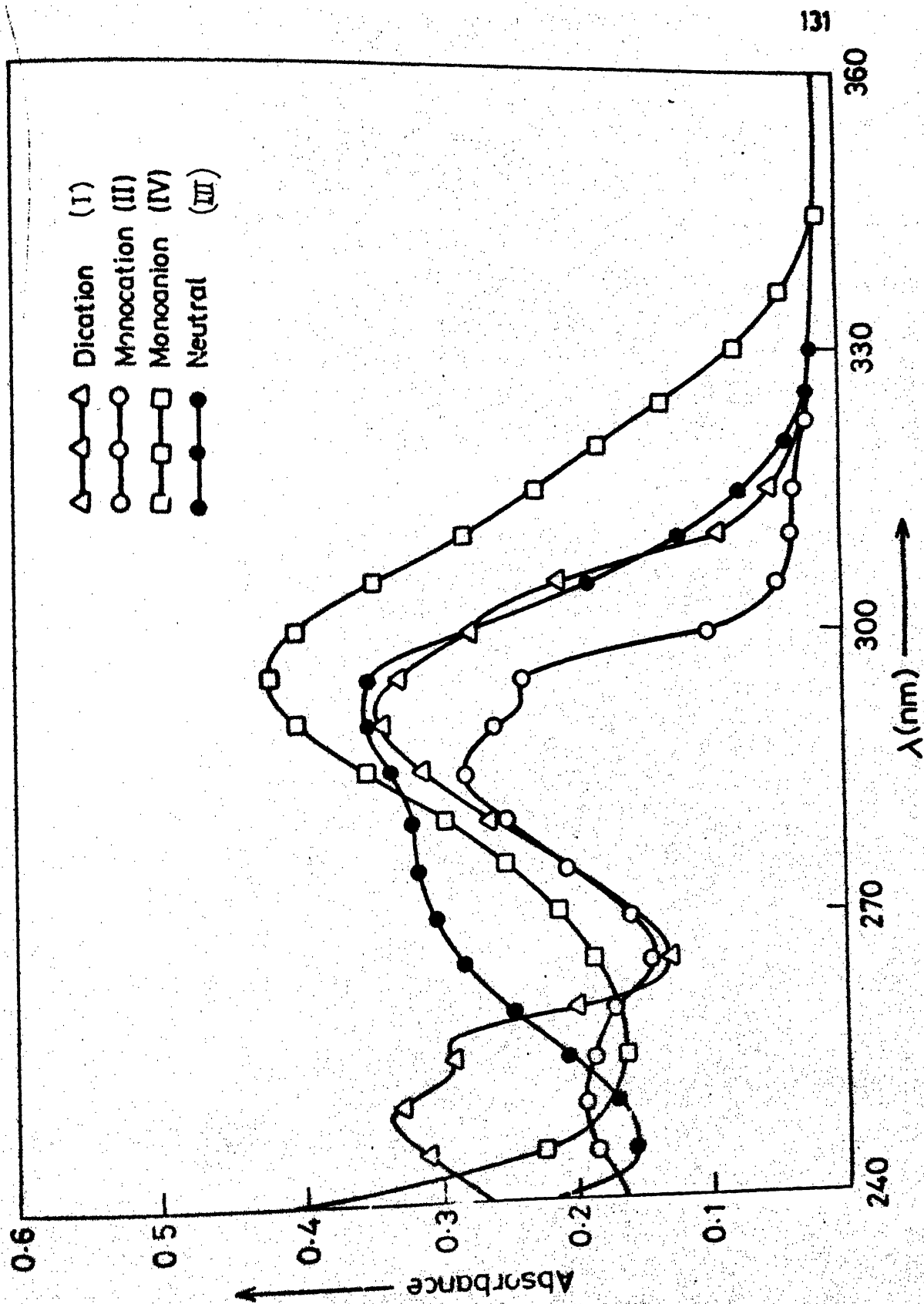
Table 4.5. Absorption maxima (log ε_{max}) and fluorescence
maxima ($\emptyset_f$) of different prototropic forms of
INH_2 at 298K.

Forms	abs(nm) λ max (log ε_{max})				flu(nm) λ max	$\emptyset_f$
Dication	249 (3.70)	256 (3.64)	291.5 (3.65)	302 (3.70)	365	0.14
Monocation*	249 (3.48)	256 (3.43)	285 (3.64)	292 (3.56)	425	0.31
Neutral	225 (4.26)	275 (3.67)	289 (3.78)	294	370	0.39
Anion			295 (3.80)		365 (77K)	

* The other monocation formed in the excited state fluoresces at
320 nm.

Table 4.6. Ground and excited state equlibria of INH_2 at 298K

Equilibrium	pK_a	pK_a^*(FT)	$\lambda_{isosbestic}$(nm)
Dication(I) ⇌ Monocation(II)	0.12	-	272
Dication(I) ⇌ Monocation(V)	-	-4.80	272
Monocation(V) ⇌ Monocation(II)	-	1.40	-
Monocation(II) ⇌ Neutral(III)	3.9	3.9	265
Neutral(III) ⇌ Anion(IV)	14.3	12.4	283
)) Anion(VI)	-	↓	

very small, which is in accordance with the solvent shifts thus reiterating the earlier conclusion that in S_o, the resonance effect (i.e. charge transfer interaction) of the lone pair of amino group is not very large. On decrease of pH from 7, the absorption spectrum of INH_2 gets slightly blue shifted and the structured spectrum resembles that of indazole.[121]. This indicates that the first protonation takes place at the amino group, similar to that observed in other arylamines.[129] On further decrease of pH, the absorption spectrum is slightly red shifted to that of monocation. This could be due to the protonation at the pyridinic nitrogen atom because similar behaviour is noticed when the protonation takes place at the similar nitrogen atom of pyrazoles[130,131] and aminoquinolines.[57-60] On increase of pH from 7, the absorption spectrum of the anion is slightly red shifted as compared to that of neutral species and could be due to the formation of anion by deprotonation of the pyrrolic nitrogen atom because as stated earlier, the deprotonation from an exocyclic amino group in the ground state usually takes place at H_- value > 16.[119-120] From the above results the various prototropic reactions in the ground state can be written and are shown in Fig. 4.10. The various ground state equilibrium constants (pK_a) are listed on arrows and in Table 4.6. The value of pK_a obtained for monocation (II)-neutral species equilibrium agrees nicely with the literature value.[132] Further the values of pK_a for monocation (II)-neutral form and neutral-monoanion (IV) form are slightly greater than those of
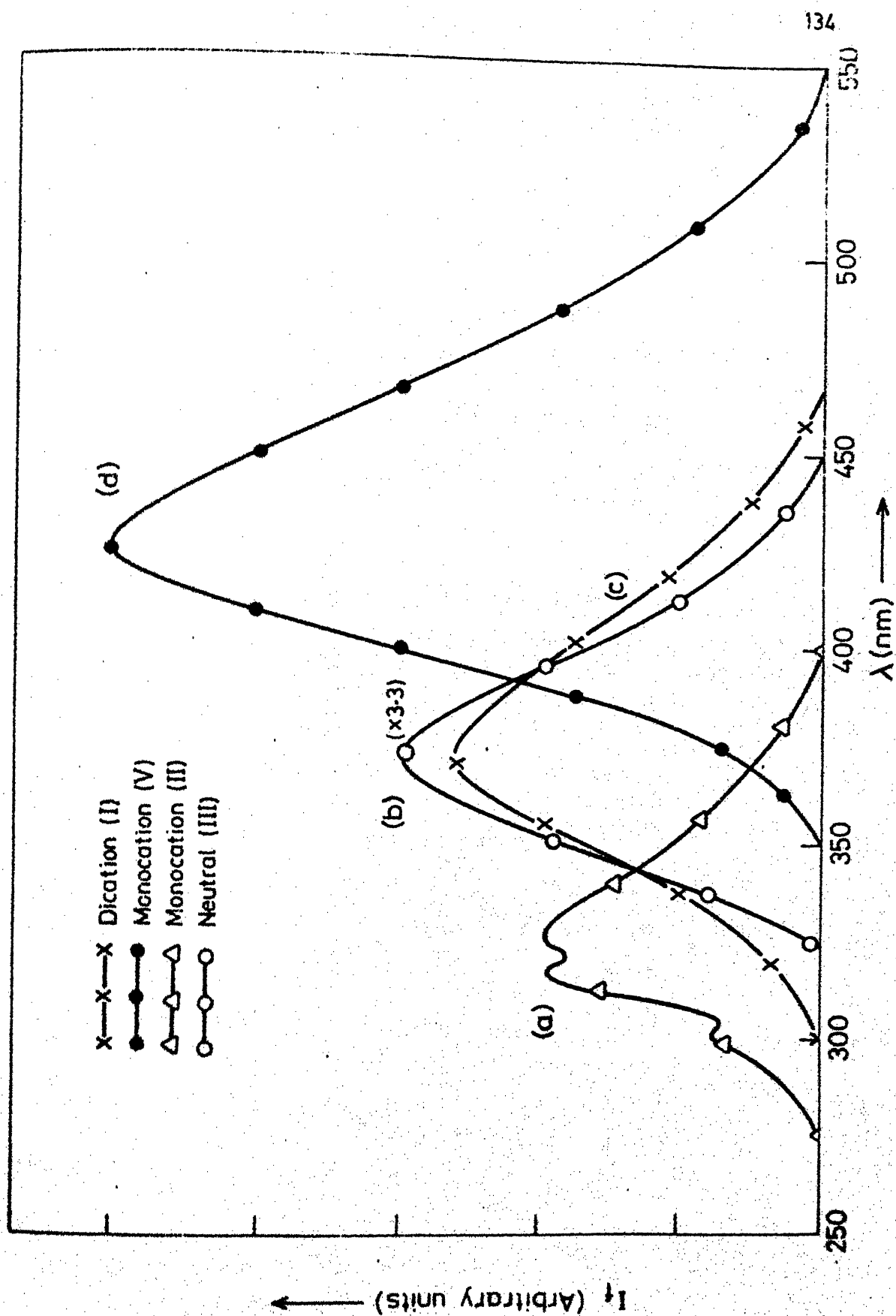
134

Fig.4.9 Fluorescence spectra of various prototropic forms of INH_2 at 298K.
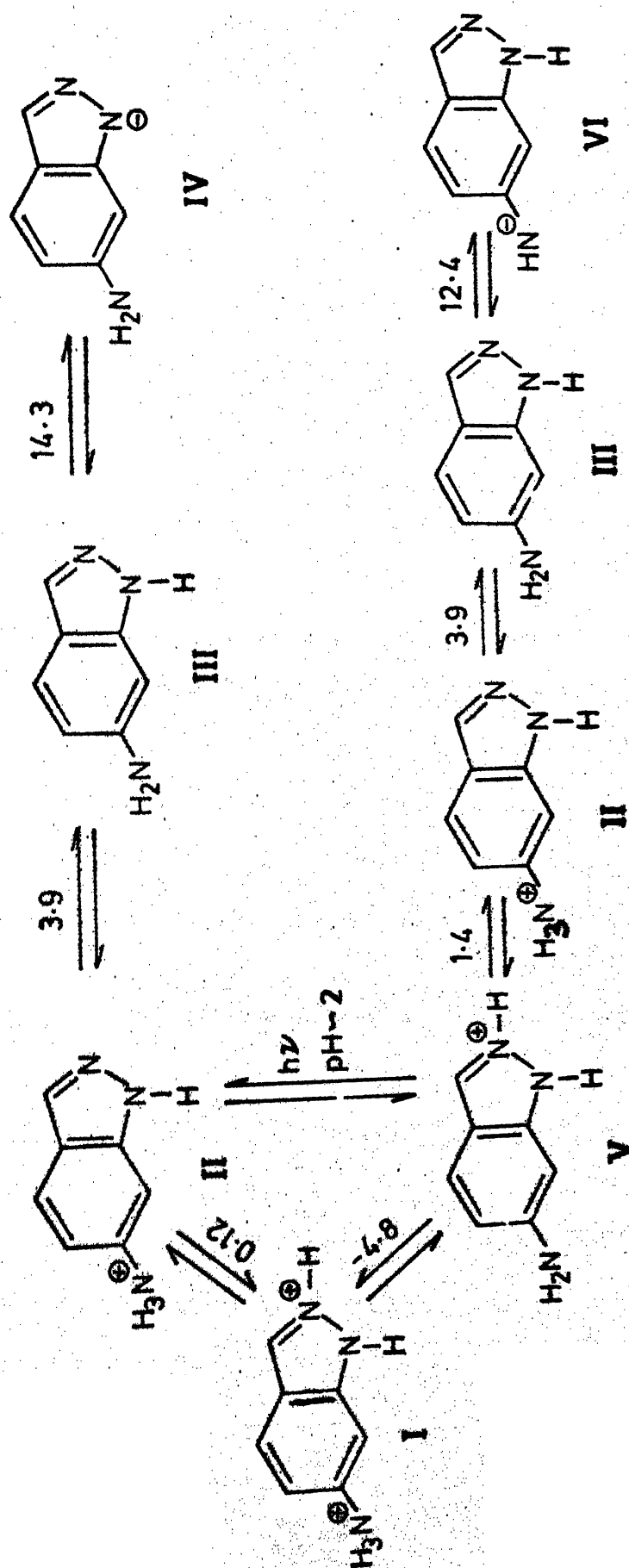
Fig. 4.10 Scheme of Ground and Excited State equilibria of INH$_2$ at different H$_o$/pH/H$_-$.

indazole.[132,86] This is consistent with the theory that the electron donating groups, such as amino and methyl , increase the basicity of the molecule.[133]

The fluorescence spectra of INH_2 have been studied in the range of H_-16 to H_o-10. The neutral species, in the pH range of 6 to 11, showes the fluorescence maxima at 370 nm. When the pH is lowered below 6, the intensity of 370 nm band starts decreasing and is quenched completely at pH 3. In this range of pH, a new blue shifted, structured fluorescence band with maxima at 320 nm starts appearing which resembles the spectrum of indazole molecule.[86] Like the ground state protonation reaction, the species present in S_1 state seems to be a monocation protonated at the amino group as it is well known that in the $\pi^* \longleftarrow \pi$ transitions, the protonation at the amino group of aromatic molecules leads to a blue shift and the fluorescence spectrum resembles with that of the parent molecule. A further decrease of pH results in the quenching of 320 nm bond, with simultaneous appearance of a new broad, structureless and red shifted band at 425 nm. The quenching of the former band is complete at a pH 0.0 and the formation of the latter band is complete at $H_o-0.5$. A further increase in the hydrogen ion concentration results in the decrease of fluorescence intensity of 425 nm band and is completely quenched at H_o-3. At H_o-2, a new fluorescence band is observed at 365 nm. Since in the INH_2 molecule there are only two probable sites of protonation, the band at 425 nm could be due to a monocation protonated at the

pyridinic nitrogen atom and the band at 365 nm could be due to the formation of a dication. On the other hand when pH is increased from 11 onward, the fluorescence intensity of 370 nm band stands decreasing and is completely quenched at pH 14, without the appearance of any other fluorescence band. The quenching seems to be due to the formation of monoanion. No fluorescence band is observed at 298K On further increase of pH, even upto H_{-16}. Fluorescence spectra of all the ionic species formed in the excited state are shown in Fig. 4.9. All the excited state equilibria are discussed below.

(a) Excited state equilibrium between the monocation(II) and neutral(III) form

In the earlier paragraph, 320 nm band had been assigned to the amino protonated species. To suppliment this, the indazole- ammonium chloride was prepared and its absorption and fluorescence spectral properties were studied. The results were quite interesting and are discussed latter, but they support the assignment of species II. The relative fluorescence intensity of both the forms versus pH are plotted in Fig. 4.11. It shows the point of intersection at pH 3.9, which is close to the ground state value. This behaviour of INH_2 is very different from other aromatic amines[57-60,106-112] (where the ammonium ion is stronger acid in S_1) and from 5-aminoindazole[49] (where the first protonation takes place at the pyridinic nitrogen atom in S_1). This only tells that the

138
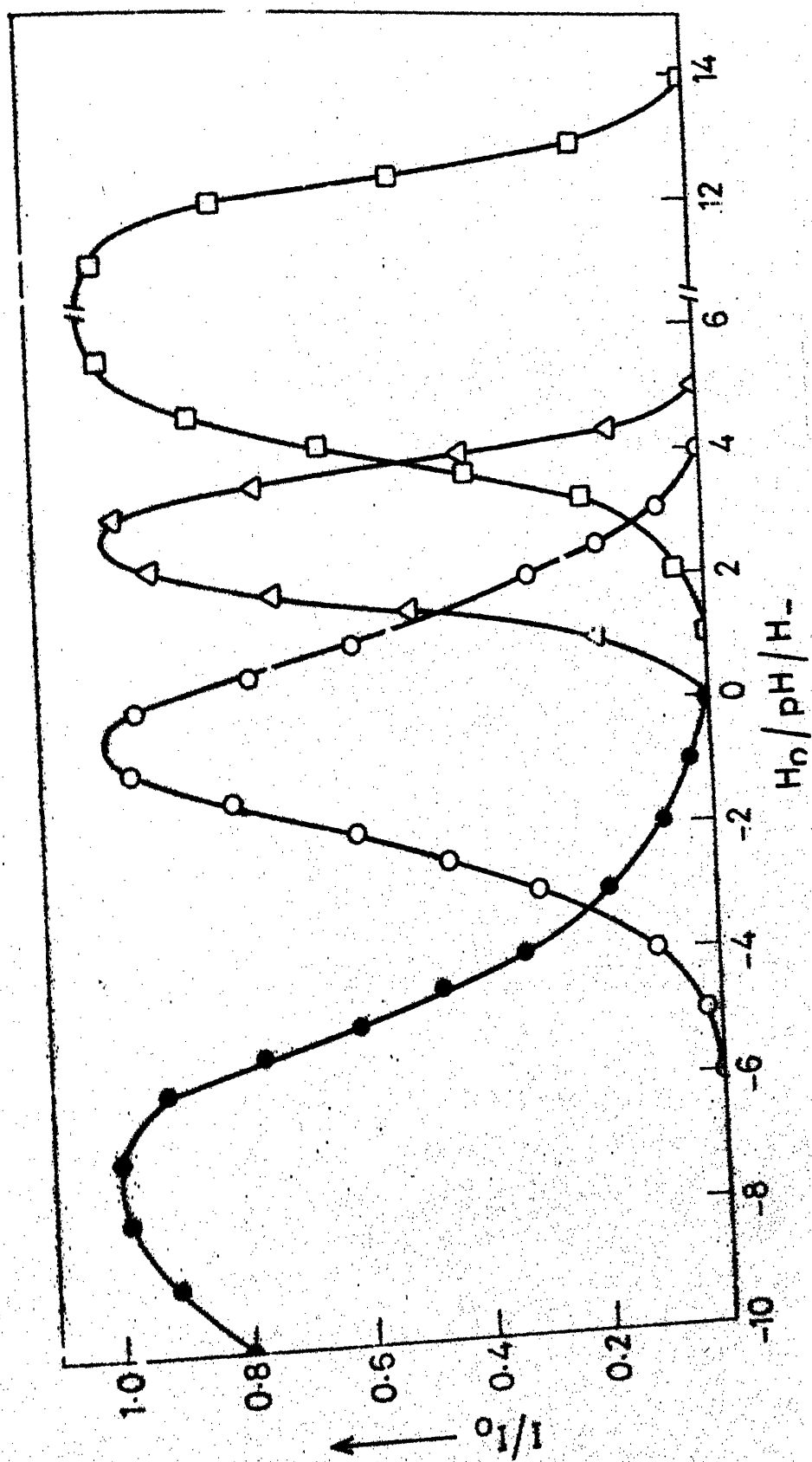
Fig. 4.11 Plot of I/I_o as a function of $H_o/pH/H_-$ of INH_2 at 298K.

radiative lifetime of the species INH_3^+ is comparable to the inverse of the dissociation rate constant of the given acid.

(b) <u>Equilibrium between indazole ammonium ion(II) and 6-aminoindazole cation(V)</u>:

In the pH range 3.9 to 0.12, only the species(II) is present at 298K in aqueous media in S_o. But as said earlier, there are two species present in S_1, one emitting at 320 nm and another at 425 nm, 320 nm band has already been discussed. The new band has been assigned to a monocation protonated at the pyridinic nitrogen atom (H^+INH_2, V). The identity of this species is further confirmed by taking absorption and fluorescence spectra of INH_2 in n-heptane and 0.01M trifluoroacetic acid. In this media only the species V is present in both S_o and S_1 states, as shown in Figs. 4.8 and 4.9. Further the fluorescence spectrum of INH_2 in this pH range and at 77K, shows only one band at 320 nm, corresponding to species II. Thus confirming the earlier results from the absorption spectrum that species II is the only ion in S_o and rearrangement of atoms is not possible in frozen state at low temperature. These results indicate that INH_3^+ dissociates in fluid aqueous state and the proton is taken up by the pyridinic nitrogen atom, forming H^+INH_2(V). Thus an equilibrium is established between the species II and V. This process could be assigned to a phototautomerism and since the two groups, protonated amino group and protonated pyridinic nitrogen atom, are widely separated, the phototautomerism could be biprotonic. The solvent dependence of the

monocations could not be studied because both species II & V are present even in S_0 state and their absorption spectra overlap each other. Hence it becomes difficult to conclude whether increase or decrease in the fluorescence intensity is due to the ground state absorbance or excited state dissociation. But it clearly reveals that it is due to the increase in the acidity of the amino group and gain in the basicity of the pyridinic nitrogen atom. This process is similar to that observed in 5-aminoindazole[49] with the difference that the reciprocal of rate constant of deprotonation of 5-indazoleammonium ion is much smaller than its radiative life-time. So the fluorescence from 5-aminoindazole (neutral) and its cation protonated at the pyridinic nitrogen atom is observed.

The relative fluorescence intensity of both the species versus pH is plotted in Fig. 4.11. The point of intersection at pH 1.4 gives the pK_a^* value of this equilibrium.

(c) Equilibrium between the Monocation(V) and the dication(I)

The H^+INH_2 cation has the fluorescence maximum at 425 nm whereas that of the dication is at 365 nm. The blue shift in the fluorescence maximum upon protonation indicates that it has taken place again at the amino group. The fluorimetric titration curve is in the Fig. 4.11. A lack of correspondence similar to aromatic amines[129,106-112] can be seen in the titration curve. This is due to proton induced quenching of the monocation as has been discussed

in earlier compounds. The accurate values of the pK_a^* and the quenching rate constant of H^+INH_2 species can only be calculated from the time dependence fluorimetry but the value of pK_a^* obtained from the rise in the formation of dication curve (-4.8) will not be too much off from the actual value. The value of pK_a^* obtained reiterates our earlier conclusion that this time the protonation has taken place at the amino group as the pK_a^* of this kind of equilibrium generally falls in this H_o range.[49,129] Further the pK_a^* obtained for the direct protonation of amino group of the neutral molecule (-5.4, calculated by Förster cycle and the fluorescence data of INH_2 and INH_3^+) does not differ too much from the protonation of H^+INH_2 species. Though this agreement could be accidental, it tells that the first protonation at the pyridinic nitrogen atom does not affect second protonation at the amino group too much.

(d) <u>Equilibrium between the Neutral III and Anion VI</u>

The effect of increase of pH from 10 onward on the fluorescence intensity of INH_2 exactly resembles that of 5-aminoindazole i.e. at pH 10, the iminoanion VI is formed (non fluorescent) in S_1 state and not the 6-aminoindazole anion IV, formed in the ground state. This is further confirmed from the fluorescence spectrum of the anion (IV) at 77K, shown in Fig. 4.12, indicating that at such a low temperature only the ground state species will be present because of the restriction on the rearrangement of atoms
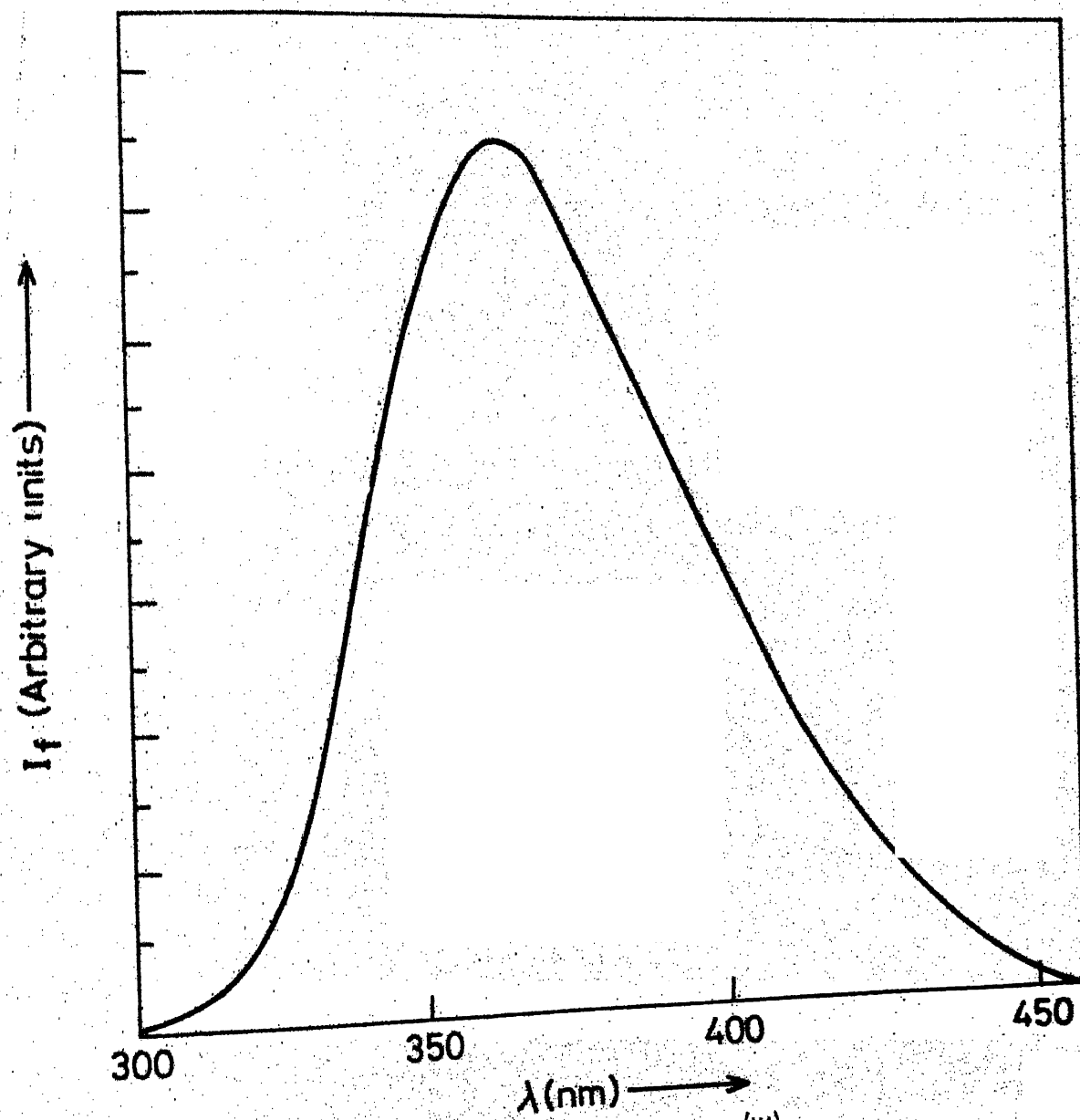
Fig.4.12 Fluorescence spectra of anion (jv) of INH_2 at 77K.

in the frozen state and moreover the fluorescence spectrum is generally observed from the species obtained by the deprotonation of the pyrrolic nitrogen atom.[130,131,134] The middle point of this quenching curve occurs at 12.4, which is the pK_a^* value for the neutral-monoanion equilibrium, showing that the aromatic amines are stronger acids in S_1 than S_0. Further increase in pH does not give rise to any fluorescence indicating that either dianion is not formed at all or it does not emit if formed.

Spectral studies of Indazoleammonium chloride (II) in different solvents

The absorption spectrum of $INH_3^+Cl^-$ has been studied in different solvents. The $\lambda_{max}^{(abs)}$ and ε_{max} are listed in Table 4.7 and the spectra are in Fig. 4.13. The absorption spectrum of $INH_3^+Cl^-$ in water exactly resembles the spectrum of indazole molecule in pH range 4 to 0.12. But in methanol and acetonitrile, besides the above structured band, a new red shifted (compared to those of $INH_3^+Cl^-$ and INH_2) and broad band appears at 315 nm, whereas in ether and dioxane, the spectrum resembles the INH_2 system. The intensity of 315 nm band increases as the hydrogen bond donating tendency of the solvent decreases i.e. it is zero in water and increases from methanol to acetonitrile. To confirm the identity of 315 nm band, the absorption spectrum of INH_2 in methanol and acetonitrile was recorded by adding 1% of 1N aqueous sulphuric acid. Exactly similar behavior (both the
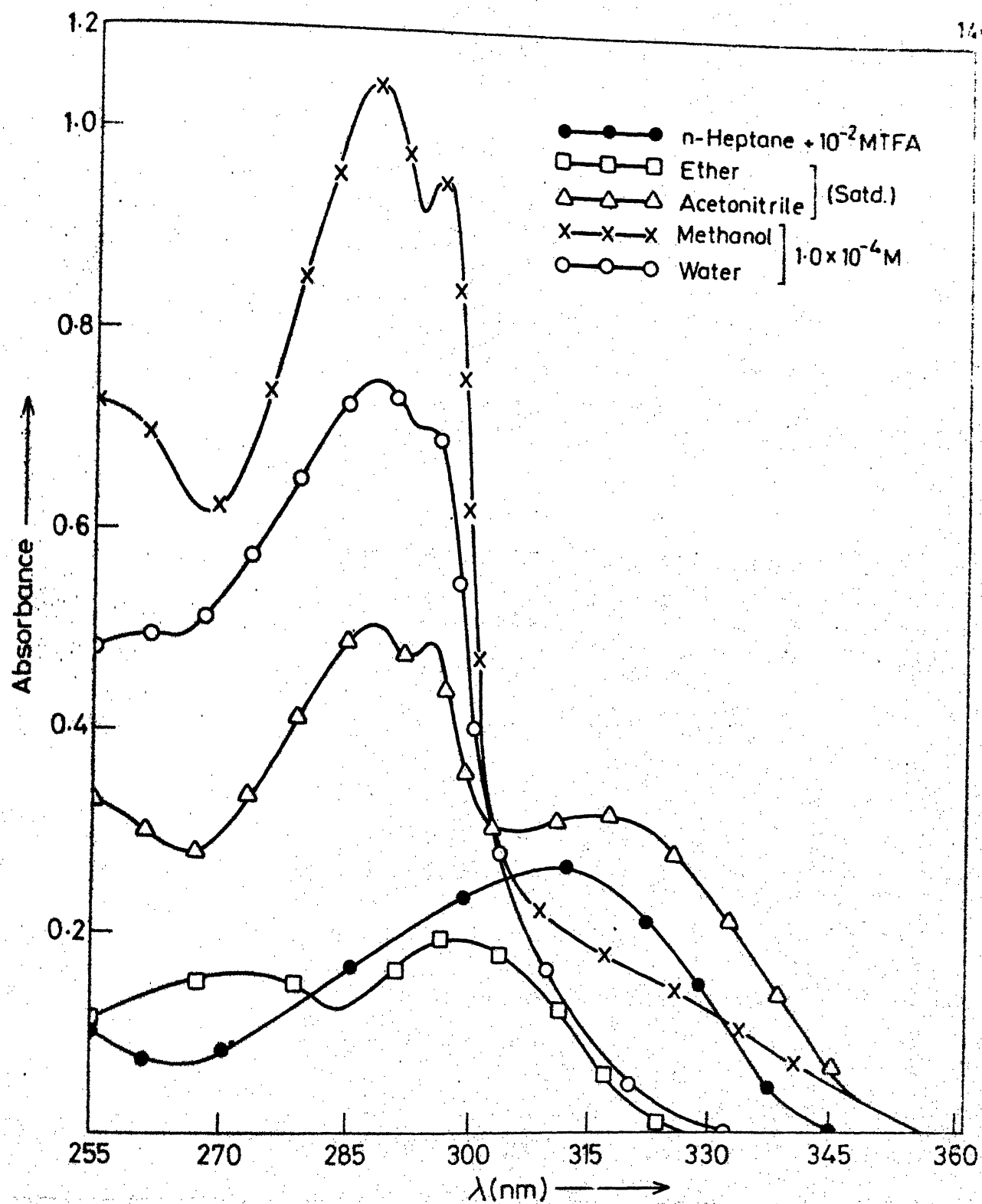
Fig.4.13 Absorption spectra of hydrochloride salt of TDH in
various solvents at 25°.

Table 4.7. Absorption maxima (log ε_{max}) and fluorescence maxima (nm) of H^+INH_2 cation in different solvents at 298K

Solvent	λ_{max}(abs)					λ_{max}(flu)	
						λ_{exc}=290nm	λ_{exc}=315nm
Ether (satd.)	250	265	275	300		350	350
Acetonitrile (satd.)	240	259	287	295	315	425 major 325	425 major 325
Methanol		260 (3.71)	287 (3.85)	296 (3.82)	315 (3.26) 250 (3.74)	410 325 major	410 major 325
Water		260 (3.52)	287 (3.69)	294 (3.68)		370 320	370 320

band systems) was observed as noticed in case of $INH_3^+Cl^-$ in methanol and acetonitrile. The absorption spectrum of INH_2 in n-heptane, 1.0×10^{-2}M in trifluoroacetic acid (TFA) gave only the 315 nm band (Table 4.8).

The fluorescence spectrum of $INH_3^+Cl^-$ in different solvents, of INH_2 n-heptane 1.0×10^{-2}M in TFA and of INH_2 in methanol and acetonitrile in 1% 1N aqueous sulphuric acid have been studied at 298K and by exciting at 315 nm and at 290 nm. The results are listed in Tables 4.7 and 4.8. It is clear from the data of Table 4.7 that $INH_3^+Cl^-$ is not stable in aqueous medium and in S_1 state at 298K, dissociates partially to neutral form, thereby getting the emission spectrum of both the neutral and INH_3^+ species. In the fluorescence spectrum of $INH_3^+Cl^-$ at 77K in aqueous medium, only one band at 320 nm is noticed. This confirms that in frozen state, the reorientation of the atoms are very slow and the emission is only observed from the excited species present in their ground state environments. Fluorescence spectrum of $INH_3^+Cl^-$ in methanol and acetonitrile at 298K as well as 77K gave again two bands, one corresponds to INH_3^+ ion, the other to a new red shifted and broad band at 425 nm, depending on the solvents. The intensities of the respective bands depend upon the nature of the solvents and the wavelength of excitation, e.g. in acetonitrile, the intensity of 425 nm band is always more than that of 320 nm band, irrespective of the wavelength of excitation whereas in methanol, the fluorescence intensity of 325 nm band is the major peak when

Table 4.8. Spectral behaviour of INH_2 in non-aqueous solvents at 298K

Solvents	$\lambda_{max}(abs)$					$\lambda_{max}(flu)$ $\lambda_{exc}=290nm$	$\lambda_{exc}=315nm$
n-Heptane +0.01M TFA	240				310	415	415
Acetonitrile +1% 1N H_2SO_4	240 (3.86)	260 (3.60)	287 (3.75)	294 (3.74)	315 (3.50)	420 major 325	420
Methanol +1% 1N H_2SO_4	245 (3.65)	260 (3.56)	287 (3.75)	295 (3.70)	315 (3.06)	415 325major	415

excited at 315 nm. This again confirms the results obtained from the absorption spectra that species with long wavelength maxima is more predominent in the solvents of weakly hydrogen bond donating ones. The existence of the species with long wavelength band is further confirmed from the fluorescence spectrum of INH_2 in heptane in 0.01M TFA where there is only one fluorescence band at 415 nm.

The above results indicate that the long wavelength band, both in absorption and fluorescence is due to the monocation of INH_2, protonated at the pyridinic nitrogen atom (H^+INH_2) of the ring.

The behaviour of $INH_3^+Cl^-$ in ether and dioxane is quite different from that in other solvents. The absorption as well as fluorescence spectra only shows the presence of neutral molecule i.e. INH_3^+ is very unstable both in S_0 and S_1 states. To see whether H^+INH_2 also behaves in a similar manner, absorption and fluorescence spectra of INH_2 in heptane 0.01M in TFA were recorded in different proportion of ether added (v/v upto 30%). The intensities of absorption and fluorescence bands of H^+INH_2 decreased drastically with the increase in the respective neutral bands. From the above results it is quite clear that ether and dioxane act as hydrogen acceptor solvents and abstract proton from INH_3^+ monocation, where as in case of H^+INH_2, ether or dioxane may be abstracting a proton from the monocation or presence of these solvents may not allow at all, the formation of H^+INH_2, because

these solvents may be completely mopping up TFA and thereby acting
as a stronger base than INH_2.

The above study has indicated that INH_3^+ is more stable in
highly polar and hydrogen bond donating solvents whereas H^+INH_2
is more stable in nonpolar and nonhydrogen-bond forming solvents,
and both are unstable in strong hydrogen bond accepting solvents
like ether or dioxane. This can be explained as follows: In case
of ammonium salt, the charge is localised on the amino nitrogen
atom and is further stabilised due to solvation by the highly polar
and hydrogen bonding solvents i.e. H_2O. As the solvent polarity
or hydrogen bond formation tendency decreases, the ammonium salt is
not so stable and forms another monocation, protonated at the
pyridinic nitrogen atom. The latter one, even in non-polar and
non-hydrogen bonding solvents like n-heptane, is stabilised due
to the following resonance phonomenon. Although the solvation can
take place in V, it seems that resonance is predominent in this
case. In contrast, this type of resonance behaviour is absent in
5-aminoindazole, thereby rendering it unstable in S_o.
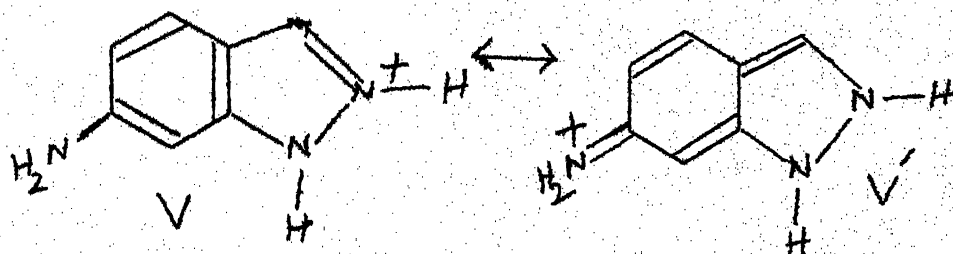
The above study, in comparison to 5-aminoindazole, has revealed the following features: i) the lifetime of INH_3^+ is comparable to the reciprocal of the rate constant of deprotonation, (ii) monocation (INH_3^+, II) is stable in water and monocation (H^+INH_2, V) is stable in n-heptane. The stability in other solvents depends on the hydrogen bond donating capacity of the solvents.

4.8.4   2-Phenylbenzimidazole(PBI)

The absorption and fluorescence spectra of PBI in different forms are given in Fig. 4.14 and their band maxima, extinction coefficients and quantum yields in Table 4.9. The following equilibria have been studied.

$$PBI^+ \quad \underset{\longleftarrow}{\overset{1}{\longrightarrow}} \quad PBI + H^+ \qquad\qquad (4.29)$$

$$PBI \quad \underset{\longleftarrow}{\overset{2}{\longrightarrow}} \quad PBI^- + H^+ \qquad\qquad (4.30)$$

The only possible site of protonation in this case is the pyridine center and as such a red shift in the absorption and fluorescence spectra on protonation is expected because it is established that $\pi \longrightarrow \pi*$ is the lowest energy transition. Contrary to the expectations a small blue shift in the long wavelength absorption band, on protonation below pH 5.2 is observed. This could be due to the partial rotation of the phenyl ring due to steric interaction of the additional proton at the pyridine or it may be due

Fig. 4.14 Absorption and fluorescence spectra of various prototropic forms of PBI at 298K.

Table 4.9. Absorption maxima (log ε_{max}) and fluorescence maxima (ϕ_f) of different prototropic forms of PBI at 298K

Forms	λ_{max}(abs) (log ε_{max})		λ_{max}(flu)	ϕ_f
Cation	240 (4.22)	295 (4.35)	358	0.14
Neutral	238 (4.15)	299 (4.36)	350	0.13
Anion	245 (4.20)	310 (4.38)	380	0.12

Table 4.10. Ground and excited state equilibria of PBI at 298K.

Equilibrium	pK_a	Föster cycle method			pK_a^*(FT)		$\lambda_{isos-bestic}$
		pK_a^* (abs)	pK_a^* (flu)	pK_a^* (ave)	buffer 0.01M	buffer 0.5M	
Cation $\rightleftharpoons$ Neutral	5.23	3.53	6.57	5.05	–	–	–
Neutral $\rightleftharpoons$ Anion	11.91	9.58	7.61	8.59	12.05	11.6	295

to normal blue shift in benzimidazole cation. A small red shift is observed in fluorescence of PBI^+ as compared to PBI. The quantum yields of PBI in different solvents, PBI^+ and PBI^- are nearly the same, indicating and as observed in fluorescence maxima that the given species do not have any specific interaction with any solvent.

The excited state pK_a's for the two equilibria were calculated using Förster cycle method and the values are given in Table 4.10. The fluorimetric titration for the equilibrium(I) could not be carried out because of too much overlap of the fluorescence spectra of cation and neutral PBI. Fluorimetric titration for the equilibrium (2) gave the ground state pK_a, clearly indicating that either the $pK_a^*(2)$ is identical to $pK_a(2)$ or the equilibrium(2) is not attained during the lifetime of the excited state species, due to their short lifetime. As has been discussed earlier, the latter seems to be true. To confirm this, fluorimetric titrations were carried out in presence of large concentration (0.5M) of phosphate buffers and no appreciable change in $pK_a^*(2)$ was noticed. Förster cycle method has shown that the PBI is more acidic in S_1 state than in S_0, as normally is the case for heterocyclic molecules when $\pi \longrightarrow \pi*$ is the lowest energy transition. The difference of 1.97 units in pK_a^* between the absorption and fluorescence data could be due to solvent relaxation and/or using the band maxima of the species rather than 0-0 transition.

The absorption data tells that PBI$^+$ is more acidic in S$_1$ than in S$_o$, whereas the fluorescence data shows the opposite behaviour. In general, as noticed, the pyridinic nitrogen atom becomes less acidic in S$_1$ if $\pi \longrightarrow \pi^*$ is the lowest energy transiton. Thus the pK$_a^*$(1) calculated using absorption data cannot be true in this case. Therefore, in absence of fluorimetric titration, the pK$_a^*$(1) determined by fluorescence data could be taken as the accurate value. The small change in pK$_a^*$(I) and pK$_a^*$(II) could be due to the presence of planar phenyl ring i.e. the electron density may be delocalized over the complete molecule, including phenyl ring, instead of only concentrating at the pyridinic nitrogen atom in the ground and the excited state.

4.8.5 2-Hydroxybenzimidazole(BIOH) and 1-methyl-2-benzimidazolinone(NMeBI)

.The absorption and fluorescence spectra of BIOH have been investigated as a function of hydrogen ion concentration in the range H$_o$-9 to H_16. The absorption and fluorescnece spectra of various species have been shown in Fig. 4.15 and 4.16 and the other data in Table 4.11. Besides BIOH (the neutral species), three new species are observed in absorption whereas only one species in fluorescent at 298K. On decrease of pH from 7, a blue shifted, structured absorption band system appears at H$_o$-2.24, which could be due to the formation of monocation. On further increase of hydrogen ion concentration, the structured band system shifts to higher wavelength with no change in the
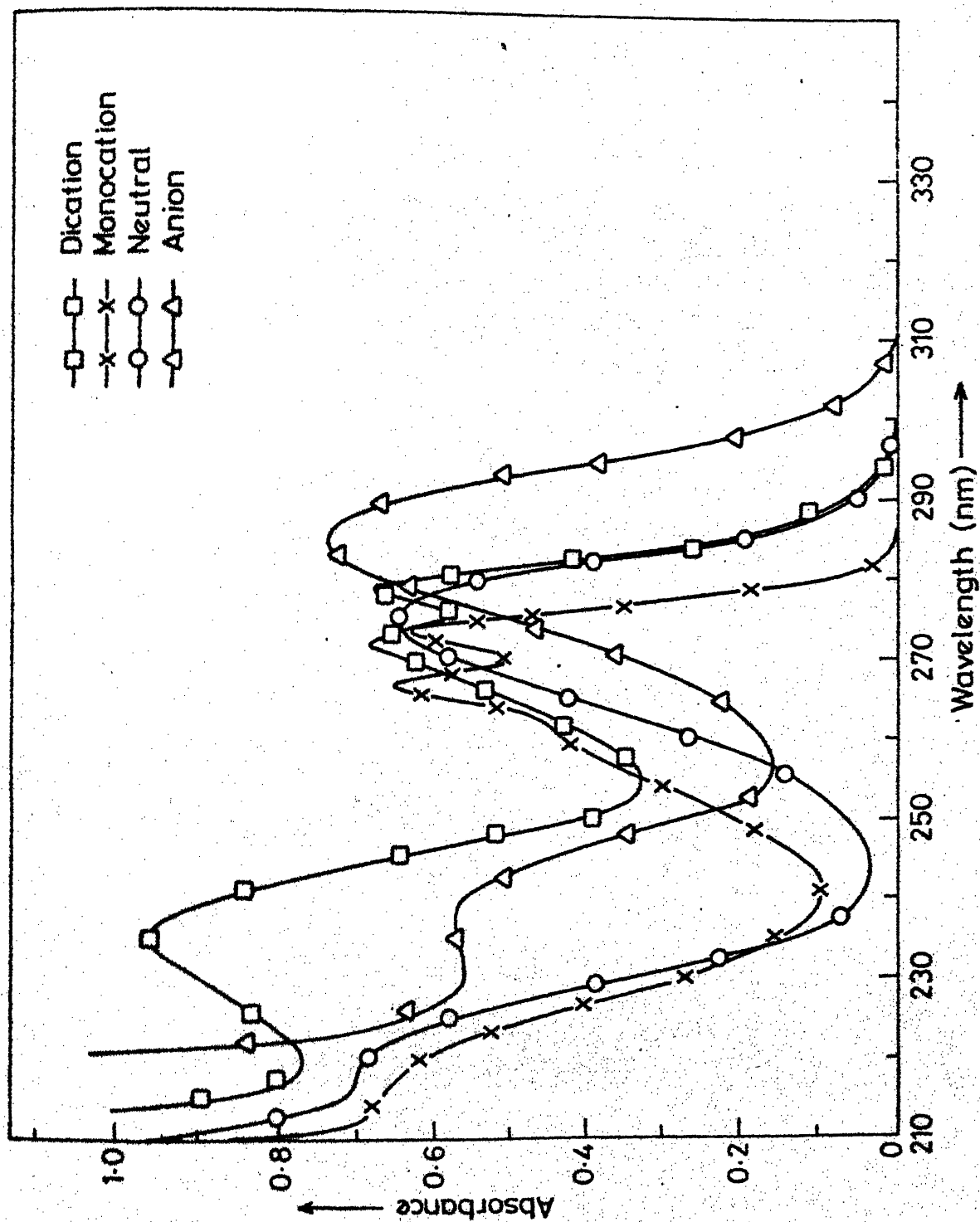
Fig.4.15 Absorption spectra of various prototropic forms of BIOH at 298K.
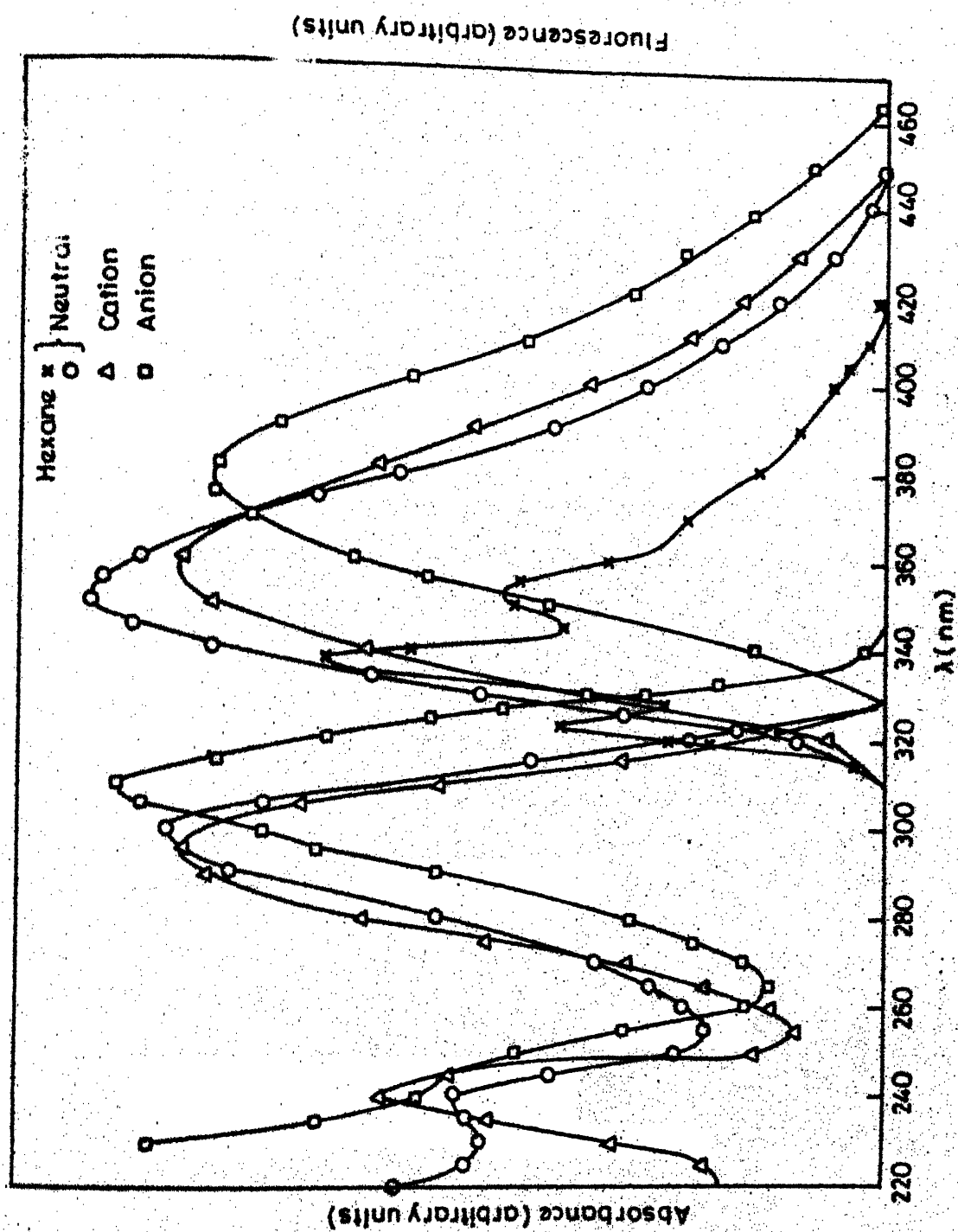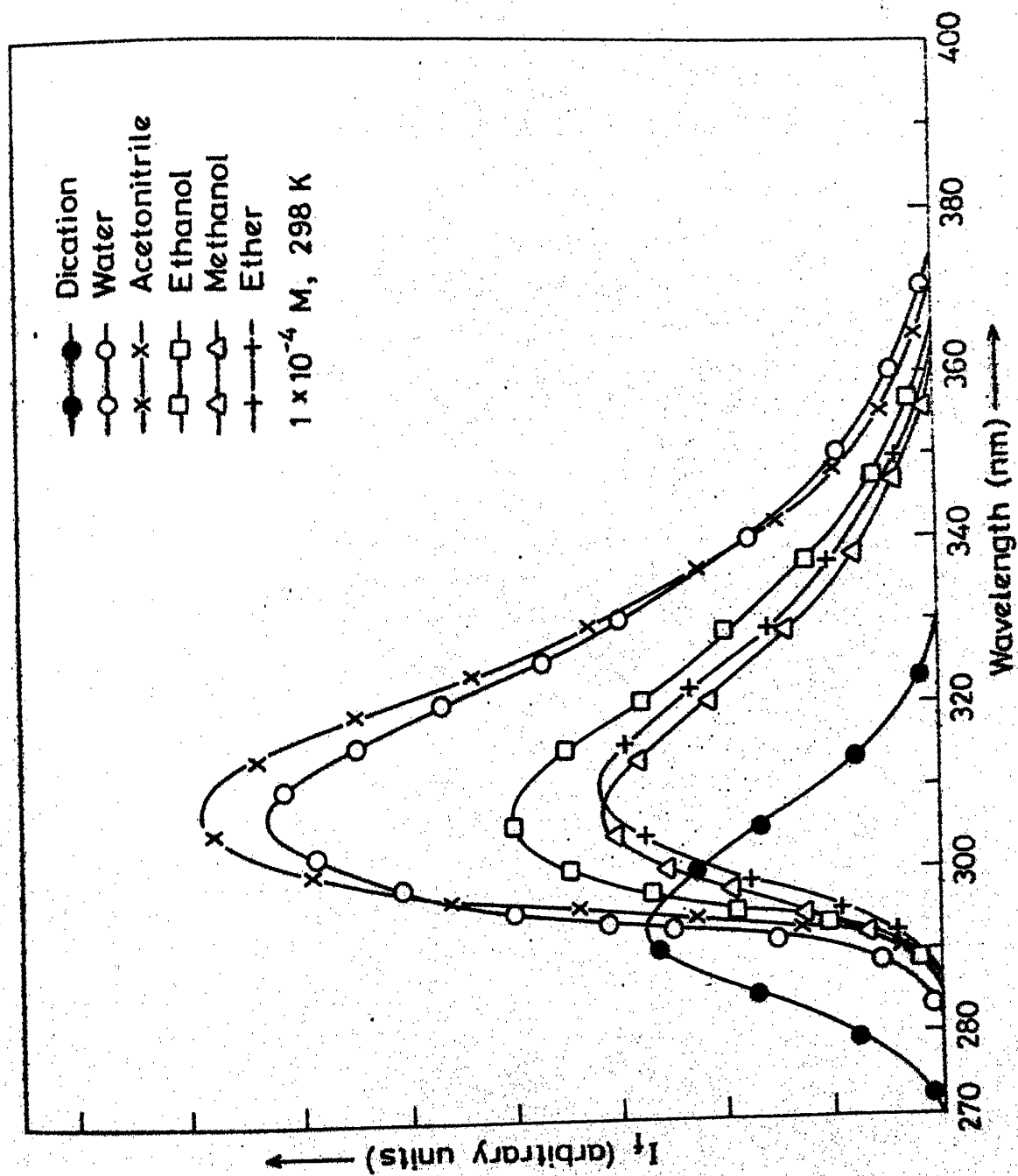
Fig.4.16 Fluorescence spectra of various prototropic forms
of BIOH at 298K.

Table 4.11. Absorption maxima (log ε_{max}) and fluorescence maxima ($\emptyset_f$) of different prototropic forms of BIOH at 298K

Forms	λ_{max}(abs) (log ε_{max})				λ_{max}(flu)	$\emptyset_f$
Dication	235 (3.93)	266	271 (4.02)	279 (4.02)	293.5	
Monocation	220 (4.13)	261	267 (4.00)	273 (4.00)		
Neutral	222 (4.02)			275 (4.01)	305	0.44
Anion	237 (4.07)			285 (4.07)		

Table 4.12. Ground and excited state equilibria of BIOH at 298K

Equilibrium	pK_a	Förstercycle method pK_a^*(abs)	pK_a^* (FT[a])	$\lambda_{isosbestic}$(nm)
Dication $\rightleftharpoons$ Monocation	-7.5	-	-7.5	272
Monocation $\rightleftharpoons$ Neutral	-2.24	-3.65	-0.02	268
Neutral $\rightleftharpoons$ Anion	11.85	9.17	11.6	277

band shapes. This occurs at a very high acid concentration (about 80% H_2SO_4) and could be due to dication. A broad structureless and red shifted band system appears at higher pH ($pK_a=12.8$). It may be due to monoanion. Only the dication species emits with a broad band maxima at 293 nm which is blue shifted as compared to neutral one. The ground state pK_a values for various equilibria were calculated spectrophotometrically and are listed in Table 4.12. $pK_a(2)$ value is much lower than the corresponding pK_a value for benzimidazole but the values of $pK_a(2)$ and $pK_a(3)$ agree with literature values.[71,135] The values of pK_a^*'s for the above equilibria have been calculated with the help of fluorimetric titrations (Fig. 4.17) and Förster cycle method. The values are listed in Table 4.12.

As established during the solvent effect studies, the neutral BIOH molecule mainly exists as species II, i.e. in keto form. pH studies also confirm this because the normal benzimidazole molecule is quite basic ($pK_a = 5.53$)[133] and becomes more basic if electron donating groups are present in the molecule. Further, a red shift should occur if $\pi \longrightarrow \pi^*$ is the lowest energy transition and protonation is taking place at pyridinic nitrogen atom. On the other hand, our results show that the absorption spectrum is blue shifted and the pK_a value is found to be -2.24, resembling more with the behaviour of carbonyl compounds rather than with benzimidazole. Förster cycle method can only be used for absorption data as the monocation is
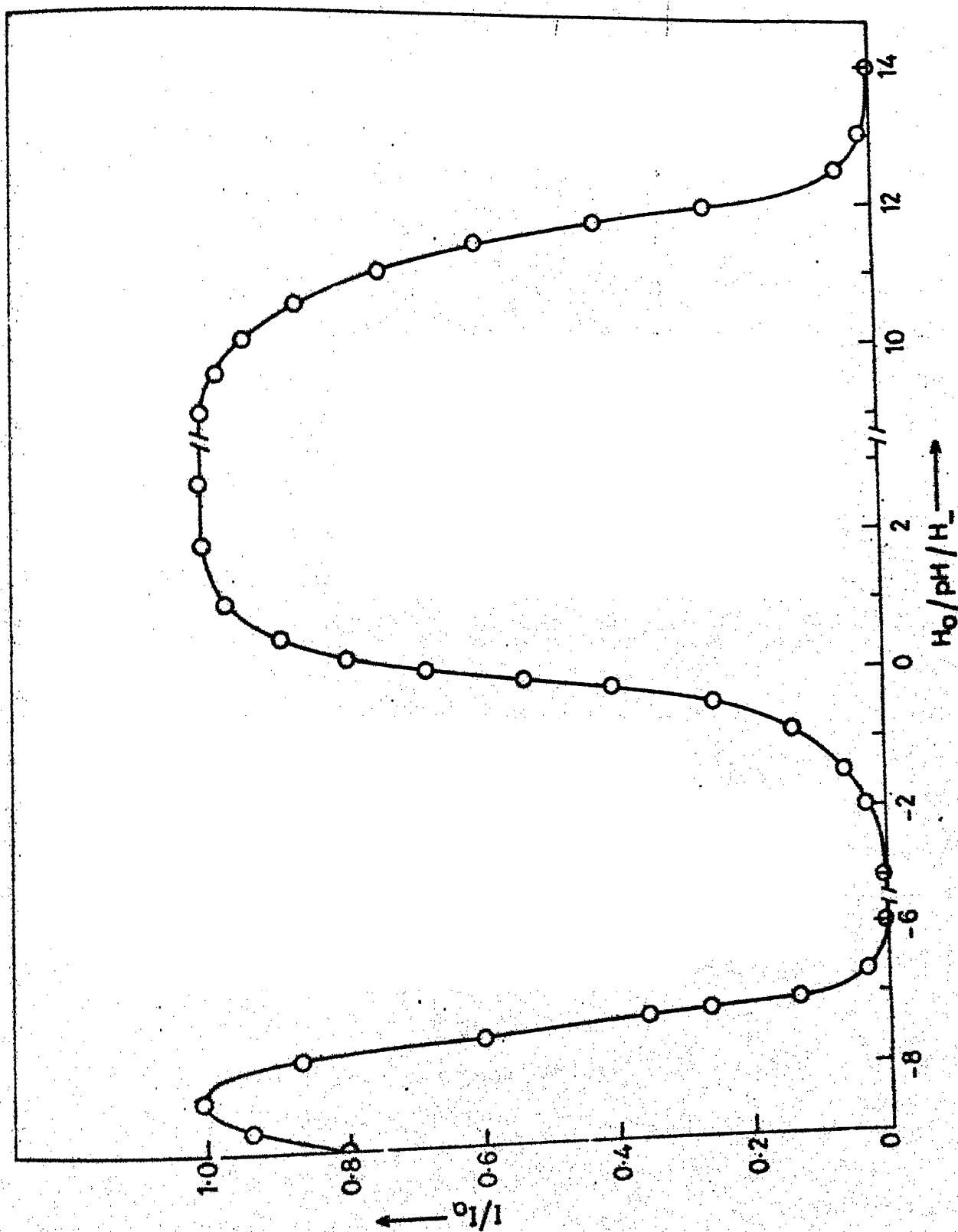
Fig.4.17 Plot of I/I_o as a function of $H_o/pH/H_-$ of BIOH at 298K.

nonfluorescent and the results indicate that the carbonyl group

is less basic in S_1 state whereas fluorimetric titration gives

the pK_a^* value as -0.02, indicating that carbonyl group is more

basic in S_1, agreeing with the normal behavior of the carbonyl

group.[136] On the other hand if the protonation had occurred

at the lone pair of the $>$N-H group (agreeing with the behaviour

of absorption spectra), then behaviour of the fluorimetric titra-

tion would have been similar to the ammonium ion[129] i.e. proton

induced quenching of neutral molecule followed by the appearance

of ammonium ion indicating that it is more acidic in S_1 state.

To the other extreme, if it is assumed that the fluorimetric

titration is following this behaviour, then there should be no

change in the absorption spectrum on further increase of the

hydrogen ion concentration. In general the fluorimetric titrati-

ons gives a better picture of equilibrium in the singlet excited

state if it is established. Hence as mentioned in the scheme

(Fig. 4.18), the first protonation takes place at the carbonyl

group.

The second addition of H^+ to BIOH molecule at very high

acid concentration could be due to the protonation of oxygen

atom of the hydroxyl group, after rearrangement of the monocation

and the equilibrium is presented in Scheme I. The red shift

observed in absorption spectrum on protonation could be due to

the restoration of aromatic character (benzimidazole molecule)

which plays the major role. The long wavelength absorption band

as well as even the shorter wavelength band system resembles with
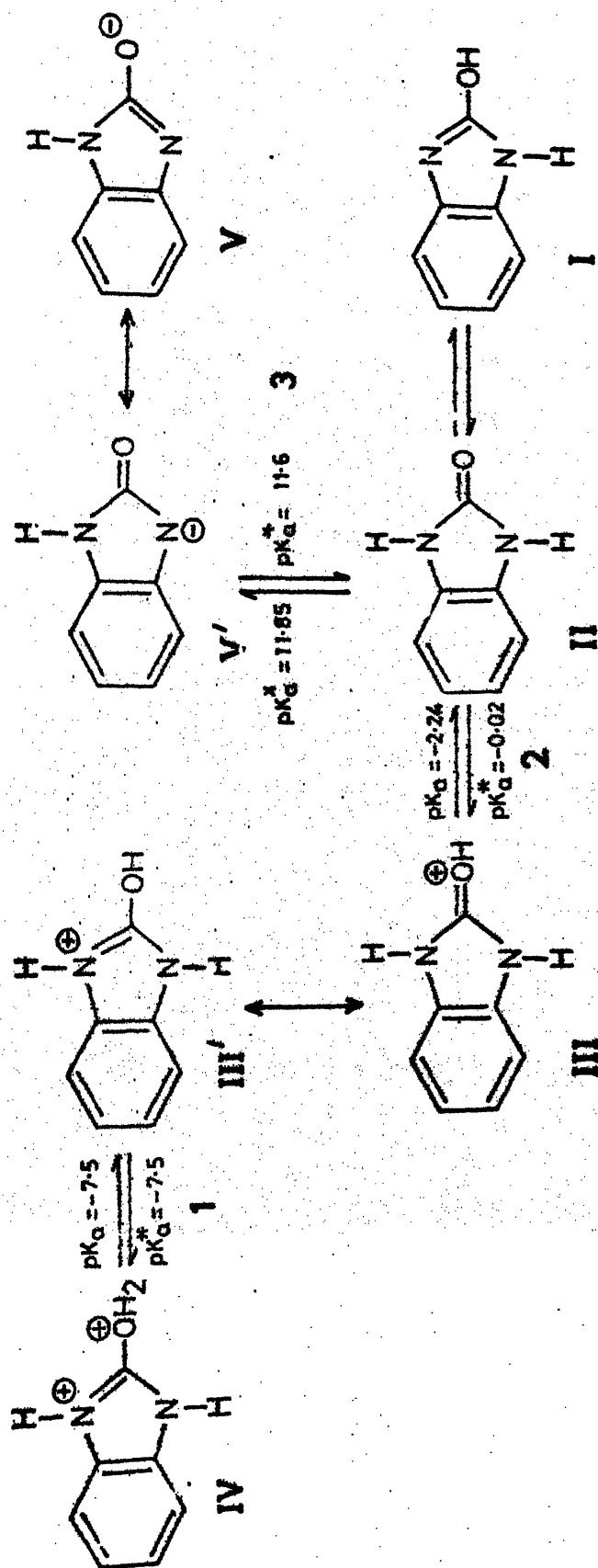
Fig.4.18 Scheme of Ground and Excited state equilibria of BIOH at different.H_o/pH/H_-.

that of the parent benzimidazole molecule. The pK_a value, calculated to be -7.5, is also obtained by fluorimetric titration. The Förster cycle method could not be used because: i) monocation is non-fluorescent and ii) the configuration of the molecule is changed on second protonation. From the above result it is clear that the dication species either has the same acidity constant in the lowest excited singlet state as in the ground state, or that the equilibrium has not been established within the lifetime of the lowest excited singlet state.

The deprotonation of BIOH at higher pH seems to be taking place from the $>$N-H group followed by rearrangement, represented in the scheme (Fig. 4.18). This is inferred as follows: i) The absorption spectrum of the anion resembles that of the parent molecule (though broad) i.e. bands at 285 nm and 237 nm. ii) The deprotonation constant of pyrrolic group in imidazole is 14.52.[133] It is lowered by the presence of electron withdrawing groups and is increased by the presence of electron releasing groups. The pK_a value of 11.85 is quite consistent with the above reasoning. The argument against the deprotonation from hydroxy group is that similar species are generally fluorescent, with extended sigmoid kind of fluorimetric titration curve, giving both the ground and excited state pK_a's.[137] Moreover the hydroxy group is a stronger acid in S_1 state. In the present case, the anion is nonfluorescent and the mid-point of the fluorescent quenching is observed at 11.6, close to the ground

state value. This is a typical behaviour of the deprotonation from the pyrrolic nitrogen atom and has been observed in many other similar compounds.[49,131,133,134] Förster cycle method could only be applied to the absorption data and as expected, have indicated that pyrrolic group becomes stronger acid in S_1 state.

The prototropic behaviour of 1-methyl-2-benzimidazolinone was similar to BIOH i.e. (i) As expected the deprotonation constant was greater than H_15 as methyl is an electron donating group increasing the basicity of other nitrogen center. (ii) monocation is nonfluorescent and (iii) dication-monocation equilibrium shifts to lower value. This is again because of the presence of electron donating methyl group making the oxygen more basic.

4.8.6 2-Aminobenzimidazole(BINH$_2$)

The absorption and fluorescence spectra of BINH$_2$ have been studied in the range of H$_0$/pH/H_ from -10 to 16. The absorption and fluorescence spectra of different prototropic forms are given in Fig. 4.19 and 4.20 respectively and their maxima are listed in Table 4.13. The long wavelength absorption maxima of monocation is structured and slightly red shifted as compared to the neutral molecule, whereas the short wavelength band of neutral molecule disappears and may be large blue shifted (< 220 nm). The absorption spectrum of dication contains both
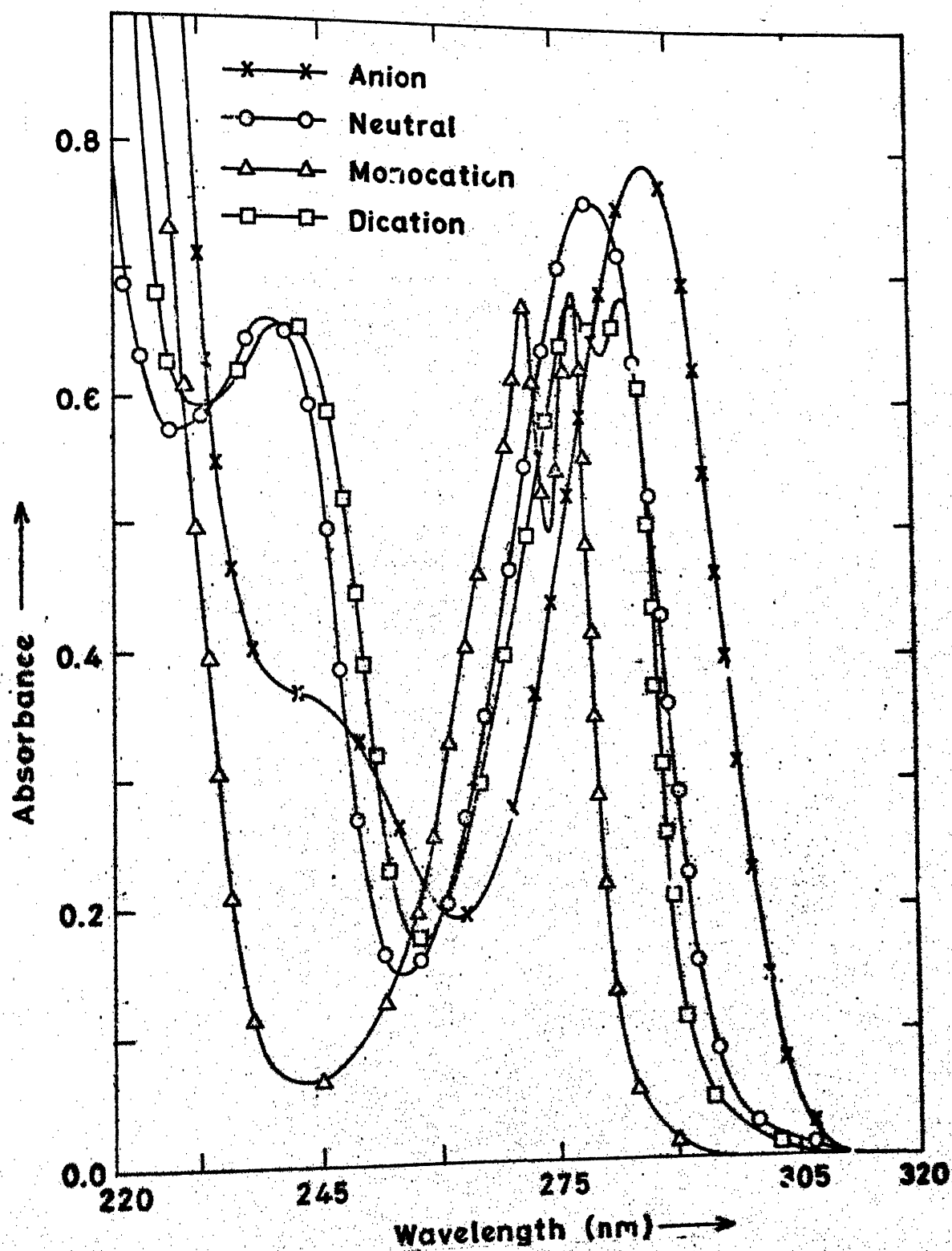
Fig.4.19 Absorption spectra of various prototropic forms of
BINH$_2$ at 298K.
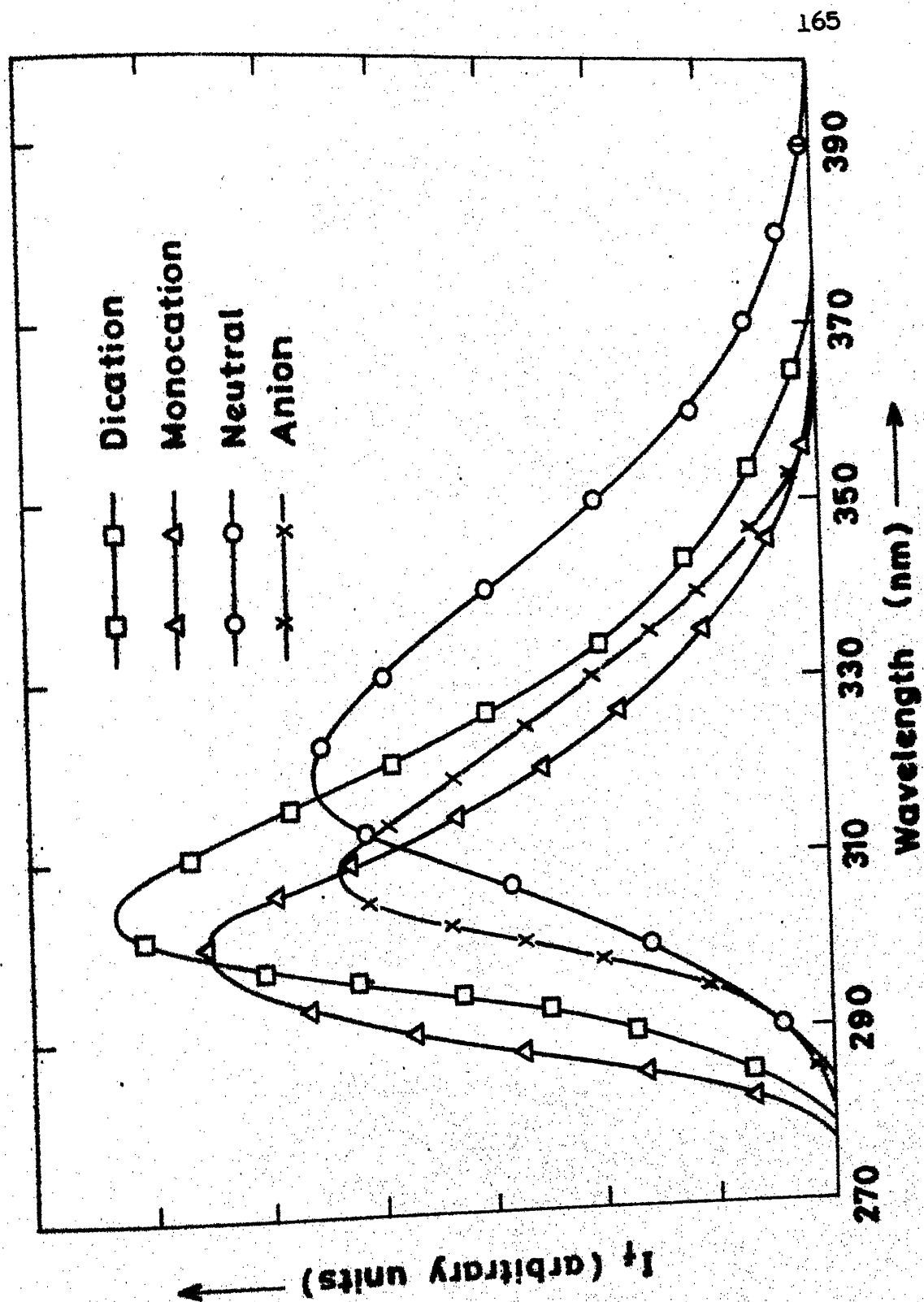
Fig.4.20   Fluorescence spectra of various prototropic forms of
BINH$_2$ at 298K, and anion at 77K.

the short and long wavelength band systems but further red shifted as compared to both neutral and monocation species. At high pH, the absorption spectrum is red shifted, could be due to formation of monoanion. The fluorescence spectrum is blue shifted followed by a red shift on increase of acid strength but the monoanion is nonfluorescent at 298K. The absorption and fluorescence spectra of the hydrochloride of BINH$_2$ have been studied in different solvents and the results are listed in Table 4.15. The data of Table 4.15 indicate that the absorption and fluorescence spectra is hardly affected by the polarity or hydrogen bond forming tendency of solvents. The λ_{max}(abs) and λ_{max}(flu) resemble with the data of monocation formed by varying the pH of the neutral molecule. Similar to the behaviour of 6-amino-indazole (P. 131) and 2-(o-aminophenyl)benzimidazole (P. 176), Cl$^-$H$^+$BINH$_2$ dissociates in ether and dioxane to give the spectra of neutral molecule at 298K. In methanol it is partially dissociated giving both the features of neutral and monocation species in absorption but of neutral molecule in fluorescence. To confirm whether this dissociation is associated with excitation, the fluorescence spectrum of salt in methanol was taken at 77K. Besides the fluorescence bands due to neutral molecule, the bands due to monocation also appeared at ~294 nm and ~288 nm, thus conforming to the above conclusion. But the results of a similar study in acetonitrile and water are quite different. Instead of fluorescence band at 297 nm, a new band at around 315-320 nm was observed at 77K. The long wavelength fluorescence

Table 4.15. Absorption maxima and fluorescence maxima of hydrochloride of $BINH_2$ at 298K.

Solvent	$\lambda_{max}(abs)$			$\lambda_{max}(flu)$
Ether	245	-	281	308
Methanol	245	275	280	310
Acetonitrile	-	273	279	298
Water	-	272	278	297

band at 77K was also present when HCl was used as protonating agent but was absent in case of H_2SO_4 as source of hydrogen ion. The new band could not be due to the fluorescence of neutral molecule because $BINH_2$ in water at 77K gave a structured fluorescence band at 307 nm and 300 nm. It may be due to some sort of interaction of Cl^- ions with the monocation present in the close distance in frozen media but no conclusive explanation is available.

In $BINH_2$ there are two sites of protonation and two sites of deprotonation. As has been said earlier, if $\pi \longrightarrow \pi^*$ is the lowest energy transition then (i) the pyridinic nitrogen atom becomes more basic[128] (ii) the aryl amines becomes less basic[105] and (iii) pyrrolic as well as amino group hydrogen atoms become more acidic in S_1 state in comparison to S_0. The effects of above behaviour are that, red shift, blue shift and red shift are observed in the absorption and fluorescence spectra in (i), (ii) and (iii) respectively. The results observed on first protonation are quite different from the general behaviour. If the protonation had occurred at the pyridinic nitrogen atom, the fluorescence and absorption spectra would have been red shifted and it would have been blue shifted in case of protonation at the amino group. But the absorption spectrum is red shifted and the fluorescence spectrum is blue shifted following no definite criteria. A similar behaviour is observed in case of 2- and 4-aminoquinolines,[59] where it was shown that the first protonation

at the pyridinic nitrogen atom is followed by a change in the hybridisation at the amino nitrogen atom, thus forming a cyclic amidine structure. It is also proposed that $BINH_2$ undergoes a similar structural change on first protonation and exists as species II (Fig. 4.22). The arguments in favour of this species are (i) the absorption and fluorescence spectra of the hydrochloride of $BINH_2$ is relatively insensitive to the polarity of the solvents as compared to other arylammonium salts,[59] thereby indicating that $Cl^-H^+BINH_2$ is less polar in S_1 as compared to S_0 states. (ii) the ground state $pK_a(II)$ value observed spectrophotometrically is higher as compared to other amino derivative of benzimidazole substituted at 5-position,[49,138] but the results are similar to 2- and 4-aminoquinolines.[59] (iii) The infrared spectra of hydrochloride of $BINH_2$ is similar to 2-benzimidazolone[91] but different from other arylamines in that absorption near ~ 3450 cm^{-1} in the normal amines and their hydrochlorides have been assigned to the antisymmetric exocyclic N-H stretching frequencies,[139] but the infrared spectrum of $Cl^-H^+BINH_2$ is red shifted to some 3260 cm^{-1}, a phenomenon which has been interpretted as characteristic of imine formation.[139,140] (iv) The absorption spectrum of species(II) is similar to that of 2(3H)-benzimidazolone i.e. the blue shift observed in the short wavelength bond (which is localised on the imidazole ring[99]) of absorption spectrum of $BINH_2$ on protonation, is due to the loss of aromatic character in the imidazole ring and long wavelength
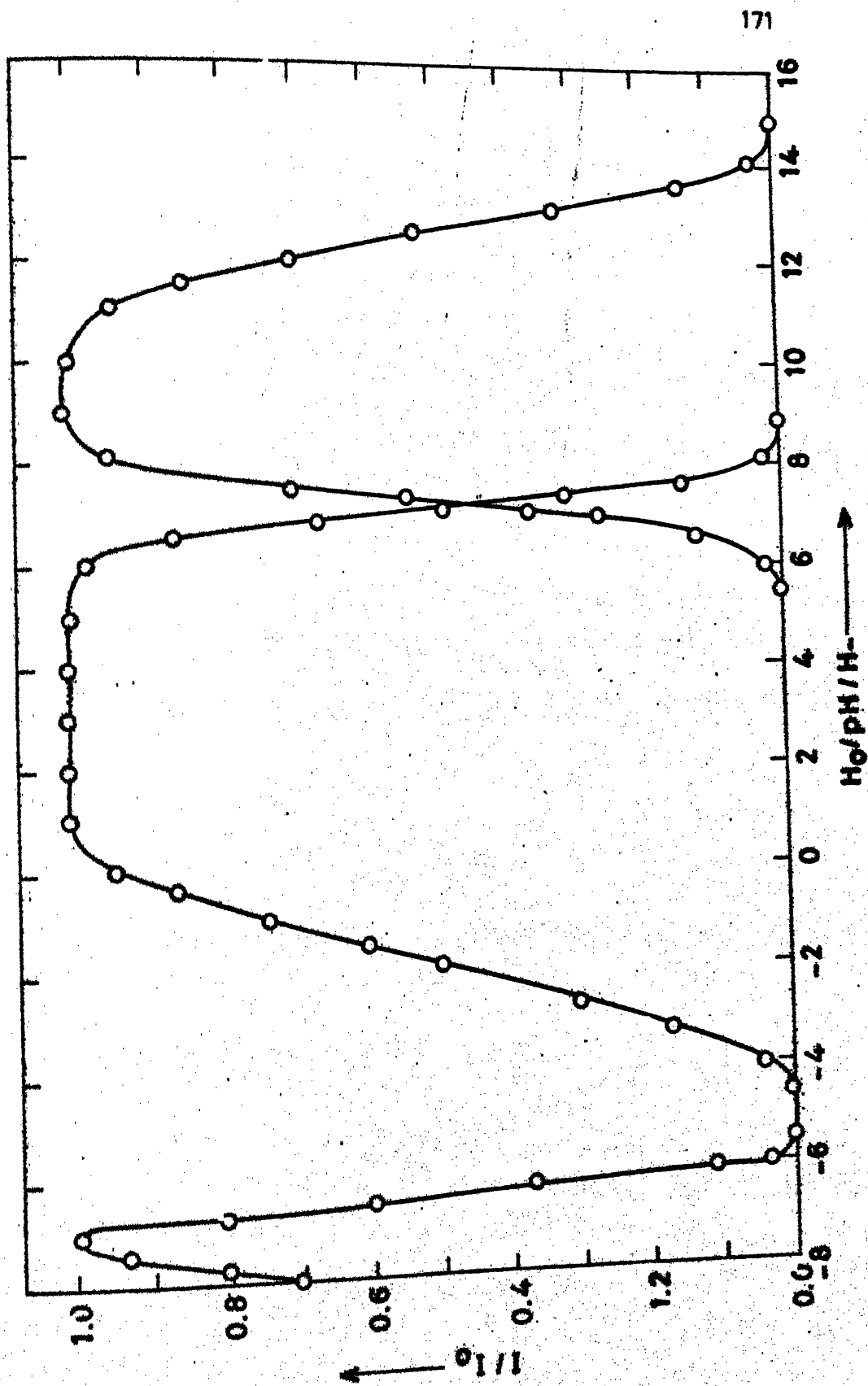
Fig.4.21 Plot of I/I_0 as a function of $H_0/pH/H_-$ of $BINH_2$ at 298K.
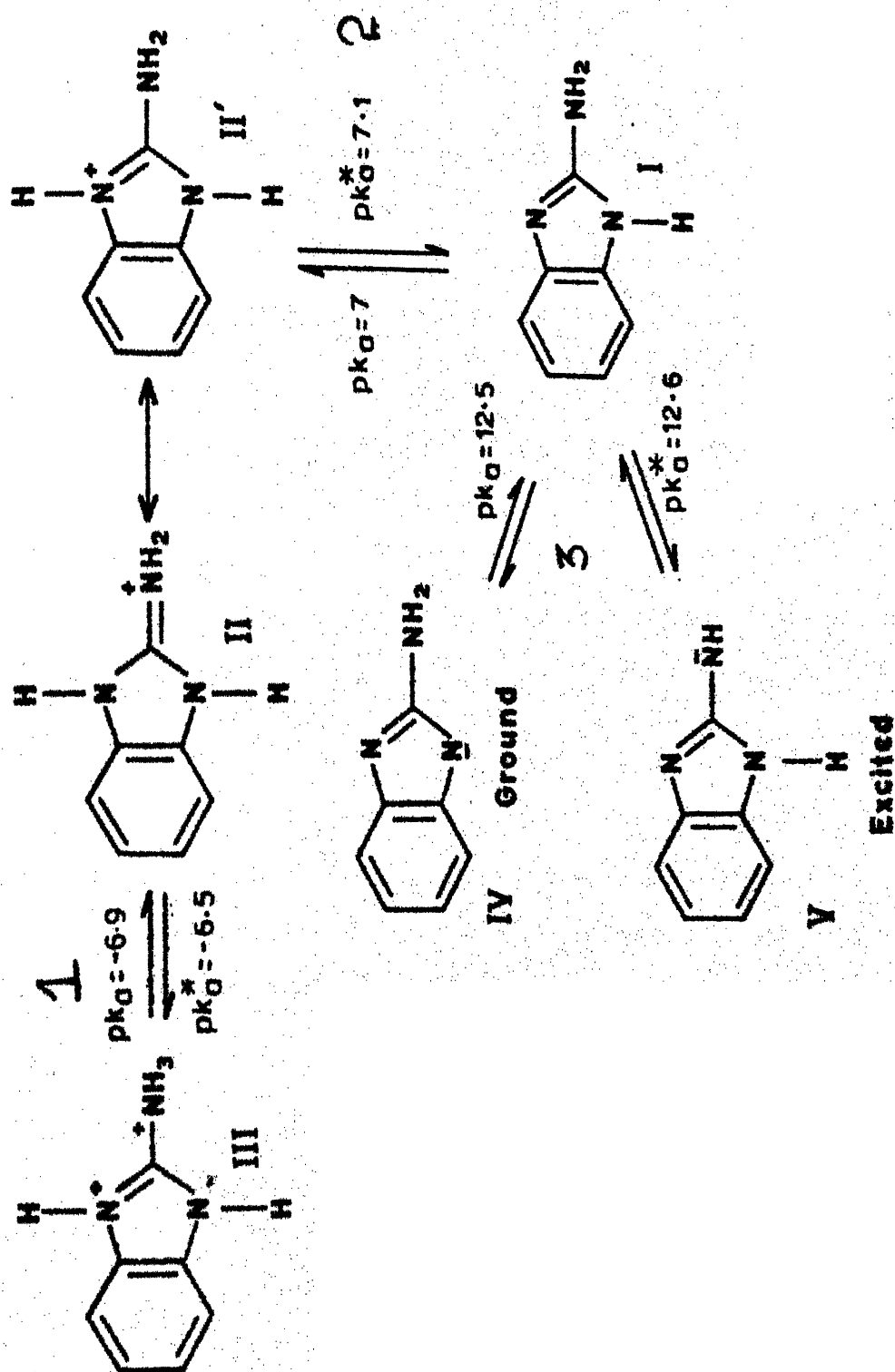
Fig. 4.22 Scheme of Ground and Excited state equilibria of $3NH_2$ at 298K.

transition which is localised on the benzene ring is slightly red shifted because of the presence of two amino nitrogen atoms, ortho to each other. The value observed agrees nicely with the value predicted from the relations given by Stevenson.[98]

Förster cycle method cannot be used to calculate $pK_a^*(2)$ because of the change in the structural behaviour as well as the nature of the transition in the conjugate acid-base pair. Fluorimetric titrations, shown in Fig. 4.21, were carried out but only gave ground state $pK_a(2)$ value, indicating that either there is no change in the dissociation constant of monocation-neutral equilibrium or it is too slow to be established during the lifetimes of the species involved.

Dication species is formed with a further increase of hydrogen ion concentration. The absorption spectrum (presence of doublet in the long wavelength bond and the appearance of short wavelength band) clearly shows that the dication is formed by the protonation of pyridinic and amino nitrogen atoms and the structure of the parent molecule i.e. benzimidazole, is preserved. It is depicted by the species III in the scheme (Fig. 4.22). Similar to the monocation-neutral equilibrium, the Förster cycle method cannot be used to calculate $pK_a^*(1)$ as the conjugate acid-base pair have different structures and transitions. Fluorimetric titrations (Fig. 4.21) of the dication-monocation equilibrium have shown that the value of $pK_a^*(1)$ in S_1 is nearly equal or slightly less negative than that of the ground state value.

This behaviour of protonation at the amino group is quite different from the arylammonium $\rightleftharpoons$ arylamine equilibrium. It is generally observed that arylammonium ions are more acidic and arylamines are less basic[105] in their first excited singlet state as compared to that in the ground state and no exception has been observed so far, where as the ketones[128] and carboxylic acids[105,141] become more basic in the lowest excited singlet state. If it is assumed that the monocations derived from $BINH_2$ are isosteric with the monocations derived from the ketones or carboxylic acids, it is possible that monocation of $BINH_2$ becomes more basic in the excited state. Now, the gain in the basicity of monocation of $BINH_2$ upon excitation could be greater than, equal to or less than the gain in acidity of the doubly protonated cation upon excitation. These results have shown that the two gains are nearly equal or the former is slightly more than the latter. A similar trend is observed in 2- and 4-aminoquinolines[59] and also in BIOH, where the former effect clearly overweighs the latter.

At high pH/H_-, the absorption studies have shown that the monoanion is formed which does not emit at 298K. The absorption spectrum of monoanion has shown that this species is structurally similar to the parent benzimidazole molecule. The formation of monoanion could be due to the deprotonation of pyrrolic hydrogen atom or from amino group. In general, deprotonation from the amino group is not observed under such conditions[142,120] in S_o

and at the same time, arylamine anions are non fluorescent with the exception of β-naphthylamine.[119] It appears from our results that the monoanions are formed from the deprotonation of pyrrolic group in S_o, but in S_1 these are formed from the deprotonation of amino group because, the monoanions formed in the former case are generally fluorescent[130,134,143] whereas formed in latter cases are non-fluorescent. This is further confirmed from the fluorescence spectrum of 2-aminobenzimidazole anion at $pH/H_- > 12$ and at 77K, shown in Fig. 4.20. At this low temperature only the excited state species in their ground state environments can exist i.e. 2-aminobenzimidazole anion can exist as confirmed by its fluorescence. Similar behaviour has also been observed in case of 5-aminoindazole.[49] It shows clearly that amino group becomes more acidic in S_1 state than in S_o and relative increase in acidity of amino group is much more than that of pyrrolic group upon excitation.

Further the nearly similar values of $pK_a(3)$ in the ground and lowest electronically excited state from fluorimetric titrations can also be due to the non-establishment of the equilibrium during the lifetimes of the conjugate acid-base pair. But this can be only possible if the deprotonation had occurred from pyrrolic nitrogen atom. So the earlier explanation seems to be more logical.

The complete equilibria is shown in the scheme (Fig. 4.22) and values of pK_a's in S_o and S_1 are shown our the arrows and in Table 4.14.

4.8.7 2-(o-Aminophenyl)benzimidazole(oBNH$_2$)

The absorption spectrum of oBNH$_2$ is studied in the H$_o$/pH/H$_-$ range of -9 to 16. Besides neutral (structure II in aqueous medium), three more new species are observed. Neutral form exists between the pH range 4 to 13. On decrease of pH from 4, all the bands are red shifted, the more prominent being the longest wavelength band and continues till pH 0.4. Further decrease of pH completely changes the structure of the band system. Two, instead of three, bands appear and resemble that of benzimidazole pattern having substituent attached at 2 position (more particularly close to that of 2-phenylbenzimidazole cation, (P.150), being blue shifted as compared to the species III. On increase of pH from 13, red shift is observed in the respective bands, keeping the three band system intact. The band maxima are listed in Table 4.16 and spectra are shown in Fig. 4.23.

The monocation formed in the pH range 0.4 to 4 can only be due to the protonation at the pyridinic nitrogen atom (species III) because the red shift of the absorption bands is normally associated with pyridinic protonation. Moreover it has been already established in solvent studies that in aqueous media this site (the pyridinic nitrogen) is not taking part in intramolecular hydrogen bond formation, thus making it available for protonation. The formation of dication can be visualised as the three band system in the absorption system is changed into
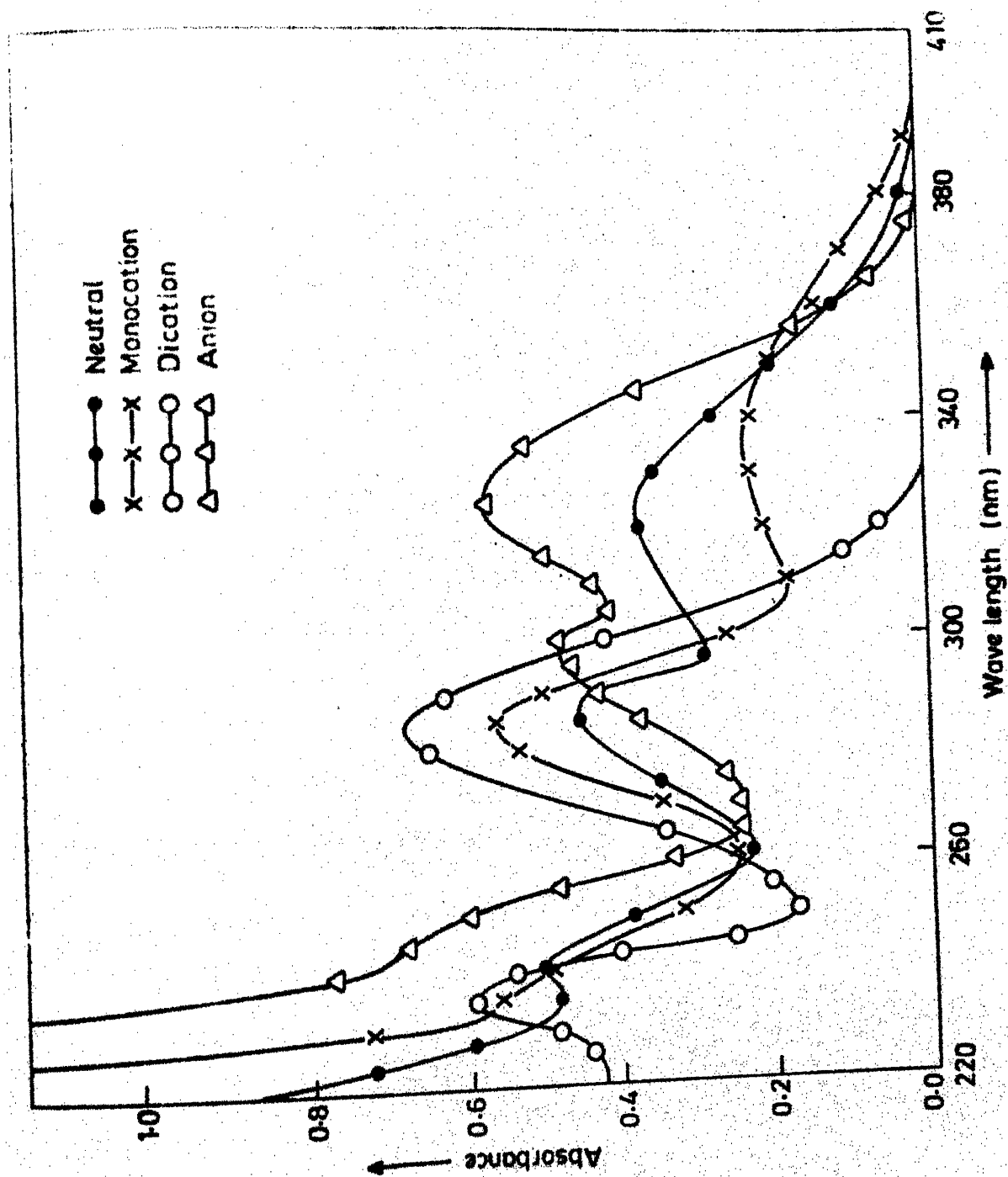
Fig. 4.23 Absorption spectra of various prototropic forms of oBNH₂ at 292K.

Table 4.16. Absorption maxima (log ε_{max}) and fluorescence maxima ($\emptyset_f$) of different prototropoc forms of $oBNH_2$ at 298K

Forms	λ_{max}(abs)				λ_{max}(flu)	$\emptyset_f$
Dication		236	284 (4.43)		391	0.430
Monocation		245 (4.27)	285 (4.32)	335 (3.94)	454	0.102
Neutral	218 (4.70)	240 (4.33)	286 (4.27)	320 (4.18)	417	0.129
Anion		247 (4.28)	297 (4.28)	324 (4.32)	505	0.375

Table 4.17. Ground and excited state equilibria of $oBNH_2$ at 298K

Equilibria	pK_a	Föster cycle method pK_a^*(abs)	pK_a^*(flu)	pK_a^*(ave)	pK_a^* (FT)	$\lambda_{isosbestic}$(nm)
Dication $\rightleftharpoons$ Monocation	0.4	–	–	–	-2.4	310
Monocation $\rightleftharpoons$ Neutral	3.5	6.0	7.6	6.8	3.9	298
Neutral $\rightleftharpoons$ Anion	12.9	12.1	–	–	12.7	345

two band system resembling more to PBI$^+$ spectrum (Fig. 4.14, P. 151). This is because, on second protonation, both the lone pairs at both the nitrogen atoms are blocked by the protons and thus the rings 3 or 4 formed due to intramolecular hydrogen bonding are absent. Moreover, the behaviour of the anilinium ion will be similar to that of phenyl group, thereby reverting back to the absorption spectrum similar to benzimidazole derivatives. The monoanion is formed due to deprotonation of the pyrrolic nitrogen atom because the deprotonation of the amino group is difficult to observe in S_o state at such a low pH.[57,136]

Fluorescence studies, carried out in the H_o/pH/H_ range of -9 to 16, also confirm the formation of the different cations or anions at various pHs and the spectra are shown in Figure 4.24. Thus the absence of proton induced quenching of oBNH$_2$ at moderate hydrogen ion concentrations preceeding protonation and the red shift observed in the fluorescence spectra suggests the first protonation to be at the pyridine nitrogen center. The blue shift in dication fluorescence is conforming to the earlier conclusion because the state from which it is fluorescing is entirely different because of the destruction of condensed four-ring structure. Fluorescence observed from the monoanion also confirms the deprotonation of the pyrrolic nitrogen atom, because, in general the imino anions (deprotonation of the amino group) formed do not fluoresce with the exception of β-napthylamine.[119]
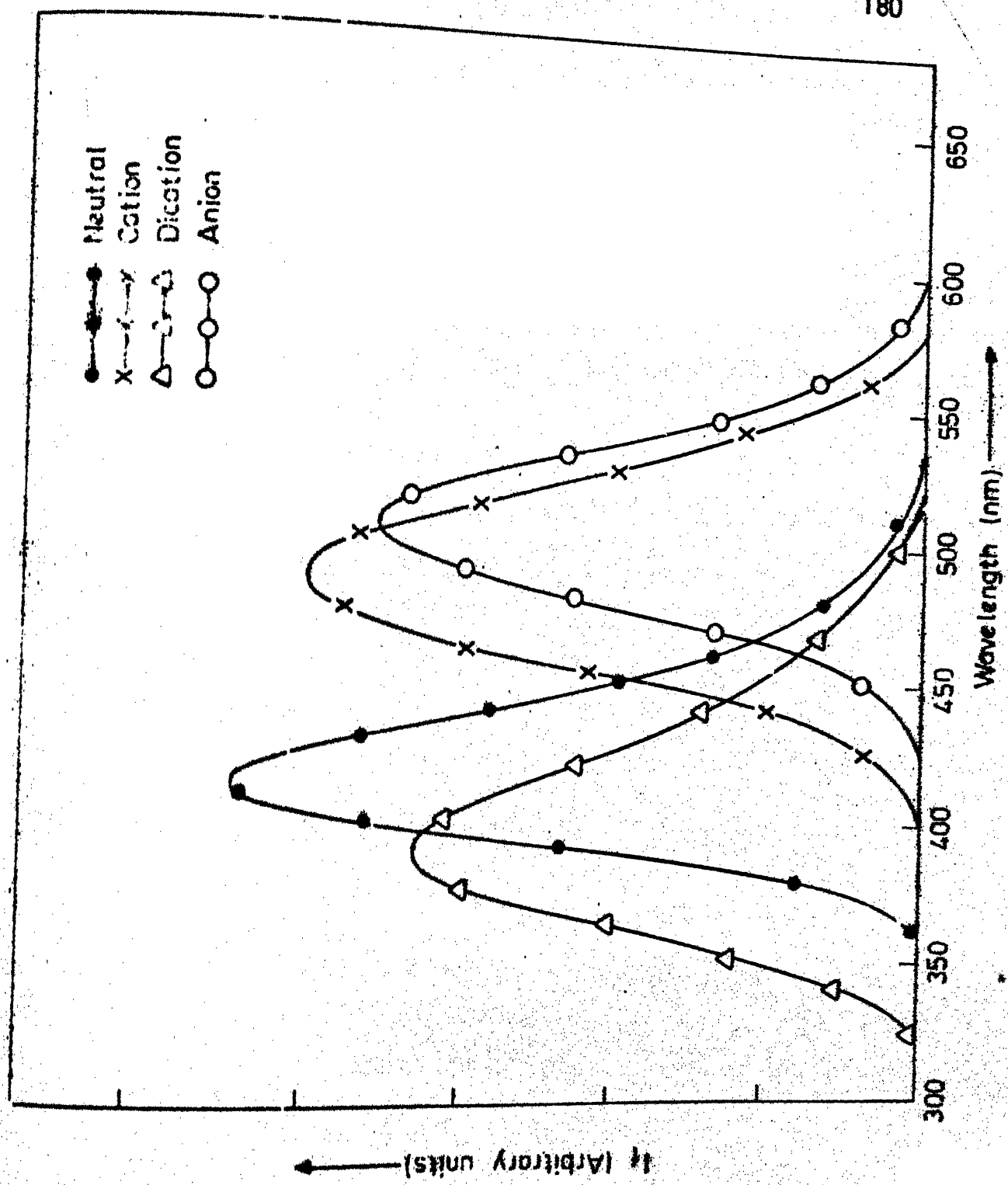
Fig.4.24   Fluorescence spectra of various prototropic forms of oBNH$_4$ at 298K.

The ground and excited state pK_a's for various equilibria are given in Table 4.17. The value of $pK_a^*(1)$ could not be calculated by using Förster cycle because the band systems observed in both the species are different. The difference between $pK_a^*(2)$, calculated by using absorption and fluorescence data is not large (i.e. 1.6 pK_a units) and could be due to different solvent relaxation in the two electronic states of the different species or due to using the band maxima instead of 0-0 transition of the neutral and monocation species. The value of $pK_a^*(3)$, using Förster cycle method could be calculated only using absorption data, indicating that pyrrolic proton is slightly more acidic in S_1 state than in S_0, as expected. The fluorescence data could not be used because after deprotonation of pyrrolic hydrogen atom, the structure of the anion formed resembles more to structure I, rather than to the structure II of the neutral molecule (II).

The fluorimetric titrations were carried out for different equilibria and the fluorescence intensities of various species as a function of $H_O/pH/H_-$ are plotted in Fig. 4.25. The values of $pK_a^*(2)$ and $pK_a^*(3)$ obtained are quite close to the ground state values as is normally the case for protonation or deprotonation of pyridinic or pyrrolic nitrogen atoms respectively. As has been stated very often this could be due to either the short lifetimes of the species in S_1 state or insufficient number of protons in the solution to establish the equilibrium.
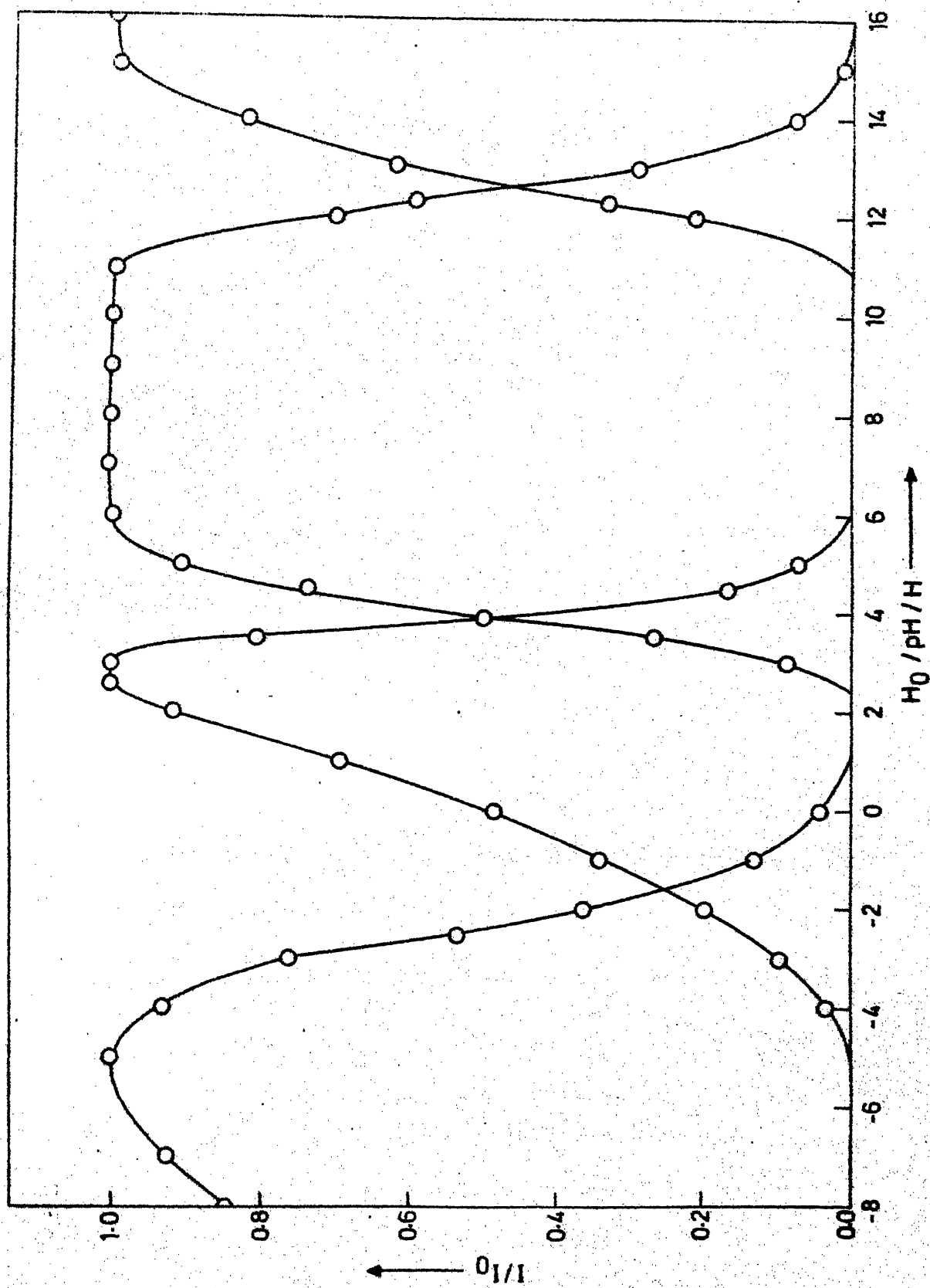
Fig.4.25 Plot of I/I_0 as a function of $H_0/pH/H_-$ of ΘΗΝΗ$_2$ at 298K.

The fluorimetric titration curves for the dication-monocation equilibrium do not intersect at the middle, indicating a slight proton induced quenching of H^+OBNH_2 which is also another indication of the fact that second protonation is at the amino group. Thus here the middle point of the rise of $H^+OBNH_3^+$ fluorescence curve $(pK_a^*(1) = -2.4)$ can be taken as being close to the true value.

The various equilibria observed under different conditions are mentioned in the scheme, (Fig. 4.26) and the pK_a's are listed on the arrows.

Absorption and fluorescence spectra of salt of $oBNH_2$

The absorption and fluorescence spectra of $oBNH_3^+$ were recorded in different solvents. Quite surprising but convincing results were observed. The absorption and fluorescence (except in acetonitrile as solvent) spectra matched with those of $oBNH_2$ (neutral) in all the solvents, indicating that $OBNH_3^+$ is unstable and dissociates into $oBNH_2$ and H^+. The above results have further proved our earlier conclusion i.e. at pH 4 (obtained when $oBNH_3^+$ was dissolved in water) $oBNH_2$ is mostly present as neutral or there may be a small amount of monocation protonated at pyridine center. In acetonitrile, fluorescence is observed from species III (λ_{max} 450 nm) and this is also observed when $oBNH_2$ is dissolved in n-heptane containing 0.01M TFA. This
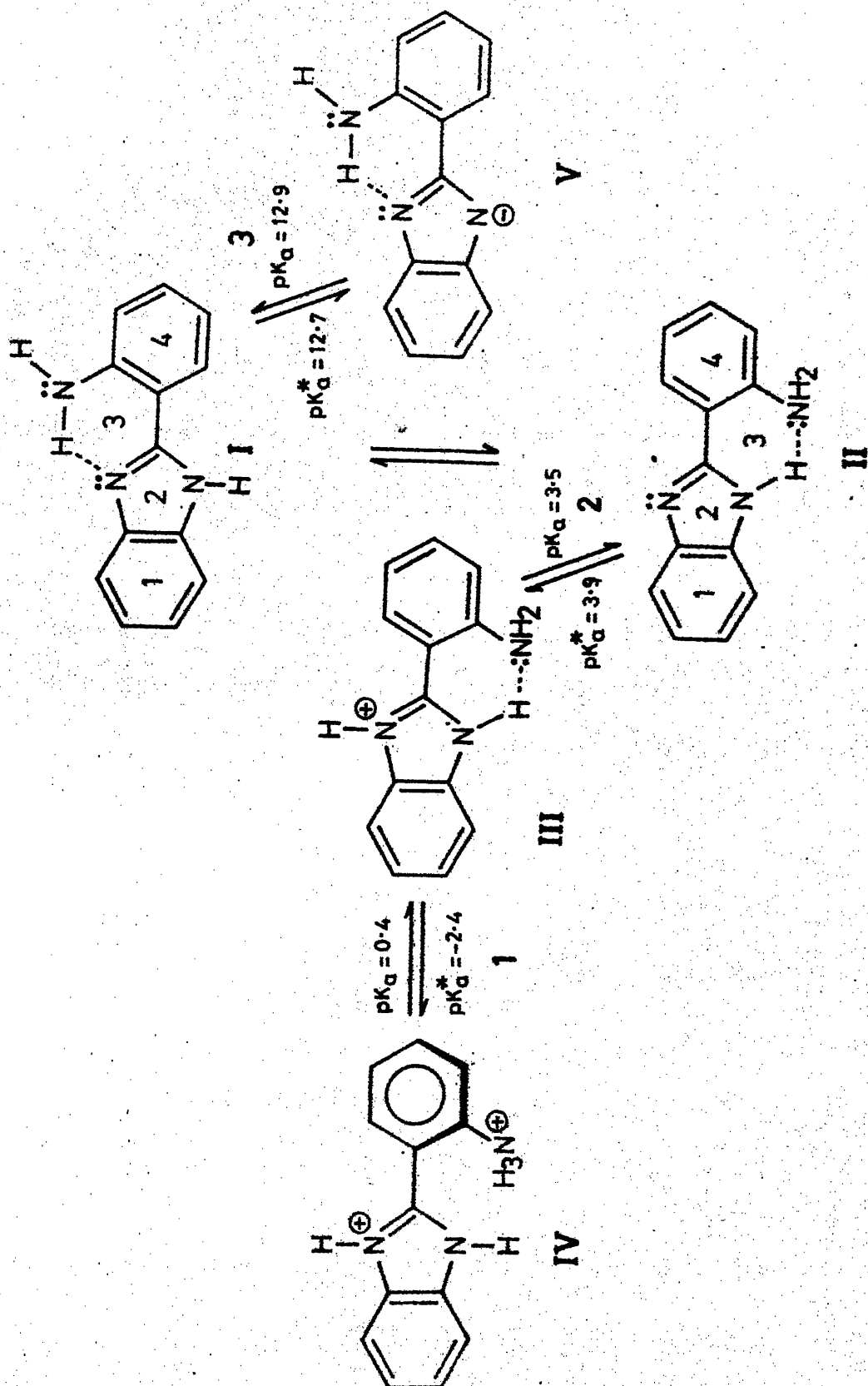
Fig. 4.26 Scheme of Ground and Excited state equilibria of oBNH₂ at 298K.

indicates that the species III is more stable in non-polar media and could be due to the presence of resonance as observed in 6-aminoindazole.

4.8.8 2-(m-Aminophenyl)benzimidazole(mBNH$_2$)

The absorption and fluorescence spectra of mBNH$_2$ are studied in the H$_o$/pH/H$_-$ range of -9 to 16. Besides the neutral form, three other species were identified. On increasing the proton concentration from pH 7, a slight blue shift in the band maxima was observed below pH 4.5 (Fig. 4.27). This absorption band was attributed to the monocation and this was found to be nonfluorescent in aqueous media at 298K. On decreasing the pH further, a red shift was observed in the longest wavelength absorption band below pH 2. This form was found to be fluorescent ($\lambda_{max}^{(flu)}$ =380 nm), which is a comparatively blue shifted band with respect to the neutral fluorescence ($\lambda_{max}^{(flu)}$ =420 nm), (Fig. 4.28). This form remained as such till H$_o$-9 without any further change in absorption or fluorescence maxima and was attributed to dication. On increasing the pH above 7, a red shifted absorption maxima was observed beyond pH 11.9, which is due to anion and was found to be nonfluorescent. The absorption and fluorescence maxima of various forms are given in Table 4.18.

mBNH$_2$ has two sites for protonation: one at the exocyclic amino group and the other at the pyridinic nitrogen atom. As has been discussed earlier for aminohydrocarbons, protonation at the
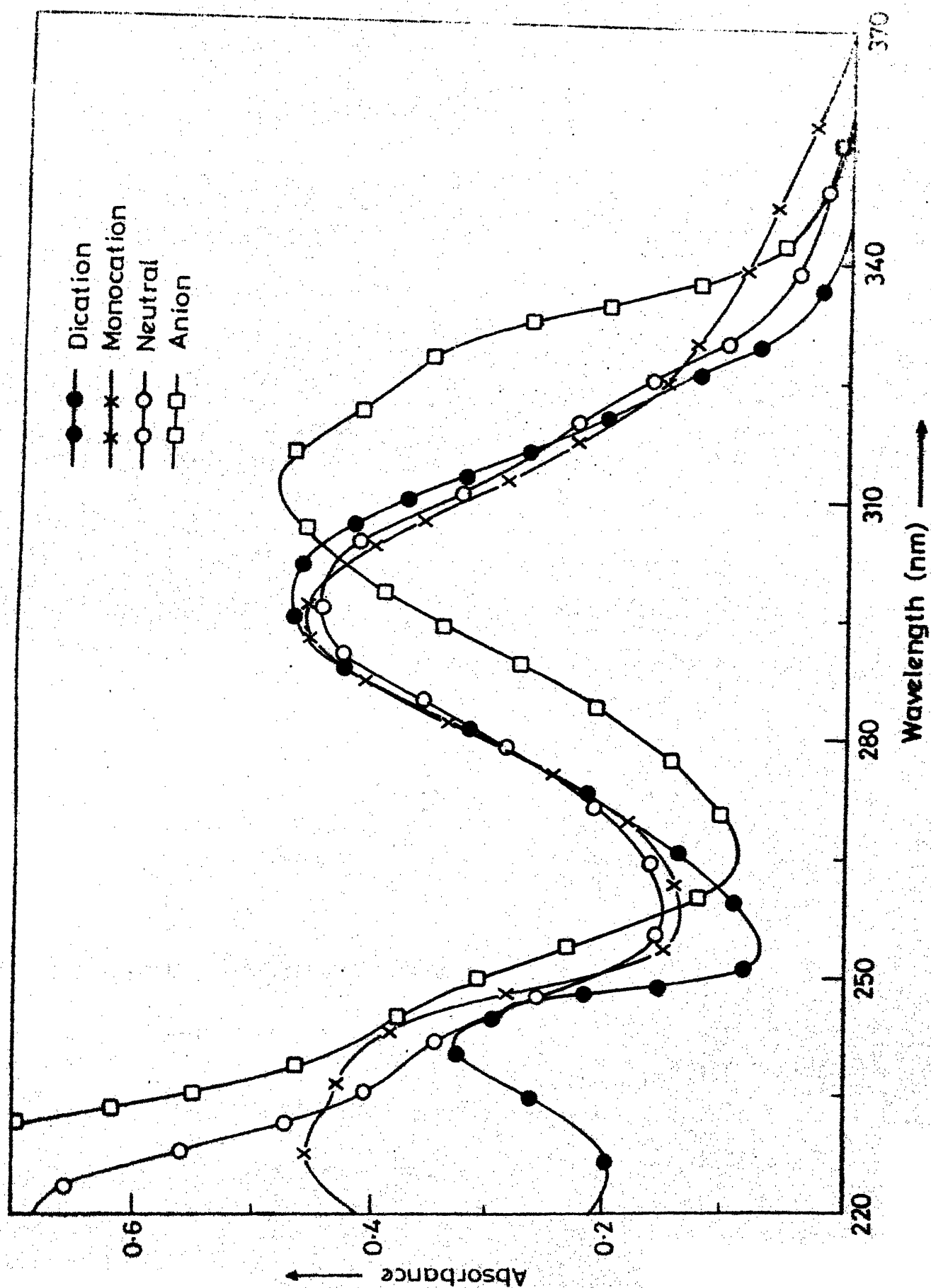
Fig.4.27 Absorption spectra of various prototropic forms of mBNH₂ at 298K.
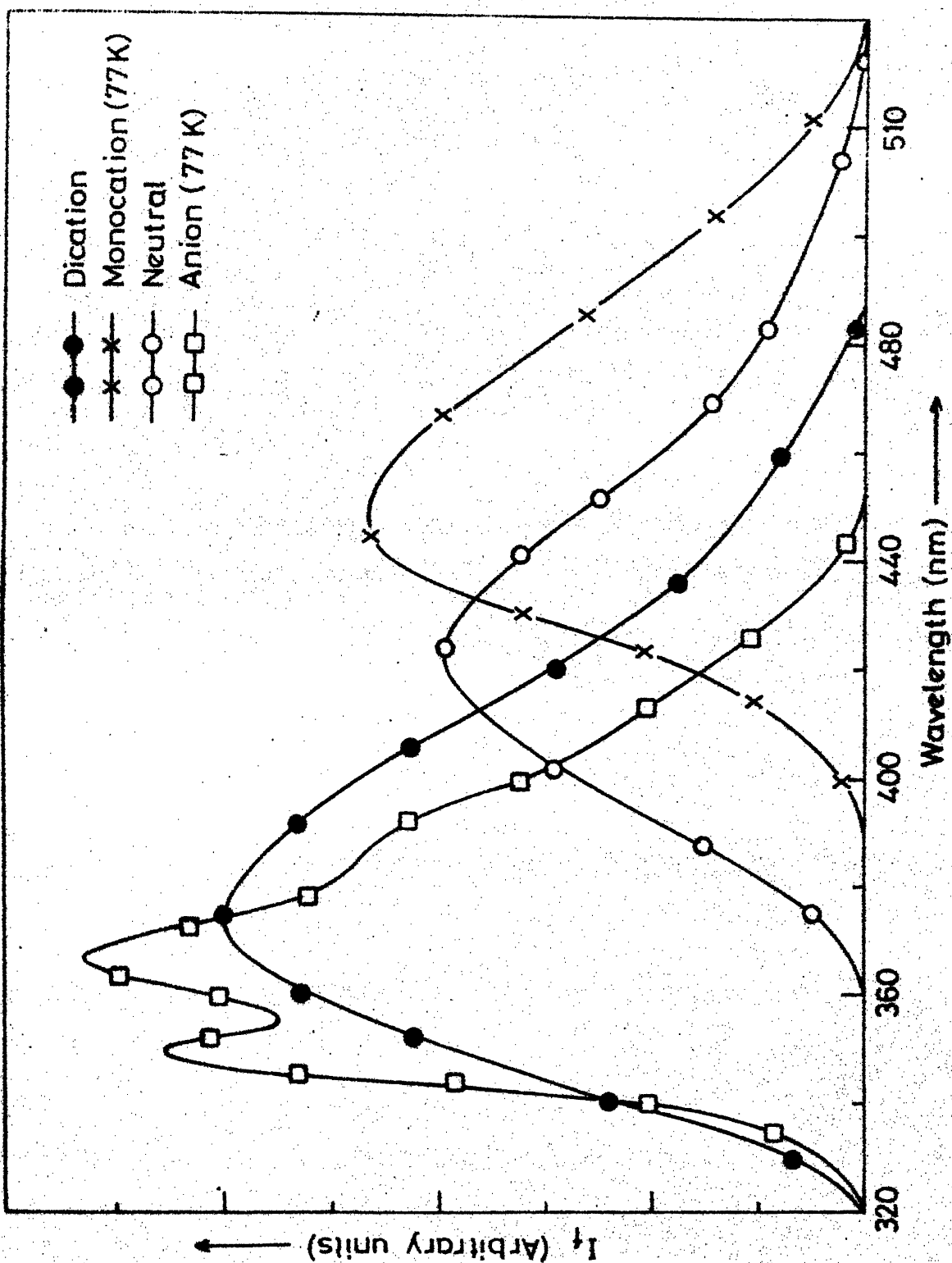
Fig. 4.28 Fluorescence spectra of various prototropic forms of mBnH$_2$ at 298K and at 77K.

Table 4.18. Absorption maxima (log ε_{max}), and fluorescence maxima ($\emptyset_f$) of different prototropic forms of $mBNH_2$ at 298K and at 77K.

Forms	λ_{max}(abs) (log ε_{max}) (nm)				λ_{max}(flu) (nm)	$\emptyset_f$
Dication	242 (4.23)	247 (4.20)	297 (4.36)		380	0.220
Monocation	227 (4.30)	240 (4.28)	294 (4.35)	340 (3.60)	450**	−
Neutral	220 (4.52)	242 (4.25)	295 (4.34)	322.5 (3.96)	420	0.132
Anion		~ 250 (4.26)	313 (4.34)	328 (4.28)	336,350,) 367,382*)	−

* At 77K and 1 x 10^{-4}M solution. ** 77K and 1×10^{-3}M solution.

amino group should exhibit the following characteristics: (i) a blue shifted band for the cation in absorbance and fluorescence, (ii) a usual ground state pK_a of ~4, (iii) in general competing proton induced fluorescence quenching observed during protonation and (iv) a higher acidity of the arylammonium ion in the excited state. Protonation at the pyridinic site is usually characterised by (i) a red shift of absorption and fluorescence spectra of the cation in comparison to neutral molecule; benzimidazole is an exception where the absorption spectra of cation gets blue shifted, (ii) an increase in the basicity of the pyridine center in its excited state, which in case of benzimidazoles is not manifested by its fluorimetric titrations. This is due to the fact that excited state prototropic equilibrium is not attained because either pK_a^* falls in the mid-pH region where the rate of proton transfer will be slower due to small concentration of H^+ ions, or the lifetime of the species are very small.

The first protonation in $mBNH_2$ has a pK_a value of 4.5 (5.3 for PBI). Below this pH the fluorescence is quenched, again reappearing as a blue shifted fluorescence at 380 nm at pH 2. Thus this resembles the behaviour of arylamino protonation. But if the protonation had occured at the amino group, there would not have been any change in absorption spectra with a further decrease of pH. Contrary to this the change in absorption spectrum is observed. Moreover for benzimidazoles it has normally been found that pK_a and pK_a^* for the protonation are

same. Hence the new fluorescence cannot be due to the formation of monocation and it is more reasonable to assume that a nonfluorescent monocation protonated at pyridinic center exists between pH 2 and 4.5. This further confirms the above point as the pK_a for the protonation of pyridinic nitrogen atom of benzimidazole is close to 5.3^{144} and that for aniline type amino group is close to $4.^{145}$ The blue shift in the monocation absorption spectrum is possibly due to the loss of conjugation due to rotation of phenyl ring or it is the normal effect of benzimidazole monocation formation. As has been suggested earlier in the introduction (P.11), it is reasonable to expect that the longer wavelength dication absorption maxima of $mBNH_2$ should match with the monocation absorption spectra of PBI. In fact this value is 297 nm for $mBNH_2$ and 295 nm for PBI.

It is not easy to offer a convincing explanation for the nonfluorescent nature of the monocation but may be explained on the same lines as is done for benzimidazole cation ($\emptyset_f$ for cation (0.06) is ten times less than that of neutral (0.67)) i.e. nonradiative processes are predominant at 298K and $\emptyset_f$ is too small for fluorescence to observe. As many collisional and vibrational nonradiative pathways can be eliminated by freezing the solution at low temperature, the above study for,$mBNH_2$ cation was done at 77K and in the pH range of 4.5 to 2. A broad band appeared at 450 nm which is red-shifted to that of the neutral species at 77K (390 nm) (Fig. 4.28). To confirm whether the 450 nm band

observed is due to monocation, the hydrochloride salt of $mBNH_2$ was prepared and its spectral behaviour had been studied in different solvents at room temperature and at low temperature (77K). The results are given in Table 4.19 and Fig. 4.30. The salt solution in water and acetonitrile show cation absorption spectra and the cation decomposes to the neutral form in methanol and dioxane. The fluorescence spectra of the salt in water was that of the neutral species (420 nm) and it could be due to an incomplete protonation of $mBNH_2$ at this pH (5.1) of salt solution, and also the cation fluorescence is quenched at 298K. The salt in methanol and dioxane also showed neutral fluorescence. Similar results were obtained for 6-aminoindazole and it was suggested that the basicity of methanol or dioxane is sufficient enough to remove the proton from $mBNH_2$ cation at very low cation concentration (10^{-5}M). A concentrated solution of the salt (10^{-3}M) in these solvents showed the presence of two fluorescence bands, one matching with the neutral fluorescence band in the respective solvents ($\sim$380 nm) and another red shifted band at 430 nm for dioxane and 470 nm for methanol. The salt in acetonitrile showed an absorption spectra matching with the cation absorption and showed two bands in fluorescence even in 10^{-5}M solution: one at 480 nm and the other at 390 nm, the latter being due to neutral fluorescence. The addition of just 5% of water to this acetonitrile solution quenched the fluorescence at 480 nm completely. This only suggests that strong hydrogen

Table 4.19. Absorption and fluorescence maxima of hydrochloride of $mBNH_2$ at 298K and 77K.

Solvent	$\lambda_{max}(abs)$ (nm) 298K[a]	$\lambda_{max}(flu)$ (nm) 298K[a]		77K[b]
Dioxane	302	– ,	388	420, –
Acetonitrile	317	480 , (major)	390 (minor)	440, –
Methanol	324	– , 450 ,	408 408[c]	430, 370
Water	330	– ,	420	450[d], –

$a = 1 \times 10^{-5}M$, $b = 1 \times 10^{-4}M$, $c = 1 \times 10^{-3}M$, $d = 1 \times 10^{-2}M$.

Table 4.20. Ground and excited state equilibria of $mBNH_2$ at 298K.

Equilibrium	pK_a	$pK_a^*(FT)$	$\lambda_{isosbestic}$ (nm)
Dication $\rightleftharpoons$ Monocation	1.9	2.0	290
Monocation $\rightleftharpoons$ Neutral	4.5	4.5	300
Neutral $\rightleftharpoons$ Anion	11.9	11.7	305
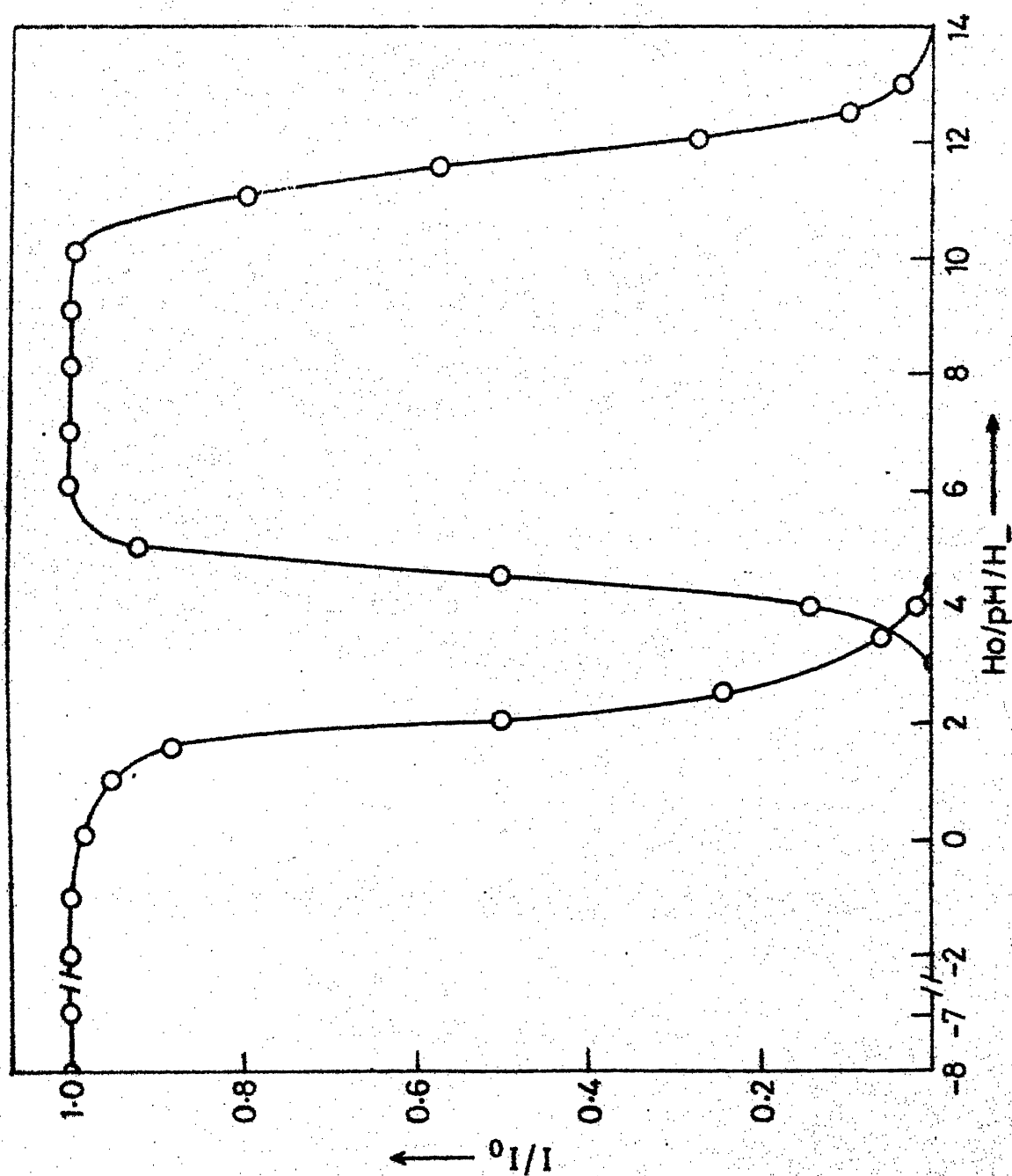
Fig.4.29 Plot of I/I_o as a function of $H_o/pH/H_-$ of mBNH$_2$ at 298K.
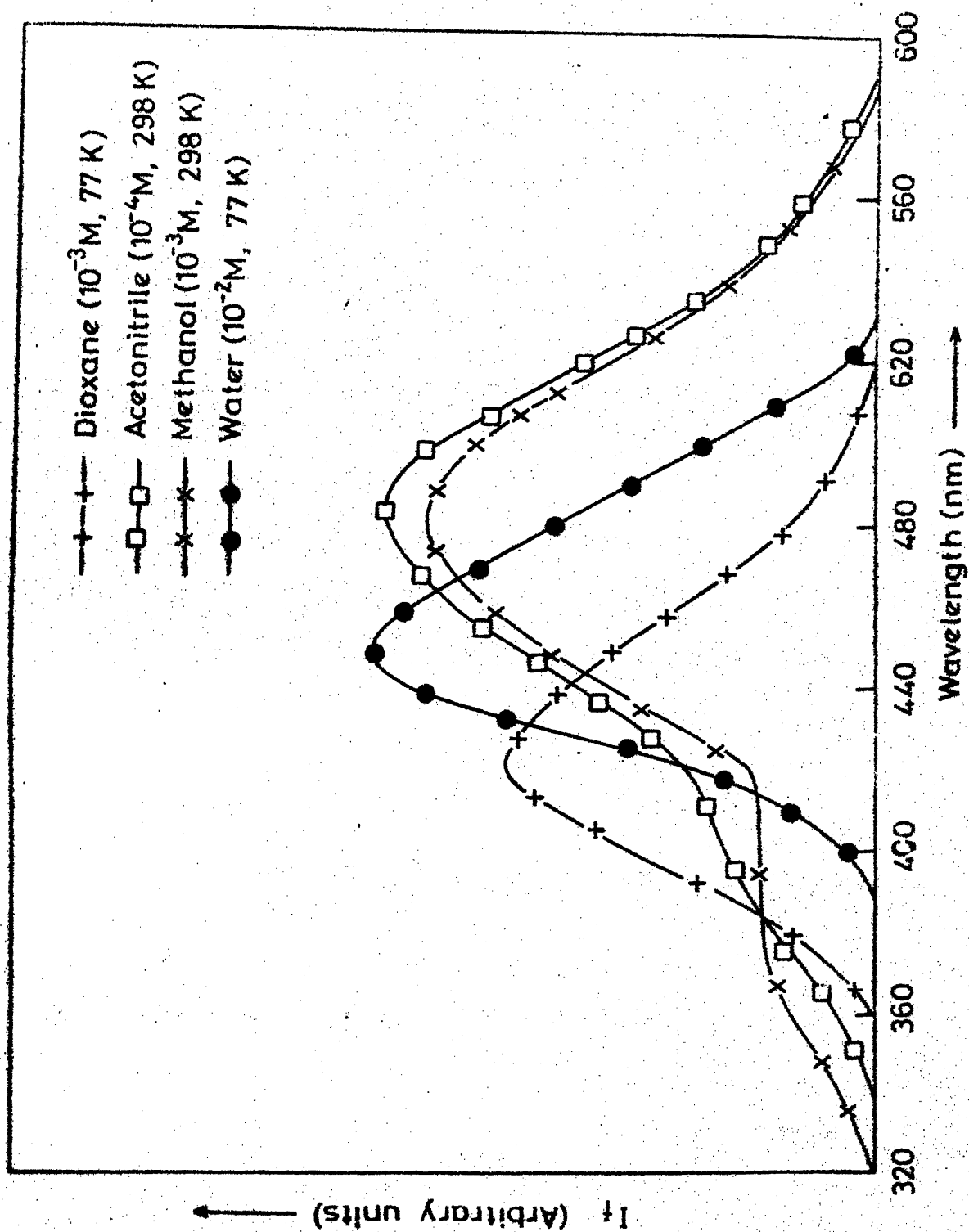
Fig.4.30 *Fluorescence spectra of hydrochloride salt of* mMNH$_2$ *in various solvents at 298K and at 77K.*

bonding solvents are efficient quencher of its fluorescence.

The red shifted fluorescence found in the $mBNH_2$ cation could be due to the fluorescence of cation or due to some excimer, though excimer formation in a charged species is unlikely. If excimer forms at 298K in liquid media, then its formation will be inhibited by freezing the solution due to slower diffusion. The low temperature (77K) fluorescence spectra of the salt in all the four solvents were taken and the results are given in Table 4.19. It is clear from the table that the longer wavelength band still exists in frozen media and in fact a band at $\sim$ 450 nm appears even in water as solvents (the λ_{max}(fluo) for neutral $mBNH_2$ at 77K is at 390 nm). Thus it is more likely that this long wavelength fluorescence is due to the cation of $mBNH_2$. It is not getting completely quenched in water at low temperature because of nonavailability of many nonradiative pathways.

The neutral fluorescence at 298K is quenched at a pH 11.9 (Fig. 4.29) which is also the pK_a for deprotonation. Thus the anion at this temperature is nonfluorescent. The fluorescence spectra of a 1M NaOH solution of the compound was taken at 77K. It was found to be fluorescent and the spectra is given in Fig. 4.28 and data in Table 4.18. A similar behavior was observed in the case of INH_2 and $BINH_2$ and thus a similar explanation can be offered. The dissociation occurs from the pyrrolic nitrogen atom in the ground state and from the exocyclic amino group in the excited state. The imino anion is generally nonfluorescent

whereas the anion from deprotonation of pyrrolic hydrogen is normally fluorescent. Thus in the frozen medium we observe anion fluorescence from ground state configuration. This also confirms that amino group becomes more acidic as compared to the pyrrolic group in S_1. The various ground and excited state equilibria are given in Table 4.20. Förster cycle values could not be calculated because of nonfluorescence of cation and anion forms, and only a very slight shift in absorption spectral maxima to give any meaningful result.

4.8.9 2-(p-Aminophenyl)benzimidazole(pBNH$_2$)

The absorption (Fig. 4.31) and fluorescence (Fig. 4.32) spectral behaviour for pBNH$_2$ is studied in the H_o/pH/H_- range of -9 to 16. The absorption and fluorescence band maxima in different forms is reported in Table 4.21. The neutral species has a long wavelength absorption maxima at 310 nm. On decreasing the pH, this band shifts to 340 nm below pH 5. With a further decrease of pH below 1.4, the 340 nm band gets blue shifted to 295 nm whereas on increasing the pH above 7, a change in absorption spectrum is observed after pH 13 i.e. the long wavelength band gets red shifted and is slightly structured. No further change in absorption spectrum is observed after pH 13. As discussed previously for other compounds this nature of absorption spectral shift clearly conforms to the followings:

(i) Monocation is formed because of the protonation at the
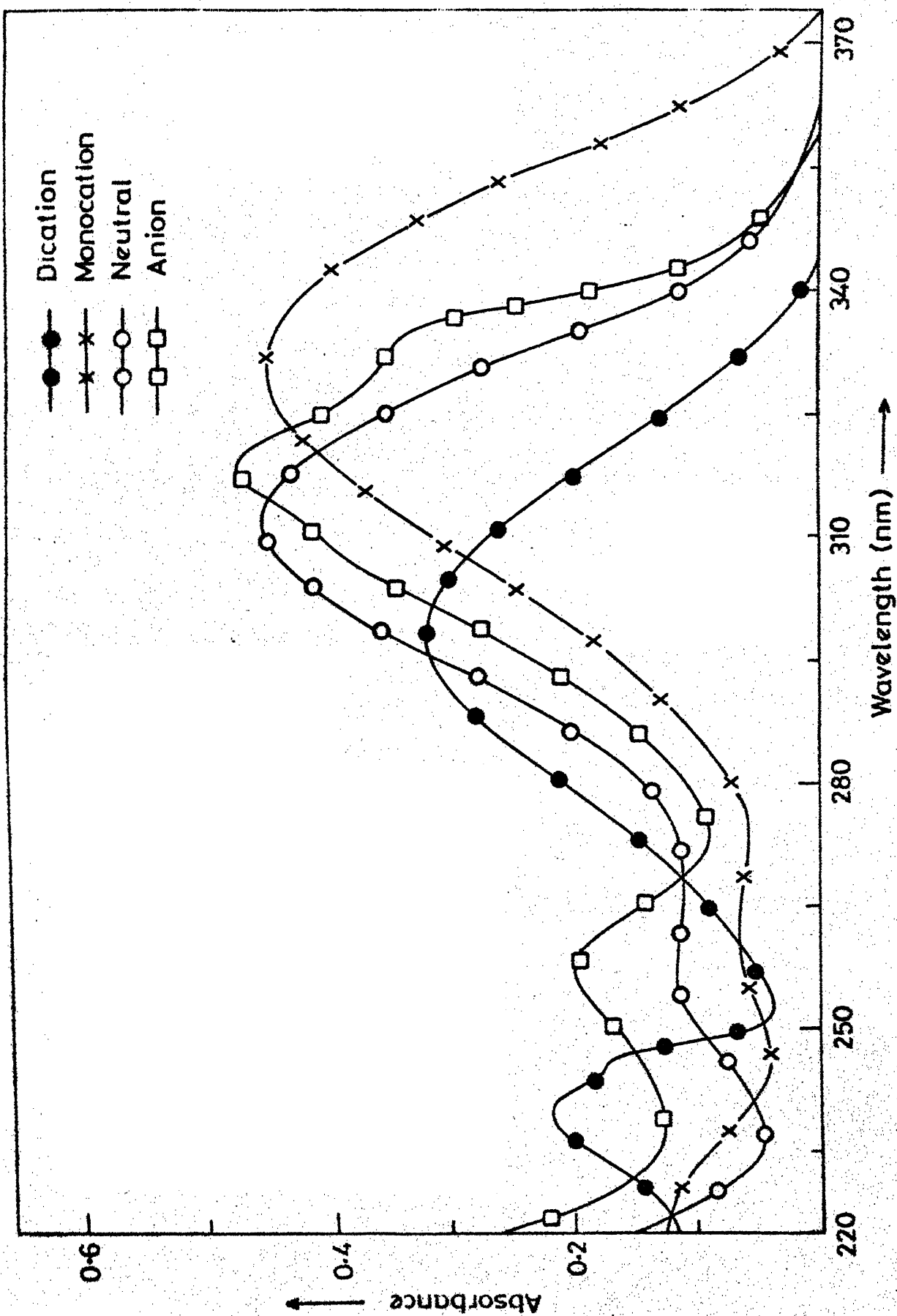
Fig.4.31 Absorption spectra of various prototropic forms of pBNH₂ at 298K.
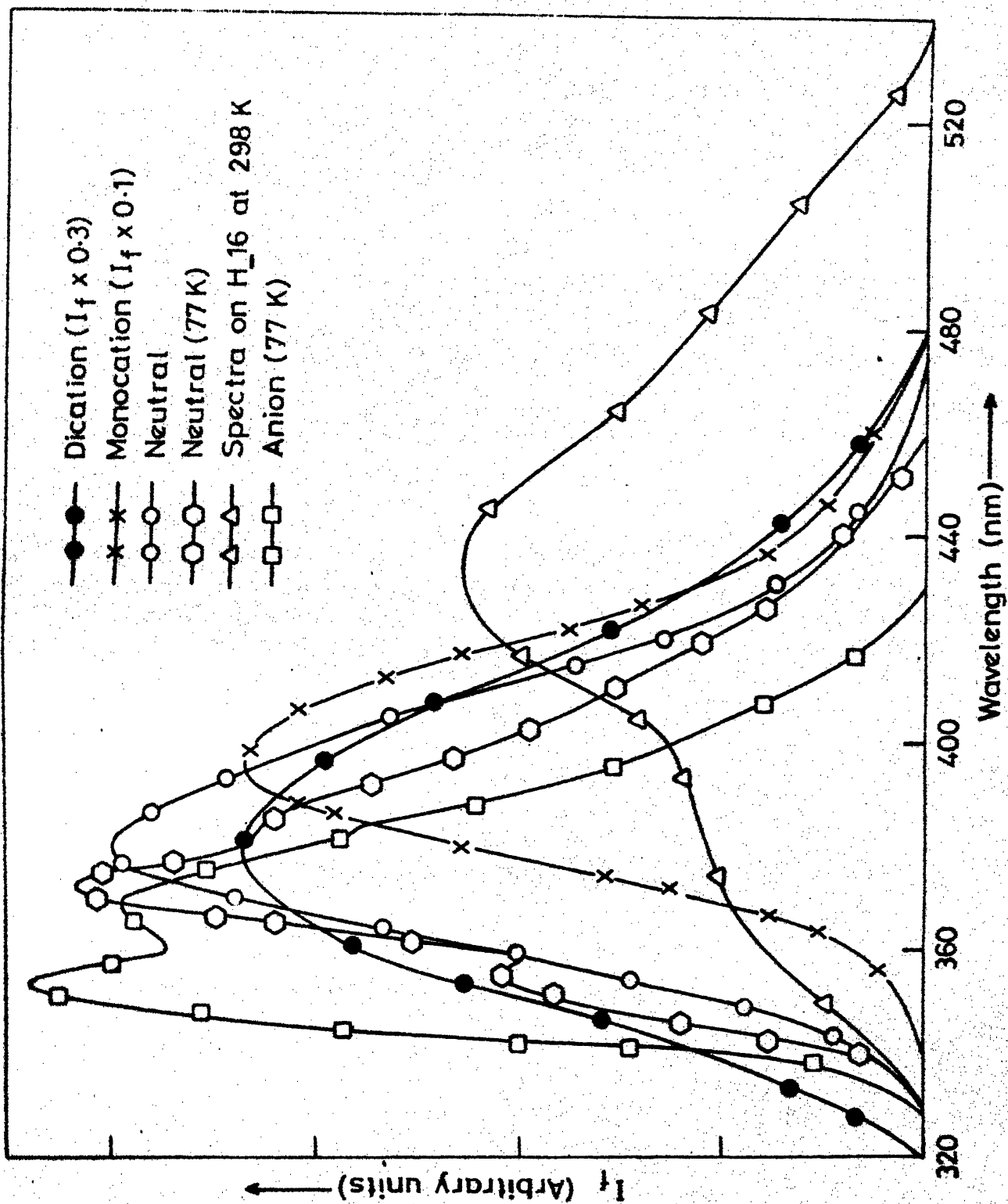
Fig.4.32 Fluorescence spectra of various prototropic forms of pBNH$_2$ at 298K and at 77K.

Table 4.21. Absorption maxima and fluorescence maxima of different prototropic forms of pBNH$_2$ at 298K.

Forms	λ_{max}(abs)			λ_{max}(flu)	ϕ_f
Dication	240	245	295	380	0.30
Monocation	230	262	340	394	0.06
Neutral		255	310	382 353,371,386,408(at 77K)	0.85
Anion		260	305⎫ 317⎬ 332⎭	430 352,368,385(at 77K)	–

Table 4.22. Ground and excit*ed* state prototropic equilibria of pBNH$_2$ at 298K.

Equilibrium	pK_a	F.C. (abs)	pK_a^* F.C. (flu)	F.C. (ave)	pK_a^* (F.T)	$\lambda_{isos.}$ (nm)
Dication ⇌ Monocation	1.40	−7.92	−0.42	−4.18	−1.6	295
Monocation ⇌ Neutral	5.05	11.03	6.58	8.80	5.00	320
Neutral ⇌ Anion	13.00	11.50	7.01	9.26	12.80	315

pyridinic center. (ii) Dication is formed by protonating the monocation at the exocyclic amino group. The blue shifted absorption band at 295 nm matches with absorption spectrum of PBI^{+} (295 nm) and that of $mBNH_2$ dication (297 nm). (iii) Deprotonation from the pyrrolic center causing red shift.

The shifts in fluorescence maxima also are similar in nature with that of the absorption maxima and these shifts occur in similar pH ranges (Table 4.22). Thus it can be inferred that the ground and the excited state species of the corresponding forms are the same. Unlike all other diaza amino compounds studied, a red shifted fluorescence band at 430 nm starts appearing at H_- 15 but its formation is not complete even at H_- 16, the highest basic concentration used .

The results of this study and those obtained from earlier studies have revealed that the pyridinic nitrogen atom becomes more basic and the ammonium ion becomes more acidic in S_1 state as compared to S_0 state. The effects of the above mentioned results on the spectral behaviour are that the shifts in the absorption spectra observed on protonation is relatively small as compared to that observed in the fluorescence spectra, thus suggesting that the first excited singlet state of the cation is relatively more stabilised in polar solvent than the ground state. The behaviour of $pBNH_2$ is different from the above mentioned one. It can be seen from the data of Table 4.21 that the spectral shift in absorption spectra (+30 nm) on protonation

of pyridinic nitrogen atom is more than that in fluorescence spectra (+12 nm). Similar changes are also observed when the second protonation takes place (i.e. -45 nm in absorption and -14 nm in fluorescence band maxima).

These results can be explained on the same lines as has been done for 2-aminobenzimidazole i.e. the presence of electron donating group may stabilize, leave it as such or destabilize the excited state more in comparison to the ground state, depending upon the interaction of two π clouds (one from the carbocyclic ring and another from aminophenyl ring). The data of Table 4.21 reveal that the interaction of these charge cloud is more favourable in neutral molecule as compared to the cation. The solvent study as well as the more favourable position of the amino group in the phenyl ring clearly tells that this charge migration from the electron donating group at the para position of the phenyl ring takes place more easily in cation than in the neutral molecule in the respective states. This kind of behaviour has been observed in the aminoquinolines where the spectral change in fluorescence as compared to quinoline is more when the amino group is substituted in carbocyclic ring as compared to heterocyclic ring.

In all the amino substituted diaza compounds studied, it has been observed that the deprotonation in the ground state takes place from the pyrrolic center and except for oBNH$_2$, the deprotonation in the excited state takes place from the exocyclic

amino group, leading to a nonfluorescent imino anion in fluid media. $oBNH_2$ anion formed after deprotonation of pyrrolic hydrogen atom was fluorescent. The behaviour of $pBNH_2$ in basic media is similar to the other compounds and not with that of $oBNH_2$. Thus the monoanion formed in S_0 state is due to the deprotonation of pyrrolic nitrogen atom and formed in S_1 state is due to the deprotonation of exocyclic amino group. If the deprotonation had occurred at the pyrrolic center in S_1 state, there would have been (i) a 1:1 correspondence between the depletion of neutral species and formation of monoanion (ii) the monoanion formed is generally fluorescent and (iii) one would have obtained at least a ground state pK_a value (if not less than pK_a) from the intersection of the fluorimetric titration curves because pyrrolic hydrogen atom becomes more acidic in S_1. The results obtained contradict all the three points mentioned above and agreeing with the earlier results that the increase in the acidity of exocyclic amino group in S_1 state is more than that in the pyrrolic group. The fluorescence spectrum of $pBNH_2$ in pH 13 to H_- 16 and at 77K (Fig. 4.32) gave structured but blue shifted spectrum as compared to neutral one at 77K and similar to the behaviour of $mBNH_2$ and INH_2. Since the fluorescence observed from the species at 77K reflects the ground state environments this only tells that monoanion of $pBNH_2$ is more stabilised in S_0 state as compared to the neutral one.

Now the red shifted fluorescence maxima (430 nm) observed
at $H_- \geq 15$ could be assigned to the dianion, formed by deproto-
nating the pyrrolic hydrogen atom, because the similar species
formed on deprotonating both the hydrogen atoms of the amino
group gives a blue shifted fluorescence spectra as compared to
both neutral and monoanion.[119] Non-complete formation of this
species only shows that the pK_a^* of this equilibrium (monoanion
$\rightleftharpoons$ dianion) is more than H_- 16.

The fluorimetric titration curves have been reported in
Fig. 4.33. The relatively low quantum yield of the cation made
it difficult to plot the relative decrease in its intensity in
the titration for dication $\rightleftharpoons$ monocation equilibrium. The
formation of anion at 298K could not be given in the fluorimet-
ric titration curve because its formation was not complete even
at H_-16 (Fig.4.33).

The various ground and excited states pK_a values obtained
by different methods are listed in Table 4.22. These values
depict the general behaviour of the benzimidazoles and proves
the assignment of various species as mentioned earlier. pK_a
values for the monocation-neutral and neutral-monoanion equilib-
ria are nearly equal to that for benzimidazole molecule, indicat-
ing that the presence of electron attracting phenyl group is
nearly balanced by the electron releasing amino group at the
proper position. The results of fluorimetric titration curves
are also consistent with the earlier findings i.e. arylammonium

ions are stronger acids in S_1, ground state pK_a value is obtained for monocation-neutral equilibrium and amino group is a stronger acid in S_1 relative to the pyrrolic center. The large difference between the pK_a^* values obtained by Förster cycle method, using absorption or fluorescence data could be due to unequal solvent relaxation or due to the use of band maxima in stead of 0-0 band. The former explanation seems to be more favourable with our earlier conclusions.

5.1 Summary

Absorption and fluorescence characteristics of two aromatic aminohydrocarbons (6-aminochrysene and 3-aminofluoranthene), 6-aminoindazole and six benzimidazoles viz. 2-hydroxybenzimidazole, 2-aminobenzimidazole, 2-phenylbenzimidazole, 2-(o-aminophenyl)benzimidazole, 2-(m-aminophenyl)benzimidazole and 2-(p-aminophenyl)benzimidazole in different solvents and at different pH have been investigated.

(i)   The study of solvent effect on spectral characteristics of aromatic amino compounds have indicated that water is acting as a hydrogen atom donor in S_0 state but as a hydrogen atom acceptor in S_1 state of amino compounds.

(ii)   pH study has clearly proved Tsutsumi's conclusion about proton induced quenching of the arylamines fluorescence before these are protonated i.e. charge migration from the amino group is concentrated at one of the atom and interaction of proton with this site is responsible for

the fluorescence quenching. All the amino compounds investigated in this study, except 3-aminofluoranthene have the above property. In the latter compound it is known that charge density is uniformly distributed over the complete molecule in S_0 and this study also indicates that the same is true in S_1 state also.

(iii) The behaviour of 6-aminoindazole (6-INH_2) is different from that of 5-aminoindazole (5-INH_2) in the sense that 6-INH_3^+ has a much shorter excited state lifetime than its counterpart of 5-INH_2 i.e. 5-INH_3^+. Due to this, fluorescence is observed from both 6-INH_3^+ (ammonium ion) and 6-H^+INH_2 (monocation protonated at the pyridinic nitrogen atom), depending upon the pH of solution, whereas over the same pH range only the former species exists in S_0. Further, the former cation is more stable in polar and strongly hydrogen bonding solvents and the latter in nonpolar solvents.

(iv) Monocations in the case of benzimidazoles in S_0 and S_1 states are always formed by protonating the pyridinic nitrogen atom, indicating that it is more basic than amino groups. Monocation of 2-aminobenzimidazole behaves as a cyclic amidine rather than a normal aromatic amine, both in S_0 and S_1 states.

(v) 2-Hydroxybenzimidazole behaves as its keto isomer [2(3H)- benzimidazolone] both in S_0 and S_1 states. Dication

is formed by protonating the hydroxyl group after reorg-
anisation of the species. The structure of the benzimi-
dazole is kept intact on forming anion.

(vi)   Intramolecular hydrogen bonding plays a major role in
the 2-(o-aminophenyl)benzimidazole and thereby forming
two hydrogen bonded isomers. The isomer I, formed with
the hydrogen atom of amino group and pyridinic nitrogen
atom is stable in nonhydrogen bonding solvents only
whereas the isomer II formed with the pyrrolic hydrogen
atom and lone pair of amino group is stable in all the
solvents in both S_0 and S_1 states. Amino group of
2-(m-aminophenyl)benzimidazole affects the spectra of
benzimidazole ring only indirectly whereas the same group
in 2-(p-aminophenyl)benzimidazole affects through a direct
conjugation.

(vii)   The increase in the acidity of the amino group is relati-
vely more than that of pyrrolic group in S_1 state i.e.
deprotonation takes place from pyrrolic group in S_0 state
and from amino group in S_1 state.

5.2 Scope of further work

In this study, the values of equilibrium constants in
the excited state have been experimentally determined by fluori-
metric titrations. These values can be further confirmed by

measuring the rate constants for the forward and reverse proton
transfer reactions with the help of time dependent fluorimetry.
In fact, this kinetic method becomes more significant in cases
where rates of deactivation processes like proton induced
fluorescence quenching of the neutral form compete with the
rate of protonation.

The rate of proton induced fluorescence quenching can be
determined from a Sterm-Volmer plot with a knowledge of the
lifetime of the species in S_1 state. In this study the life-
time has been estimated approximately using Strickler and Berg's
formula. The rate can be measured with accuracy only by measur-
ing the lifetime experimentally with the help of time dependent
fluorimetry.

LIST OF REFERENCES

1. M. Kasha, Disc. Faraday. Soc., 9, 14 (1950).

2. H. McConnell, J. Chem. Phys., 20, 700 (1952).

3. N.S. Bayliss and E.G. McRae, J. Phys. Chem., 58, 1002 (1954).

4. E. Lippert, Z. Elektrochem., 61, 962 (1957).

5. E.G. McRae, J. Phys. Chem., 61, 562 (1957).

6. P. Suppan and C. Tsiamis, Spectrochim. Acta., 36A, 971 (1950).

7. N. Mataga, Y. Kaifu and M. Koizumi, Bull. Chem. Soc. Japan, 29, 465 (1956).

8. H.H. Jaffe and M. Orchin, "Theory and Applications of Ultraviolet Spectroscopy", John Wiley, New York (1962).

9. (a) H. Suzuki, "Electronic Absorption Spectra and Geometry of Organic Molecules", Academic Press, New York (1967).

   (b) N. Mataga and T. Kubota, "Molecular Interactions and Electronic Spectra", Marcel Dekker Inc., New York (1970).

10. P. Pringsheim, "Fluorescence and Phosphorescence", Interscience Publishers, Inc., New York (1949).

11. Th. Förster, "Fluoreszenz Organisher Verbindungen", Vandenhoeck and Rupreht, Gottingen (1951).

12. B.L. Van Durren, Chem. Rev., 63, 325 (1963).

13. N. Mataga and S. Tsuno, Bull. Chem. Soc. Japan, 30, 711 (1957).

14. N. Mataga and Y. Kaifu, Mol. Phys., 7, 137 (1964).

15. N. Mataga, Bull. Chem. Soc. Japan, 31, 487 (1958).

16. I.B. Berlman, J. Phys. Chem., 74, 3085 (1970).

17. S.B. Costa, A.L. Maccanita and M.J. Prieto, J. Photochem., 11, 109 (1979).

18. P. Suppan, Chem. Phys. Letts., 94, 272 (1983).

19. A.C. Capomacchia, J. Casper and S.G. Schulman, J. Pharm. Sci., 63, 1272 (1974).

20. P.J. Kovi, C.L. Miller and S.G. Schulman, Anal. Chim. Acta., 61, 7 (1972).

21. S.G. Schulman and K. Abate, J. Pharm. Sci., 61, 1576 (1972).

22. R.J. Strugeon and S.G. Schulman, J. Pharm. Sci., 65, 1833 (1976).

23. K. Weber, Z. Phys. Chem. (Leipzig), B15, 18 (1931).

24. Th. Förster, Z. Elektrochem., 54, 42 (1950).

25. Th. Förster, Z. Elektrochem., 54, 531 (1950).

26. Th. Förster, "Photochemistry in the Liquid and Solid States", Ed. F. Daniels, John Wiley and Sons, Inc., New York (1960).

27. A. Weller, Z. Elektrochem., 56, 662 (1952).

28. D.D. Rosebrook and W.W. Brandt, J. Phys. Chem., 70, 3851 (1966).

29. W. Bartok, P.J. Lucchesi and N.S. Snider, J. Amer. Chem. Soc., 84, 1842 (1962).

30. J.C. Haylock, S.F. Mason and B.E. Smith, J. Chem. Soc., 4897 (1963).

31. S.F. Mason, J. Philip and B.E. Smith, J. Chem. Soc., 3051 (1968).

32. H.H. Jaffe and H. Lloyd Jones, J. Org. Chem., 30, 964 (1964).

33. H.H. Jaffe, D.L. Beveridge and L. Jones, J. Amer. Chem. Soc., 86, 2962 (1964).

34. E.L. Wehry and L.B. Rogers, J. Amer. Chem. Soc., 87, 4235 (1965).

35. E. Vander Donckt, "Progress in Reaction Kinetics", Ed. G. Porter, Pergman Press, New York, Vol. 5, (1970), P.273.

36. S.G. Schulman, Rev. in Anal. Chem., 1, 85 (1971).

37. J.F. Ireland and P.A.H. Wyatt, "Advances in Physical Organic Chemistry", Vol.12, Ed. V. Gold and D. Bethell, Academic Press, New York (1976), P.131.

38. S.G. Schulman, "Physical Methods in Heterocyclic Chemistry", Ed. A.R. Katritzky, Academic Press, New York, Vol.VI (1974), P.147.

39. S,G. Schulman, R.M. Threatte, A.C. Capomacchia and W.L. Paul, J. Pharm. Sci., 63, 876 (1974).

40. S.G. Schulman and A.C. Capomacchia, J. Phys. Chem., 79, 1337 (1975).

41. A.C. Capomacchia and S.G. Schulman, J. Pharm. Sci., 64, 1256 (1975).

42. S.G. Schulman, D.V. Naik, A.C. Capomacchia and T. Roy, J. Pharm. Sci., 64, 982 (1975).

43. P.J. Kovi and S.G. Schulman, Anal. Chim. Acta., 63, 39 (1973).

44. S.G. Schulman, "Modern Fluorescence Spectroscopy", Vol.2, Ed. E.L. Wehry, Plenum Press, New York (1976), P.239.

45. S.G. Schulman, "Fluorescence and Phosphorescence Spectroscopy: Physicochemical Principles and Practice", Pergamon Press, New York (1977).

46. U. Pandey, N.B. Joshi and D.D. Pant, Chem. Phys. Lett., 72, 209 (1980).

47. M. Swaminathan and S.K. Dogra, Can. J. Chem., 61, 1064 (1983).

48. K. Tsutsumi, A. Aoki, H. Shizuka and Monta, Bull. Chem. Soc. Japan, 44, 3245 (1971).

49. M. Swaminathan and S.K. Dogra, J. Am. Chem. Soc., 105, 6223 (1983).

50. T.K. Adler, Anal. Chem., 34, 685 (1962).

51. H.U. Schutt and H. Zimmerman, Ber. Bunsenges Phys. Chem., 67, 54 (1963).

52. J.H. Longworth, R.O. Rahn and R.G. Schulman, J. Chem. Phys., 45, 2930 (1966).

53. H.C. Borrensen, Acta. Chem. Scand., 17, 921 (1963).

54. M. Kondo and H. Kuwano, Bull. Chem. Soc. Japan, 42, 1433 (1969).

55. P. Svejda, R.R. Anderson and A.H. Maki, J. Amer. Chem. Soc., 100, 7131 (1978).

56. S.G. Schulman, A.C. Capomacchia and B. Tussey, Photochem. Photobiol., 14, 733 (1971).

57. A.C. Capomacchia and S.G. Schulman, Anal. Chim. Acta., 58, 91 (1972).

58. S.G. Schulman and L.B. Sanders, Anal. Chim. Acta., 56, 83 (1971).

59. P.J. Kovi, A.C. Capomacchia and S.G. Schulman, Anal. Chem., 44, 1611 (1972).

60. K. Abate, A.C. Capomacchia, P.J. Jackman, P.J. Kovi, and S.G. Schulman, Anal. Chim. Acta., 65, 59 (1973).

61. P.C. Tway and L.J. Cline Love, J. Phys. Chem., 86, 5223, 5227 (1982).

62. R. Argauer and C.E. White, "Fluorescence Analysis", Dekker, New York (1970).

63. C.E. White, May Ho and E.Q. Weimer, Anal. Chem., 32, 438 (1960).

64. C.A. Parker and W.T. Rees, Analyst, 85, 587 (1960).

65. W.H. Melhuish, J. Opt. Soc. America., 52, 1256 (1962).

66. R.F. Chen, Anal. Biochem., 20, 339 (1967).

67. C.A. Parker, "Photoluminescence of Solutions", Elsevier Publications, New York (1968).

68. C.A. Parker, Nature, 182, 1002 (1958).

69. J.A. Riddick and W.B. Bunger, "Organic Solvents", Wiley Interscience, New York (1970).

70. D.W. Hein, R.J. Alheim and J.J. Leavitt, J. Amer. Chem. Soc., 79, 427 (1957).

71. L.S. Efros, B.A. Porai-Koshits and S.G. Farbenshtein, J. Gen. Chem. USSR, 23, 1691 (1953).

72. L.P. Hammett and A.J. Deyrup, J. Amer. Chem. Soc., 54, 2721 (1932).

73. M.J. Jorgenson and D.R. Hartter, J. Amer. Chem. Soc., 85, 878 (1963).

74. G. Yagil, J. Phys. Chem., 71(4), 1034 (1967).

75. G.G. Guilbault, "Practical Fluorescence", Marcel Dekker Inc., New York (1973), P.12.

76. Ref. 75, P.14.

77. A.R. Katritzky and A.P. Ambler, "Physical Methods in Heterocyclic Chemistry", Vol.II, Academic Press, New York and London (1963). The Characteristic benzimidazole peaks and amino group peaks were matched.

78. J.R. Platt, J. Chem. Phys., 17, 484 (1949).

79. Ref. 8, P.355.

80. D.J. Rabiger and M.M. Joullie', J. Org. Chem., 29, 476 (1964).

81. G. Leandri, A. Mangini, F. Montanari and R. Posserini, Gazz. Chim. Italiana, 85, 769 (1955).

82. R.D. Gordon and R.F. Yang, Can. J. Chem., 48, 1722 (1970).

83. H. Zimmermann and N. Joop, Z. Elektrochem, 65, 68 (1961).

84. M. Tichy, R. Zahradrik, J.A. Vollmin and W. Simon, Collect. Czech. Chem. Comm., 37, 1962 (1972).

85. E.W. Thulstrup, M. Nepros, V. Dvorak and J. Michl, J. Mol. Spectroscopy, 59, 265 (1976).

85. (a) W.L.F. Armarego, "Physical Methods in Heterocyclic Chemistry", Vol.III, Ed. A.R. Katritzky, Academic Press (1963), P.96.

86. A.K. Mishra, M. Swaminathan and S.K. Dogra, J. Photochem., in press.

87. P. Brocklehurst, Tetrahedron, 18, 299 (1962).

88. O. Dann and P. Nickel, Ann. 667, 101 (1963).

89. L.S. Efros and A.V. El'tsov, J. Gen. Chem. USSR, 27, 755(1957).

90. P. Nuhn, G. Wagner and S. Leistner, Z. Chem., 9, 152 (1969).

91. P.N. Preston, "Benzimidazoles and Congeneric Tricyclic Compounds", Part 1, Ed. P.N. Preston, Interscience (1981), P.355.

92. J. Heller, Prakt. Chem., 111, 1 (1925).

93. J. Elbs, Prakt. Chem., 83, 21 (1911).

94. V. Mond, Gazz., 76, 365 (1946).

95. D. Brown, J. Chem. Soc., 1974 (1958).

96. D. Harrison, J.J. Ralph and A.C.B. Smith, J. Chem. Soc., 2930 (1963).

97. D. Harrison and A.C.B. Smith, J. Chem. Soc., 3157 (1959).

98. F.A. Matson, R.F. Becker and D.R. Scott, "Techniques of Organic Chemistry", Vol.IX, Part I, Ed. W. West, Interscience, New York, (1968), P.271, 273 and references listed there.

99. Ref. 91, P.64.

100. Ref. 8, P.560.

101. S.G. Schulman, P.T. Tidwell, J.J. Cetorelli and J.D. Winefordner, J. Amer. Chem. Soc., 93, 3179 (1971).

102. S.G. Schulman and A.C. Capomacchia, Spectrochim. Acta., 28A, 1 (1972).

103. W.L. Levshin, Z. Phys., 43, 230 (1931).

104. Ref. 44, P.266-275.

105. A. Weller, "Progress in Reaction Kinetics", Vol.I, Ed. G. Porter, Pergamon Press, New York (1961), P.187.

106. K. Tsutsumi and H. Shizuka, Chem. Phys. Lett., 52, 485(1977); Z. Phys. Chem. N.F., 111, 129 (1978).

107. H. Shizuka, K. Tsutsumi, H. Takeuchi and I. Tanaka, Chem. Phys. Lett., 62, 408 (1979).

108. H. Shizuka and K. Tsutsumi, J. Photochem., 9, 334 (1978).

109. K. Tsutsumi and H. Shizuka, Z. Phys. Chem., N.F., 122, 129 (1980).

110. H. Hafner, J. Worner, W. Steiner and M. Hauser, Chem. Phys. Lett., 72, 139 (1980).

111. C.M. Harris and B.K. Sellinger, J. Phys. Chem., 84, 891, 1366 (1980).

112. K. Tsutsumi, S. Sekiguchi and H. Shizuka, J. Chem. Soc., Faraday Trans. I, 78, 1087 (1982).

113. Z.R. Grabowski and A. Grabowska, Z. Phys. Chem. N.F., 101, 197 (1976).

114. S. Tobita and H. Shizuka, Chem. Phys. Lett., 75, 140 (1980).

115. A. Weller, Z. Phys. Chem. N.F., 3, 238 (1955).

116. S.J. Strickler and R.A. Berg, J. Chem. Phys., 37, 814 (1962).

117. Ref.8, P.330.

118. J. Michl and R. Zahradnik, Collect. Czech. Chem. Comm., 31, 3453 (1966).

119. Th. Förster, Z. Elektrochem., 54, 531 (1950).

120. M. Swaminathan and S.K. Dogra, Can. J. Chem., 61, 1064(1983).

121. A.K. Mishra, M. Swaminathan and S.K. Dogra, unpublished results.

122. S.G. Schulman, A.C. Capomacchia and M.S. Rietta, Anal. Chim. Acta., 56, 91 (1971).

123. Ref.8, P.344.

124. J. Michl, K. Bocek and R. Zahradnik, Collect. Czech. Chem. Comm., 31, 3471 (1966).

125. J. Michl, R. Zahradnik and W. Simon, Collect. Czech. Chem. Comm., 31, 3464 (1966).

126. J.B. Birks, "Photophysics of Aromatic Molecules", Wiley Interscience, London (1970), P.126.

127. Ref. 126, P.123.

128. Ref. 37, Chap.II, P.159.

129. See the protonation equilibria in CNH_2 and FNH_2, P.114,122.

130. M. Swaminathan and S.K. Dogra, J. Photochem., $\underline{21}$, 245(1983).

131. M. Swaminathan and S.K. Dogra, Ind. J. Chem., in press.

132. D.D. Perrin, "Dissociation Constants of Organic Bases in Aqueous Solution", Butterworths, London (1965), P.274.

133. C.A. Matuszak and A.J. Matuszak, J. Chem. Educ., $\underline{53}$, 280 (1976).

134. M. Swaminathan and S.K. Dogra, Ind. J. Chem., $\underline{22A}$, 278(1983).

135. D. Brown, J. Chem. Soc., 1974 (1958).

136. H. Boaz and G.K. Rollefson, J. Amer. Chem., $\underline{72}$, 3435 (1950).

137. M. Swaminathan and S.K. Dogra, J. Chem. Soc., Perkin Trans.II, to be published.

138. Ref. 132, P.262.

139. S.F. Mason, J. Chem. Soc., 1281 (1959).

140. C. Angyal and R. Werner, J. Chem. Soc., 2911 (1952).

141. C.J. Marzzacco, G. Deckey and A.M. Halpern, J. Phys. Chem., $\underline{86}$, 4937 (1982).

142. See deprotonation of CNH_2, FNH_2, INH_2, P.114,122,130.

143. M. Swaminathan and S.K. Dogra, Ind. J. Chem., $\underline{22}$, 407(1983).

144. D.D. Perrin, "Dissociation Constant of Organic Bases in Aqueous Solution", Butterworths, London (1965), P.261.

145. Ref. 144, P.58.

146. Ref. 8, P.338.

147. A.K. Mishra and S.K. Dogra, J. Photochem., $\underline{23}$, 163 (1983).

148. A.K. Mishra and S.K. Dogra, J. Chem. Soc., Perkin Trans.II, in press.

149. A.K. Mishra and S.K. Dogra, Spectrochim. Acta., $\underline{39A}$, 609 (1983).

150. Ref. 37, P.189.

VITAE

Born on March 10, 1959 at Dhananjayapur, Ganjam (Orissa), the author had his early education at P.S. High School, Saintala. He obtained his pre-university and 'First Year Degree Science' degrees from Jawaharlal College, Patnagarh, B.Sc.(Hons) degree from D.A.V. College, Titilagarh, Sambalpur University and M.Sc. degree from Delhi University in 1980.

LIST OF PUBLICATIONS

1. "Effect of solvents and pH on the absorption and fluorescence spectra of 2-phenylbenzimidazole", A.K. Mishra and S.K.Dogra, Spectrochimica Acta, 39A, 609 (1983).

2. "Excited state prototropism of 6-aminochrysene", A.K. Mishra and S.K. Dogra, Journal of Photochemistry, 23, 163 (1983).

3. "Photoluminescence of 3-aminofluoranthene", A.K. Mishra and S.K. Dogra, Journal of Chemical Society, Perkin-II, in press.

4. "Some effects of phosphate buffers on the excited state prototropic equilibria of indazole", A.K. Mishra, M. Swaminathan and S.K. Dogra, Journal of Photochemistry, in press.

5. "Photoluminescence of 2-(o-aminphenyl)benzimidazole", A.K. Mishra and S.K. Dogra, communicated.

6. "Prototropic equilibria in the lowest excited singlet state of 2-hydroxybenzimidazole 2(3H)-benzimidazolone , A.K. Mishra and S.K. Dogra, communicated.

7. "Luminescence characteristics of 6-aminoindazole in different solvents and at various pH", A.K. Mishra and S.K. Dogra, Communicated.

8. "Electronic spectra of 2-aminobenzimidazole", A.K. Mishra and S.K. Dogra, communicated.

9. "Prototropism in 2-(m-aminophenyl)benzimidazole in the first excited singlet state", A.K. Mishra and S.K. Dogra, communicated.

10. "Prototropism in 2-(p-aminophenyl)benzimidazole in the first excited singlet state", A.K. Mishra and S.K. Dogra, communicated.